SAN-1591-1

DEVELOPMENT OF A SOLAR DESICCANT DEHUMIDIFIER

Volume 1: Summary.

Volume 2: Detailed Technical Information

M. E. Gunderson
K. C. Hwang
S. M. Railing

March 31, 1978

Work Performed Under Contract No. EG-77-C-03-1591

Garrett Corporation
AiResearch Manufacturing Company
Los Angeles, California

U.S. Department of Energy

Solar Energy

Technical Progress Report

DEVELOPMENT OF A SOLAR DESICCANT DEHUMIDIFIER

Volume 1: Summary

78-14957-1

March 31, 1978

Prepared by M.E. Gunderson, K.C. Hwang, and S.M. Railing

Approved by

Rousseau

J. Rousseau

Prepared for

Department of Energy

GARRETT

AIRESEARCH MANUFACTURING COMPANY
OF CALIFORNIA

SAN-1591-1
Distribution Category UC-59c

INTRODUCTION AND SYSTEM DEFINITION

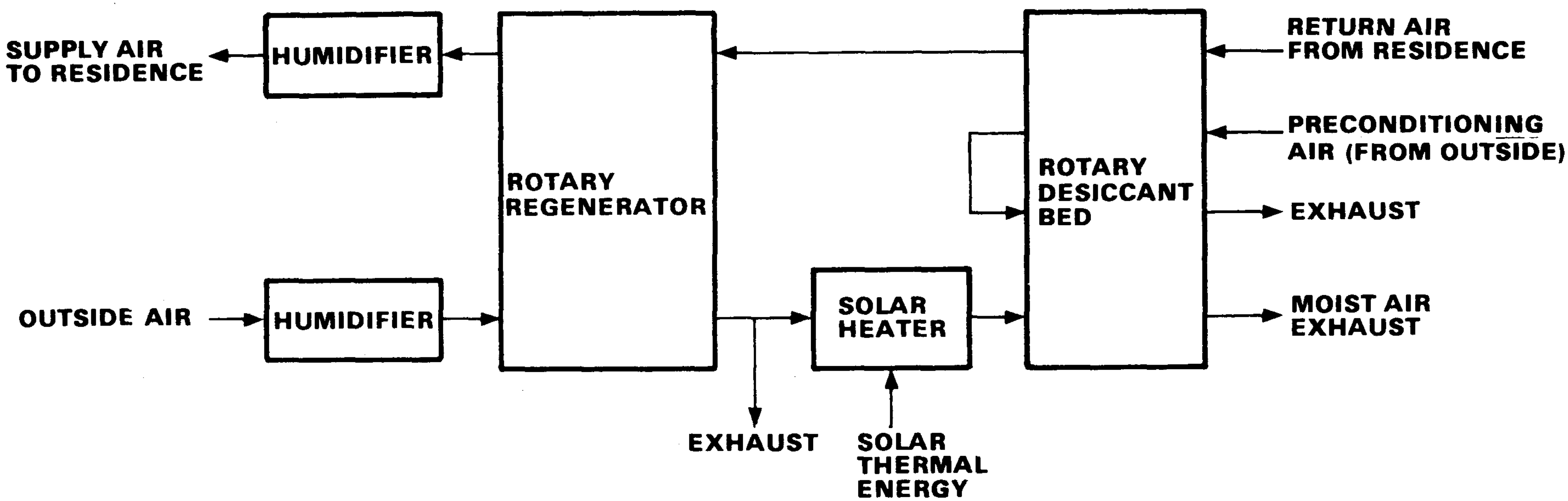

INTRODUCTION AND SYSTEM DEFINITION

This is the first technical progress report prepared by AiResearch Manufacturing Company of California for the Department of Energy under Contract No. EG-77-C-03-1591. The report covers activities from October 1, 1977 to April 1, 1978. This volume contains a summary of the work completed under this contract. Detailed information is given in Volume 2, as Appendixes A through K.

This program is aimed at the development of a solar desiccant dehumidifier featuring a rotary bed of granular silica gel and a rotary regenerator. This dehumidifier can be used for air conditioning through adiabatic saturation of the process airstream. The accompanying system schematic illustrates a complete air conditioning system based on this principle.

DEHUMIDIFIER CROSS SECTION

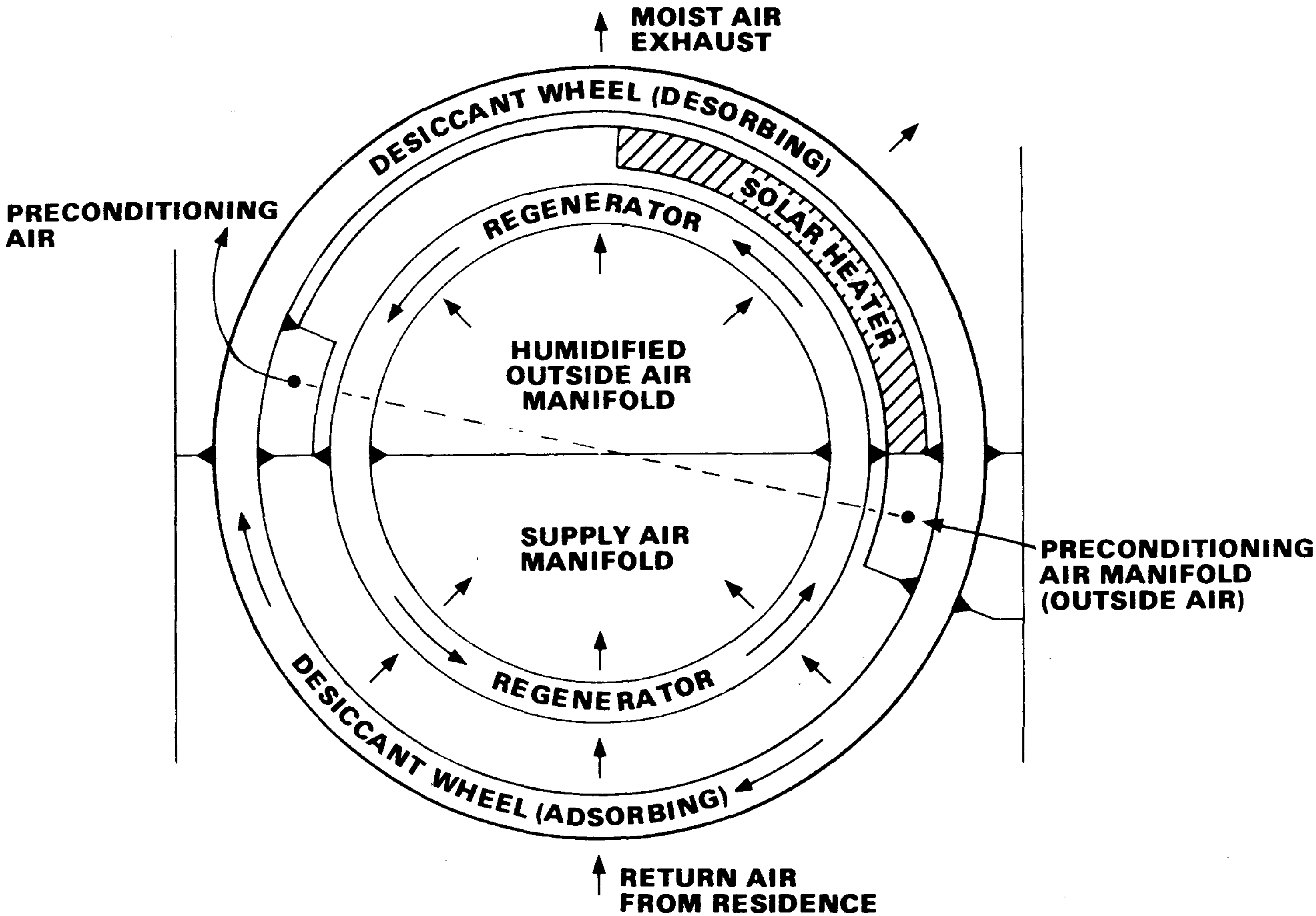

DEHUMIDIFIER CROSS SECTION

This illustration shows the two counterrotating concentric drums that comprise the desiccant subsystem. The outer drum contains the silica gel desiccant, and the inner drum contains the regenerator matrix. A solar heat exchanger fits in the annulus to supply energy to desorb the desiccant. Process and desorbing air streams flow radially through the two drums.

TASK I-0. MANAGEMENT

PROGRAM TASKS	MANPOWER LOADING, MAN-HOURS
PHASE I -- CONCEPTUAL DESIGN	
TASK I-1. REVIEW OF THE LITERATURE	120
TASK I-2. DESIGN REQUIREMENTS AND EVALUATION CRITERIA	200
TASK I-3. CANDIDATE COOLING SUBSYSTEMS	160
TASK I-4. SUBSYSTEM COMPUTER MODEL	320
TASK I-5. SUBSYSTEM PERFORMANCE MAP	300
TASK I-6. SYSTEM PERFORMANCE MODEL	200
TASK I-7. COLLECTOR TRADE STUDIES	240
TASK I-8. SYSTEM OPTIMIZATION	240
TASK I-9. PRELIMINARY ENVIRONMENTAL ASSESSMENT	160
TASK I-10. SUBSYSTEM PRELIMINARY DESIGN	1000
TASK I-11. COMMERCIALIZATION	480
TASK I-12. COST-EFFECTIVENESS STUDIES	240
TASK I-13. DOCUMENTATION (TECHNICAL PROGRESS)	400
	4060
PHASE II -- DETAILED DESIGN	
TASK II-1. SUBSYSTEM UPDATE	400
TASK II-2. SYSTEM UPDATE	400
TASK II-3. SUBSYSTEM DETAILED DESIGN	3400
TASK II-4. SUBSYSTEM/SYSTEM SPECIFICATION	600
TASK II-5. DOCUMENTATION (TECHNICAL PROGRESS)	600
	5400
PHASE III -- FABRICATION, TESTING, AND EVALUATION (PROTOTYPE REVIEW; TEST REVIEW; RECOMMENDATIONS)	
TASK III-1. DEHUMIDIFIER FABRICATION	1980 *
TASK III-2. DEHUMIDIFIER TEST STAND DEVELOPMENT	500 *
TASK III-3. DEHUMIDIFIER TESTING	2400
TASK III-4. SOLAR SYSTEM SIMULATOR DEVELOPMENT	500 *
TASK III-5. SOLAR SYSTEM TESTING	680
TASK III-6. TEST DATA EVALUATION	700
TASK III-7. SYSTEM/SUBSYSTEM DESIGN UPDATE	300
TASK III-8. COMMERCIALIZATION DATA UPDATE	220
TASK III-9. COST/EFFECTIVENESS DATA UPDATE	160
TASK III-10. PLANS AND RECOMMENDATIONS	240
TASK III-11. DOCUMENTATION (TECHNICAL PROGRESS)	400
	8080

MONTHS AFTER CONTRACT AWARD: 1–36

OCT. 1, 1977 (month 1) — APR. 1, 1978 (month 7)

*DOES NOT INCLUDE HARDWARE

S-15997-A

TASK I-0. MANAGEMENT

AiResearch progress on the solar desiccant dehumidifier contract has been close to original plans. The original program time schedule, shown here, covers three years, and has been revised to cover two years. The accelerated shcedule was submitted to DOE for approval, but as yet no reply has been received. In anticipation of approval, work is progressing according to the accelerated schedule.

Some work on system computer modeling has been postponed due to the decision by DOE to substitute standardized climate and house models for those already developed by AiResearch. The work in these areas will resume when the information is received from DOE.

PHASE I EXPENDITURES AND COMMITMENTS

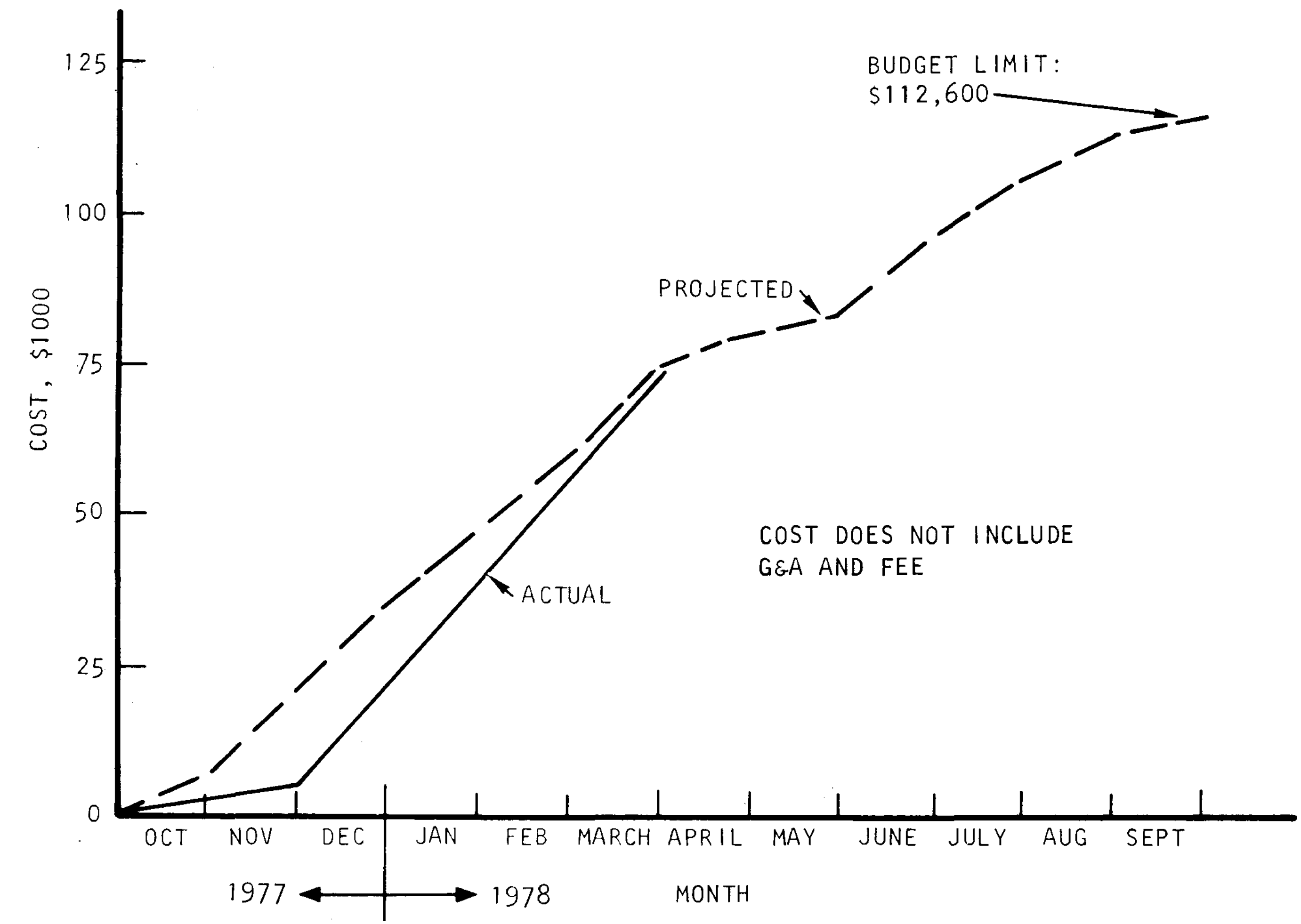

PHASE I EXPENDITURES AND COMMITMENTS

Expenditures and commitments were slightly lower than original forecasts during the early months of the contract. It appears that the budget will be closely followed for the remainder of Phase I.

ADDITIONAL MANAGEMENT ACTIVITIES

<u>SUBCONTRACTING</u>

- CONSULTATION WITH STEPHEN FITCH (BRY-AIR) CONTINUING
- MANUFACTURING DETAILS DISCUSSED WITH DUNHAM-BUSH

<u>MEETING AND DISCUSSIONS</u>

- PAPER PRESENTED AT SAN FRANCISCO WORKSHOP, FEBRUARY 1978
- ROUND-TABLE DISCUSSION AT SERI, NOVEMBER 1977
- DOE, BNL, PRC REPRESENTATIVES REVIEW PROGRAM, TORRANCE, FEBRUARY 1978

ADDITIONAL MANAGEMENT ACTIVITIES

Mr. Stephen Fitch of Bry-Air, Inc., Sunbury, Ohio, has been engaged as a subcontractor in the area of desiccant subsystem design. Mr. Fitch has extensive experience with similar industrial dehumidifiers and has been quite helpful. AiResearch personnel have travelled to Sunbury to discuss this project with Mr. Fitch.

Dunham-Bush, the proposed manufacturers of the final solar desiccant unit, has been consulted regarding construction techniques. It is desired to eliminate the need for any special skills on the part of manufacturing, installation, and service personnel so that the solar desiccant system will easily fit into the HVAC trade.

A paper entitled "Preliminary Design of a Solar Desiccant Air Conditioner" was presented at the Third Workshop on the Use of Solar Energy for the Cooling of Buildings in San Francisco. This paper summarizes work completed under this contract through January 1978.

AiResearch participated in a round-table discussion of desiccant systems at SERI in Golden, Colorado. In this meeting, valuable information was obtained from current DOE contractors and other people interested in the desiccant field.

AiResearch progress was reviewed by personnel from DOE, Brookhaven National Laboratory (BNL), and Planning Research Corporation (PRC) in February at the AiResearch plant at Torrance. The meeting included a detailed discussion of the work completed, and the direction of future work.

Details of management activities are given in Appendix A of Volume 2.

TASK I-1. REVIEW OF THE LITERATURE

STATE-OF-THE-ART SURVEY

- INSTITUTE OF GAS TECHNOLOGY (IGT)
- SOLARON
- CENTER FOR THE ENVIRONMENT AND MAN (CEM)
- COMMONWEALTH SCIENTIFIC AND INDUSTRIAL RESEARCH ORGANIZATION, AUSTRALIA (CSIRO)
- COMPREHENSIVE REVIEW OF STATE-OF-ART AT SERI MEETING

TASK I-1. REVIEW OF THE LITERATURE

A literature survey has been made covering (1) determination of the performance of, and design problems encountered with, various desiccant subsystems already in existence or currently under development and (2) a search for a sorbent with better performance than selica gel. Four major contributors to the previous state-of-the-art in desiccant cooling have been found. The first of these is the IGT system. This unit is based upon the original Munters Environmental Control (MEC) system, and was designed as a gas-fired air conditioner. A solar heat exchanger has been added as a retrofit. The desiccant is molecular seive impregnated asbestos paper. The desiccant and regenerator disks are vertically mounted, and are turned by peripheral rollers.

The second existing system has been designed by Solaron and constructed and tested by Bry-Air. This system is based upon a standard Bry-Air dehumidifer design. Two horizontal disks constructed of perforated steel comprise the desiccant beds. The desiccant is 6 to 8 mesh silica gel.

CEM has designed a third system. The philosophy in this case is to try to approach the thermodynamically ideal isothermal desiccant bed by using four beds with intercoolers and interheaters. The performance improvement expected from this approach must be balanced against the increased complexity and pressure drop.

A large amount of development work by CSIRO has lead to the fourth system. Vertical disks are used, as in the IGT system, but they are mounted on a central shaft. The desiccant is molecular seive impregnated asbestos paper. Rotary regenerators are constructed of mylar film. A fairly comprehensive analytical model of desiccant performance has been developed. Unfortunately, there is not a sufficient amount of directly comparable performance data available to be able to evaluate these systems with respect to each other, or to the proposed AiResearch system.

A comprehensive review of the state-of-the-art was held at the SERI meeting in Golden, Colorado. This meeting was well-timed for AiResearch because it was held in the early phase of the current project, at a time when concepts were still being considered.

SORBENT SELECTION

- SILICA GEL (VARIOUS MESH SIZES)
- MOLECULAR SIEVE
  - PELLETS (VARIOUS MESH SIZES)
  - ASBESTOS PAPER SUBSTRATE
- ACTIVATED ALUMINA
- LITHIUM CHLORIDE

8 TO 10 MESH SILICA GEL SELECTED

S 25331

SORBENT SELECTION

Silica gel, molecular sieve, and activated alumina were given serious consideration as sorbents. The 8 to 10 mesh silica gel was found to have the best combination of mass transfer properties, pressure drop characteristics, longevity, and cost. The comparisons were made on the basis of published data, manufacturers' quotations, and AiResearch experimental data. Molecular sieve pellets were found to have similar properties to silica gel, but at somewhat higher costs; molecular sieve paper is about ten times as expensive as pellets. Activated alumina has the best mechanical strength properties, but does not perform as well as silica gel in the pressure and temperature ranges encountered in this project. Lithium chloride also was examined, but was found not to be practical because of deliquesence.

Details of the state-of-the-art survey and SERI meeting highlights are documented in Appendix B of Volume 2. The sorbent examination and comparison is documented in Appendix C.

TASK I-2. DESIGN REQUIREMENTS AND EVALUATION CRITERIA

- GEOGRAPHIC LOCATIONS*

  NEW YORK: TYPICAL OF LARGE POPULATION CENTER
  PHOENIX: TYPICAL OF DESERT AREA
  LAKE CHARLES: TYPICAL OF HUMID CLIMATE

  (DESIGN YEAR CLIMATIC DATA AVAILABLE FROM CONTRACT NAS 8-32091)

- SINGLE-FAMILY RESIDENCE MODEL (1775 SQ FT)*

  ASHRAE 90 - 75 STANDARD OR BETTER

DESIGN LOAD	SENSIBLE	LATENT	TOTAL
NEW YORK	24,200	9900	34,100
PHOENIX	32,000	8900	40,900
LAKE CHARLES	25,600	12,000	37,600

- COST MODEL

  PRESENT VALUE AND UNIFORM ANNUAL COST

* MAY BE REPLACED BY STANDARDIZED MODELS FROM DOE

TASK I-2. DESIGN REQUIREMENTS AND EVALUATION CRITERIA

The work in Task I-2 was intended to establish the required design point performance for the desiccant dehumidifier, and to develop criteria for the evaluation of the thermodynamic and economic performance of the system with respect to more conventional systems.

Three geographic locations have been selected for which design year weather data are available. New York City is representative of the large East Coast population center, and hence of an area requiring a large amount of air conditioning. Lake Charles, Louisiana is typical of Southeastern and Gulf Coast locations, where the ambient relative humidity is very high during the cooling season. Phoenix, Arizona is representative of the Southwestern United States desert, where ambient humidity is low and sensible cooling loads are high. These three locations are expected to indicate the requirements of most of the United States requiring air conditioning.

A basic single-family residence has been designed in sufficient detail to determine time-dependent instantaneous loads when combined with the design year climatic data for the three geographic locations. This house depends upon conventional construction techniques, modified only to the extent necessary to accommodate the solar collectors and other solar equipment. ASHRAE Standard 90-75 is met or exceeded in all respects. The geographic locations and house model developed by AiResearch may be replaced by standardized models developed by DOE.

Present value and uniform annual cost are the two methods of economic analysis that will be used to indicate financial viability of the solar desiccant system. Estimates of conventional fuel and electricity costs have been made which account for real cost escalation plus inflation.

LiBr/H_2O ABSORPTION CHILLER PERFORMANCE

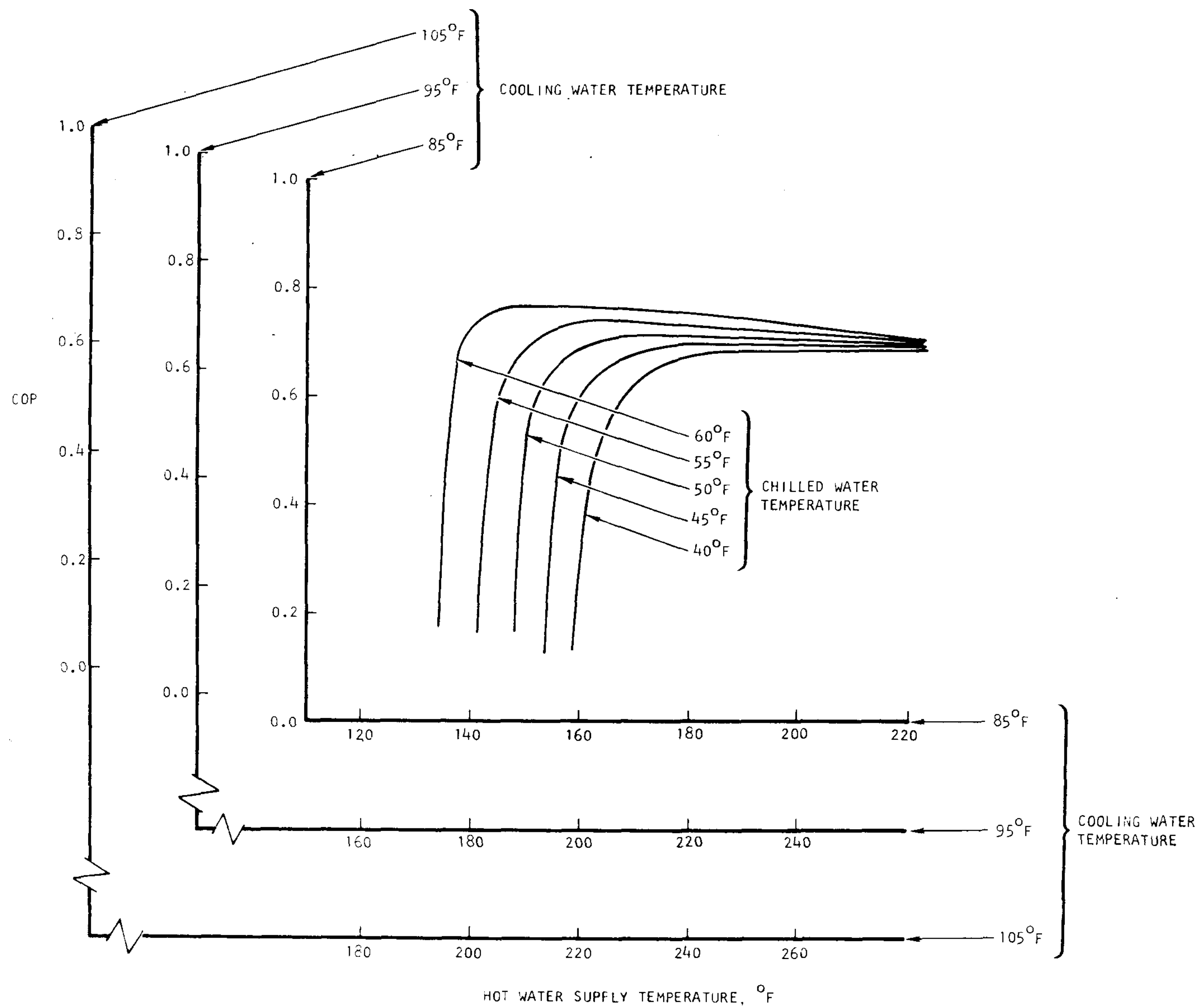

$LiBr/H_2O$ ABSORPTION PERFORMANCE

For comparison of thermodynamic performance of the desiccant system with other solar cooling systems, the characteristics of absorption and Rankine-reverse Rankine configurations have been researched. These include development programs of several manufacturers, as well as production equipment.

Shown here is typical design point performance for a single-effect $LiBr/H_2O$ absorption chiller. This information is compiled from Arkla, Trane, Carrier, and AiResearch performance predictions.

RANKINE COOLING SYSTEM PERFORMANCE

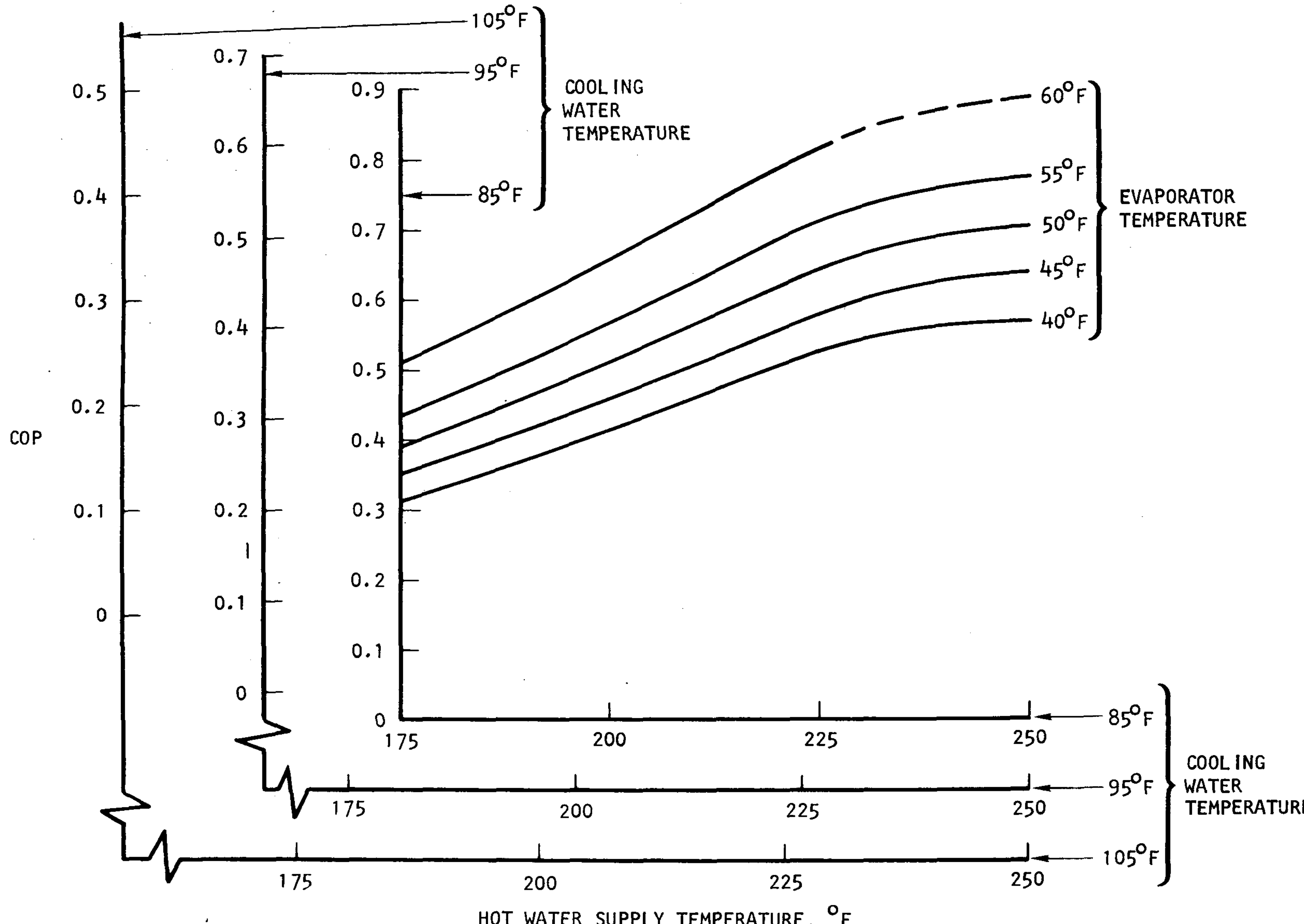

S-22183

RANKINE COOLING SYSTEM PERFORMANCE

This illustration shows predicted performance for the AiResearch 3-ton solar Rankine cooling system. This system comprises a Rankine power generation cycle driving a reverse-Rankine refrigeration cycle. Both cycles use R-11 as the working fluid and share a common condenser. It is felt that this represents the performance that can be achieved by sophisticated Rankine equipment in small tonnage sizes.

The geographic locations, single-family residence model, cost model, and conventional systems for comparison are documented in Appendices D, E, F, and G, respectively.

TASK I-3. CANDIDATE COOLING SUBSYSTEMS

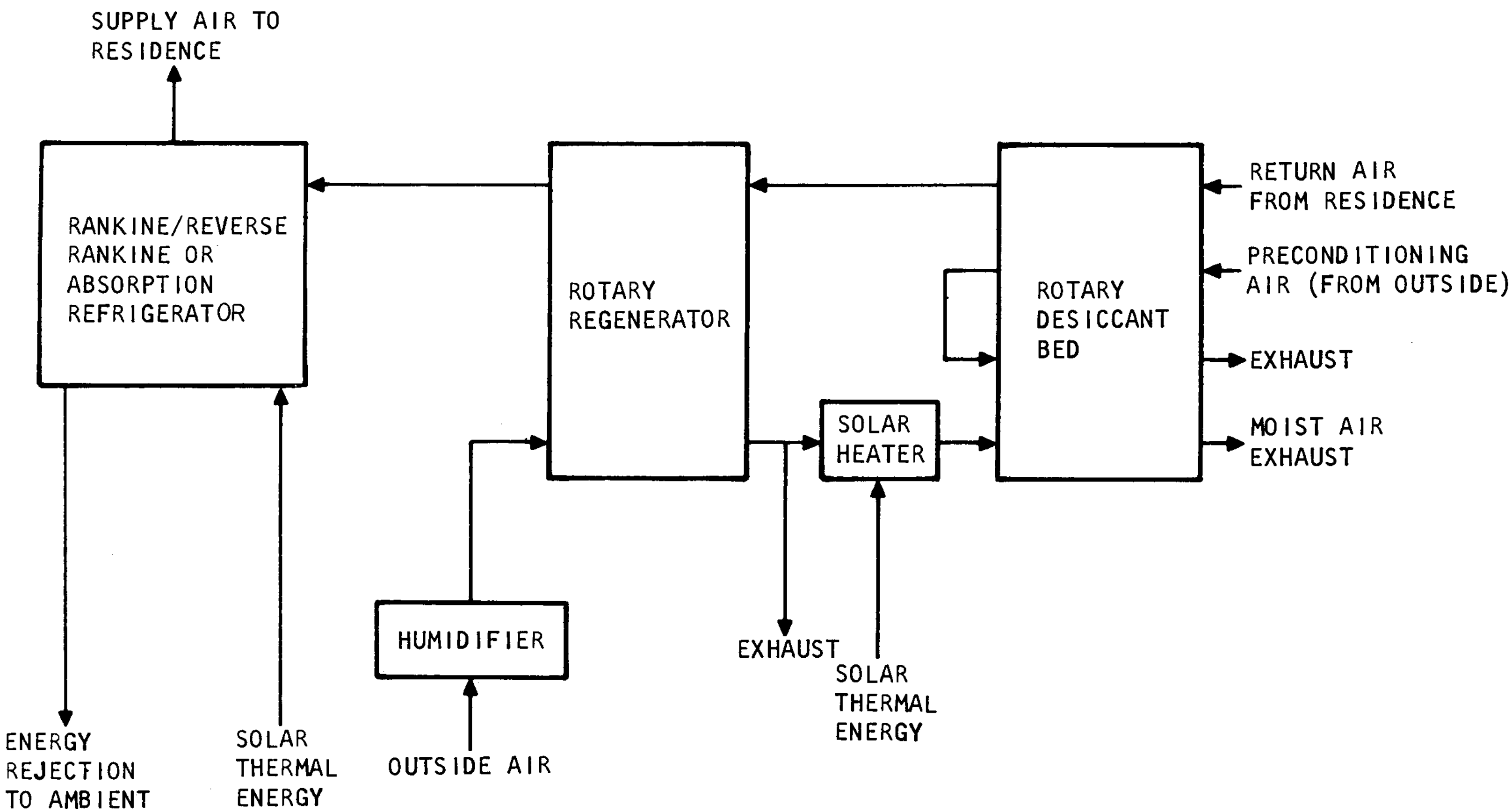

S-25015

TASK I-3. CANDIDATE COOLING SUBSYSTEM

While a complete air conditioning system can be constructed by combining the solar desiccant subsystem with adiabatic saturators, in many cases superior thermodynamic performance can be realized by hybrid systems. As shown in this illustration, dehumidification of the process air stream could be done by the desiccant equipment, with sensible cooling capacity added by means of a solar-powered refrigeration subsystem.

Two solar-powered cooling subsystems have been considered as serious candidates to be coupled to the solar desiccant dehumidifier. The first is the AiResearch Rankine-reverse Rankine refrigerator. In this unit, a Rankine solar power cycle drives a reverse Rankine refrigeration cycle. This unit is currently under development by AiResearch.

A lithium bromide, single-effect absorption refrigerator is the second candidate An advantage with this system is the ready availability of absorption hardware, and well-established performance data.

Design point performance for these two cooling subsystems is the same as previously shown under Task I-2.

IMPORTANCE OF SENSIBLE HEAT FACTOR

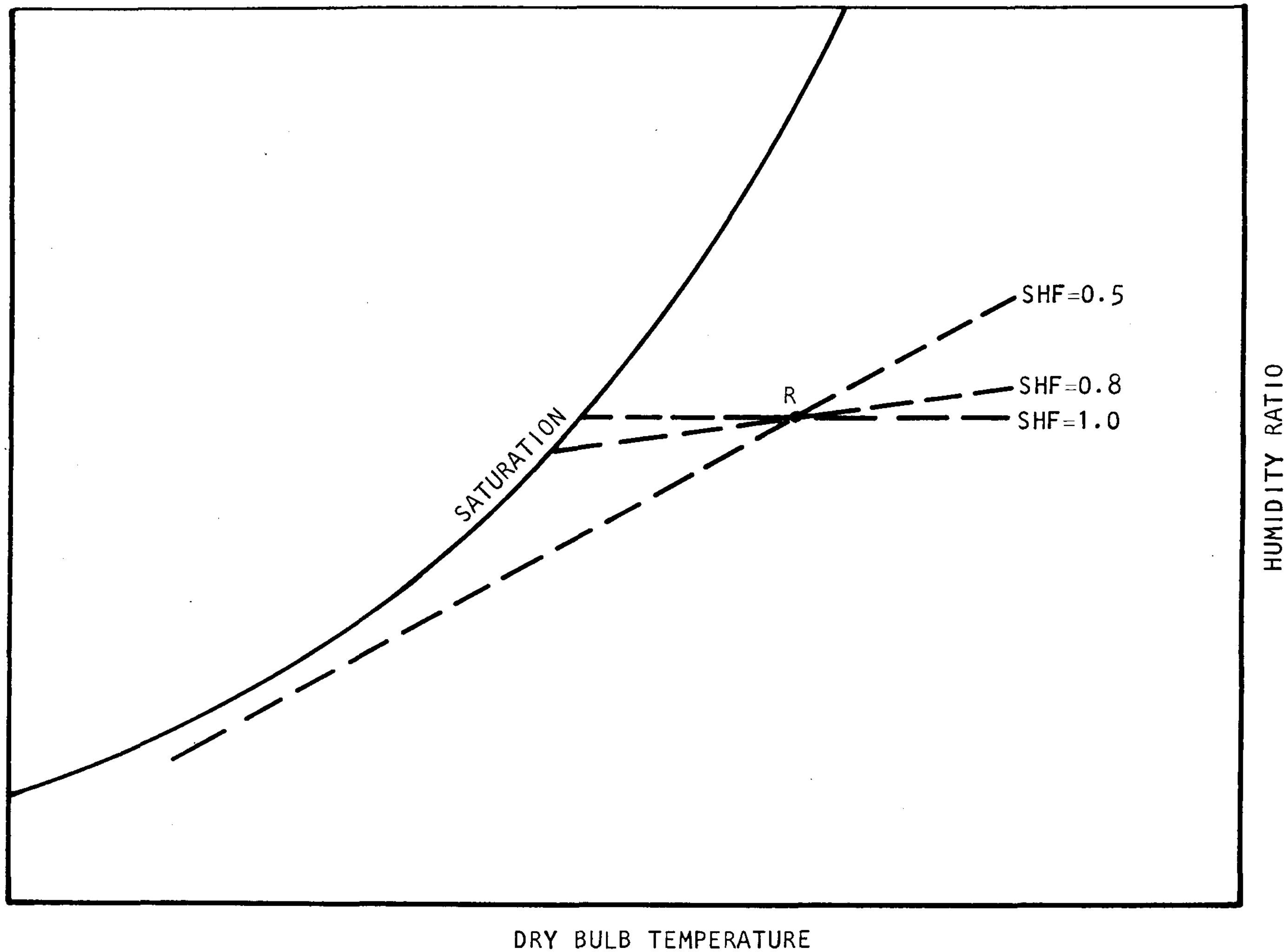

S-25014

IMPORTANCE OF SENSIBLE HEAT FACTOR

Hybrid systems will have superior performance to either purely desiccant or purely conventional systems in a variety of situations. The largest advantages occur when latent cooling loads are high.

The skeleton psychrometric chart in this illustration shows a return air state at point R. Three lines are drawn through R, representing sensible heat factors (SHF) of 1.0, 0.8, and 0.5. SHF is defined as the fraction of the total cooling load that is sensible; therefore, SHF = 1.0 implies that no moisture need be removed from the air, and SHF = 0.5 implies that one-half the cooling load is made up of moisture removal, and so on. The supply air to a conditioned space must fall on the SHF line drawn through R for the energy and moisture removal rates to balance the addition rates imposed by the load. In general, the lower the SHF, the more advantage gained from a hybrid system.

SIMPLE AND HYBRID SOLAR SYSTEM PERFORMANCE

SENSIBLE HEAT FACTOR = 0.8 (TYPICAL RESIDENCE)

SYSTEM	COP
SOLAR DESICCANT DEHUMIDIFIER WITH EVAPORATIVE COOLING	0.52
SOLAR ABSORPTION REFRIGERATION SYSTEM	0.71
SOLAR RANKINE REFRIGERATION SYSTEM	0.58
SOLAR DESICCANT DEHUMIDIFIER WITH ABSORPTION REFRIGERATION (HYBRID)	0.70
SOLAR DESICCANT DEHUMIDIFIER WITH RANKINE REFRIGERATION (HYBRID)	0.60

SENSIBLE HEAT FACTOR = 0.5 (COMMERCIAL KITCHEN)

SYSTEM	COP
SOLAR DESICCANT DEHUMIDIFIER WITH EVAPORATIVE COOLING	0.70
SOLAR ABSORPTION REFRIGERATION SYSTEM*	0.54
SOLAR RANKINE REFRIGERATION SYSTEM*	0.44
SOLAR DESICCANT DEHUMIDIFIER WITH ABSORPTION REFRIGERATION (HYBRID)	0.72
SOLAR DESICCANT DEHUMIDIFIER WITH RANKINE REFRIGERATION (HYBRID)	0.68

* REQUIRES REHEAT; NOT INCLUDED IN COP CALCULATIONS. SEE APPENDIX H FOR DISCUSSION.

S-25338

SIMPLE AND HYBRID SOLAR SYSTEM PERFORMANCE

This chart shows that the advantages of hybrid systems over simple absorption and Rankine solar cooling systems are significant in high latent load (i.e., low SHF) applications. No particular advantage is shown for the residence, but the commercial kitchen desiccant-absorption hybrid shows a 33 percent improvement over the simple absorption system, and the desiccant-Rankine hybrid shows a 55 percent improvement over the simple Rankine system. In addition, the two simple systems require reheating of the return air. In this analysis it was assumed that this could be done by waste energy, so it was not included in the COP calculations. In an application where use of waste heating was impractical, the simple system COPs would be much lower.

Parasitic power consumption is one important factor that does not show up in the COP analysis. The solar desiccant dehumidifier with evaporative cooling is shown as having about the same COP as the two hybrids for the kitchen application. However, both hybrids should have lower fan power requirements.

This will be a significant factor in overall system feasibility. In addition, since an air conditioner very seldom operates at design capacity, a favorable preliminary evaluation should be followed by a yearly performance evaluation. Only by this technique can the actual solar and auxiliary energy consumption be meaningfully determined.

A detailed discussion of candidate cooling subsystem selection and hybrid system performance is given in Appendix H.

TASK I-4. SUBSYSTEM COMPUTER MODEL

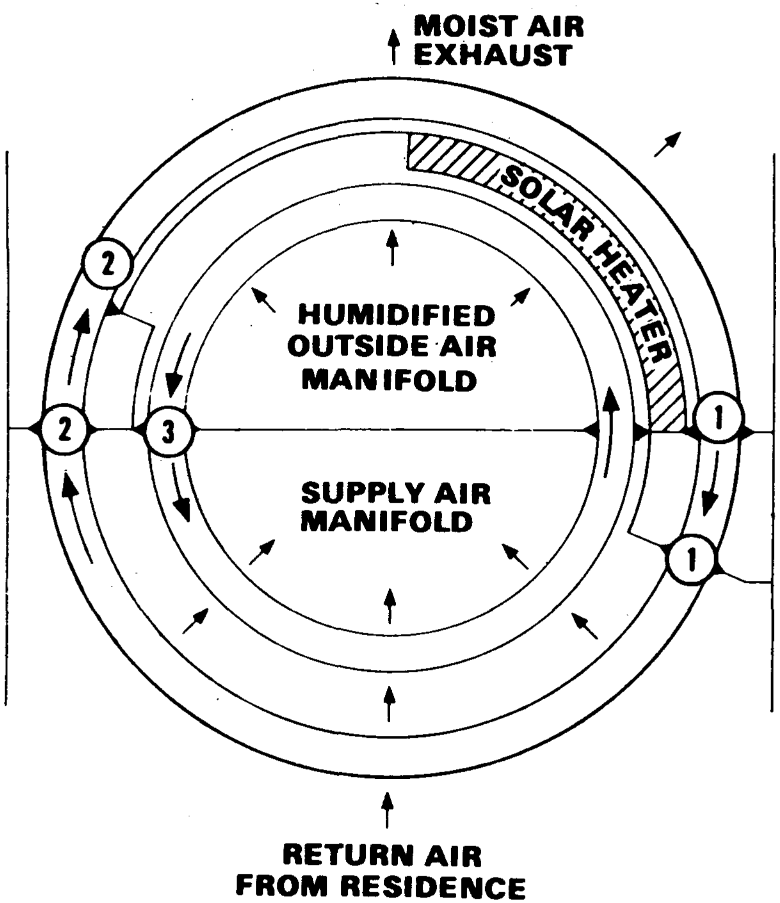

SORBENT BED MODEL

- ACCOUNTS FOR TRANSIENT THERMAL AND MASS TRANSFER PHENOMENA AROUND PERIPHERY AND IN RADIAL DIRECTION
- MASS TRANSFER MODEL INCLUDES MASS TRANSFER THROUGH GAS FILM AND DIFFUSIVITY WITHIN PARTICLE
- CALCULATION TIME INTERVAL DETERMINED BY MAX. LOADING RATE OR TEMPERATURE CHANGE AT ANY POINT (0.5 PERCENT OR 1°F)

DEHUMIDIFIER MODEL

1. ASSUME LOADING AND TEMPERATURE PROFILE
2. CALCULATE ADSORBING BED PERFORMANCE AND AIR CONDITIONS AT BED OUTLET
3. CALCULATE REGENERATOR PERFORMANCE AND AIR CONDITIONS AT OUTLET
4. CALCULATE DESORBING BED PERFORMANCE
5. REPEAT UNTIL STABILIZED CONDITIONS OBTAINED

TASK I-4. SUBSYSTEM COMPUTER MODEL

The design of the desiccant air conditioner involves the optimization of a number of parameters that describe the system. The energy and mass transfer models are quite complex and interdependent, so sophisticated computer techniques are required to make meaningful results available in reasonable amounts of time.

The dehumidifier computer model is based on the AiResearch sorbent model, which has been used successfully in the design of several spacecraft environmental control units. The basic model accounts for transient thermal and mass transfer through the gas film and solid particles. Calculation time intervals are continuously updated by the mass loading and temperature changes that occur between iterations.

The dehumidifier model is constructed by assuming that the desiccant bed is made up of a large number of small sorbent beds.

Initial loading and temperature profiles are assumed, and iterative calculations performed until stabilized operating conditions are obtained.

CANDIDATE REGENERATOR MATRICES

MATERIAL	SPECIFIC SURFACE AREA, FT^2/FT^3	PRESSURE DROP, IN. - H_2O	MATRIX COST, $
GLASS BEADS	280	0.7	1538
CRUSHED RECLAIMED GLASS	280	0.8	38
METAL TURNINGS	500	0.5	333 TO 1149
PLASTIC PELLETS	280	0.7	373 TO 3776
PLASTIC SCREENS	980	0.2	1314 TO 7721
ALUMINUM SCREEN	980	0.2	271
GALVANIZED STEEL SCREEN	980	0.2	293

CANDIDATE REGENERATOR MATRICES

One of the most influential of all decisions in the desiccant subsystem design was the selection of a regenerator matrix material. A regenerator effectiveness of 90 percent is considered necessary for reasonable subsystem performance; this could lead to higher pressure drops than are conventional in heat exchanger design. Also affected by the material are the matrix cost, weight, rotation speed, and containment method.

Some of the most important regenerator parameters are shown in the above table. Pressure drop is the lowest with the screen materials, which also have the highest specific surface area, a factor which influences the mass of material required. Plastics, particularly Teflon, would be ideal in all respects except cost. The long-term corrosion resistance of Teflon ($7721 matrix cost) would be a very expensive advantage, for example.

Galvanized steel screen was selected as a good compromise among the various performance and cost parameters.

BASELINE DESICCANT SUBSYSTEM CHARACTERISTICS

MAJOR SUBSYSTEM DIMENSIONS

DESICCANT BED

GRANULAR SILICA GEL (8 TO 10 MESH)
BED DIAMETER: 46 IN.
BED THICKNESS: 1.15 IN.
WEIGHT: 193 LB
ROTATING SPEED: 5 RPH
WORKING CAPACITY: 3.7 PERCENT

REGENERATOR

DIAMETER: 30 IN.
THICKNESS: 0.85 IN.
MATRIX: STEEL SCREEN
24 BY 24 BY 0.014 IN.
WEIGHT: 290 LB
ROTATING SPEED: 15 RPM
EFFECTIVENESS: 0.90

DESIGN POINT PERFORMANCE

DESIGN CONDITIONS

- CAPACITY: 3 TONS
- CONDITIONED SPACE TEMPERATURES: 78°F db, 67°F wb
- OUTSIDE AIR TEMPERATURES: 95°F db, 75°F wb
- SOLAR THERMAL ENERGY TEMPERATURE LEVEL: 200°F

PERFORMANCE

- CONDITIONED SPACE AIRFLOW: 1550 CFM
- OUTSIDE AIRFLOW: 1850 CFM
- RETURN AIR (TO CONDITIONED SPACE) TEMPERATURES: 62.6°F db, 61°F wb
- SYSTEM COP: 0.52

BASELINE DESICCANT SUBSYSTEM CHARACTERISTICS

The subsystem model has been used to optimize the baseline configuration with respect to desiccant bed cycle time, process air flow rate, regenerator cooling air path, preconditioning air flow and path, regenerator effectiveness, and solar heater size. The optimized COP is 0.52 at design conditions.

The operation of the subsystem computer model is discussed in Appendix I. Parametric design data are also presented that illustrate the influences of variations in the configuration on performance and capacity.

TASK I-5. SUBSYSTEM PERFORMANCE MAP

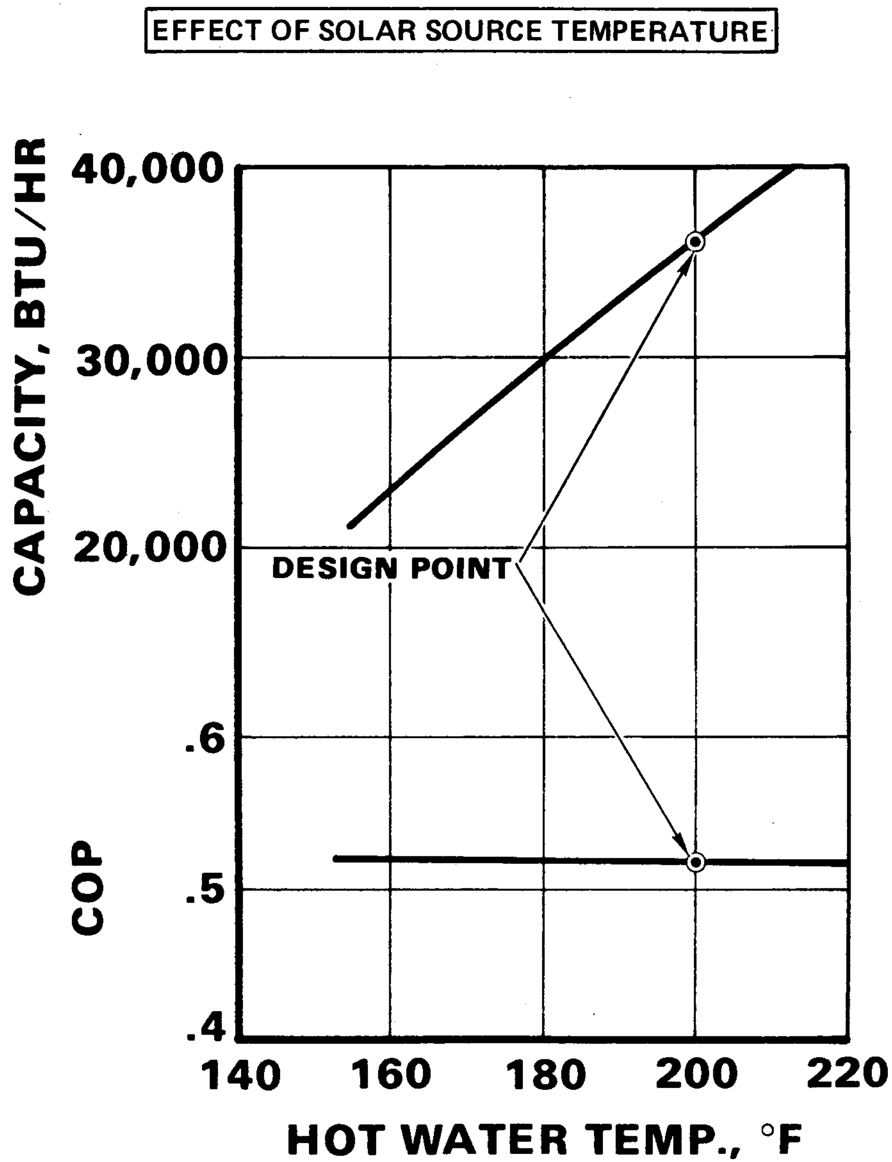

TASK I-5. SUBSYSTEM PERFORMANCE MAP

The subsystem performance computer model has been used to generate off-design performance predictions for the desiccant air conditioning system. Some of the most likely variables to change during operation have been varied over reasonable ranges, keeping all other parameters constant.

Solar source temperature will most likely change during the daily operation cycle, as well as over the yearly cycle. Increased inlet temperature increases the capacity of the cooling system, but the COP remains approximately constant, as shown above.

PERFORMANCE AND CAPACITY VS. OUTSIDE CONDITIONS

– – – – CONDITIONED SPACE AIR RECIRCULATED

——— 100 PERCENT VENTILATED SYSTEM

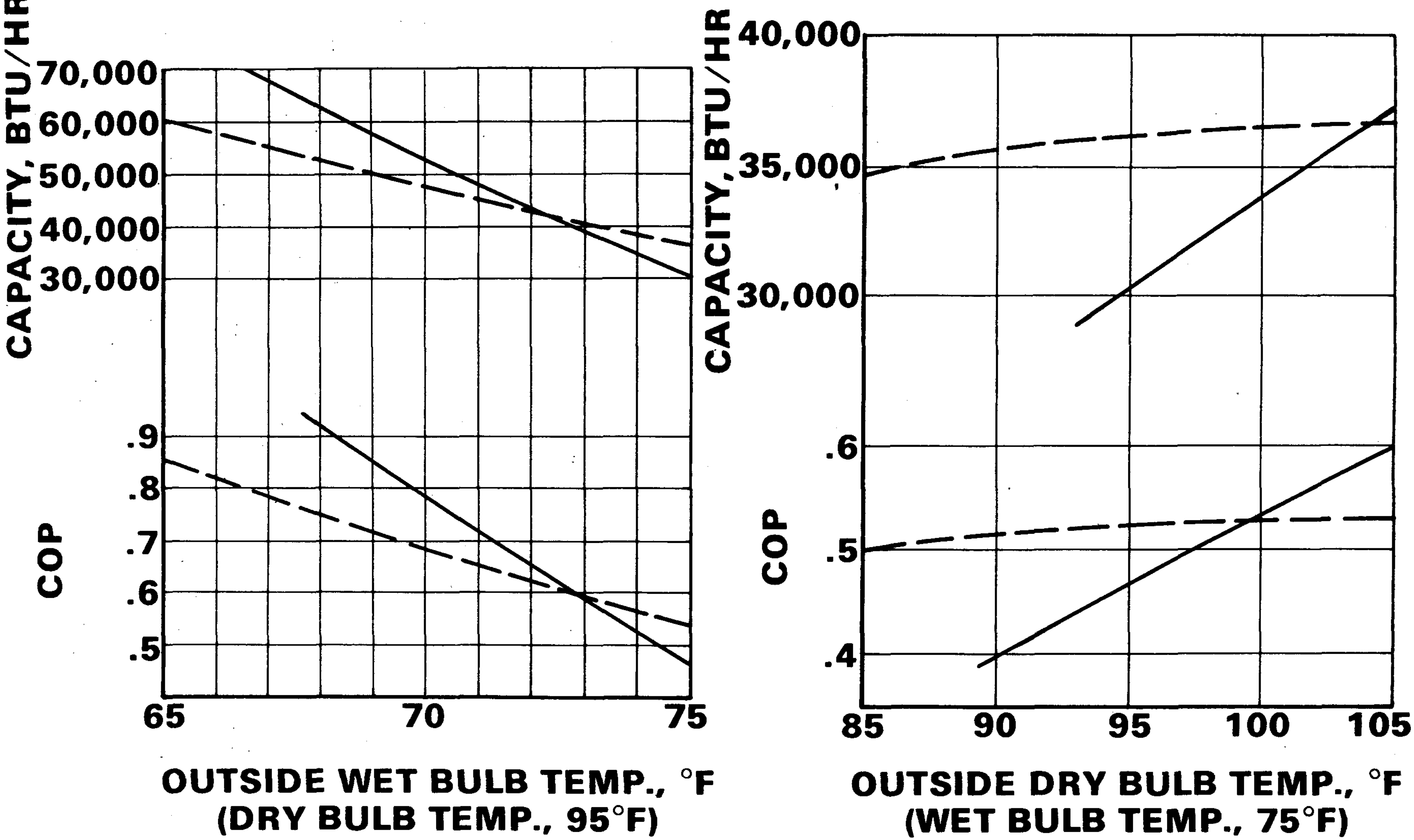

PERFORMANCE AND CAPACITY VS. OUTSIDE CONDITIONS

Outside wet bulb temperature increases will decrease capacity and COP, as shown above. This is due primarily to the influence of the outside air stream on the desorption process.

PERFORMANCE AND CAPACITY VS. INSIDE CONDITIONS

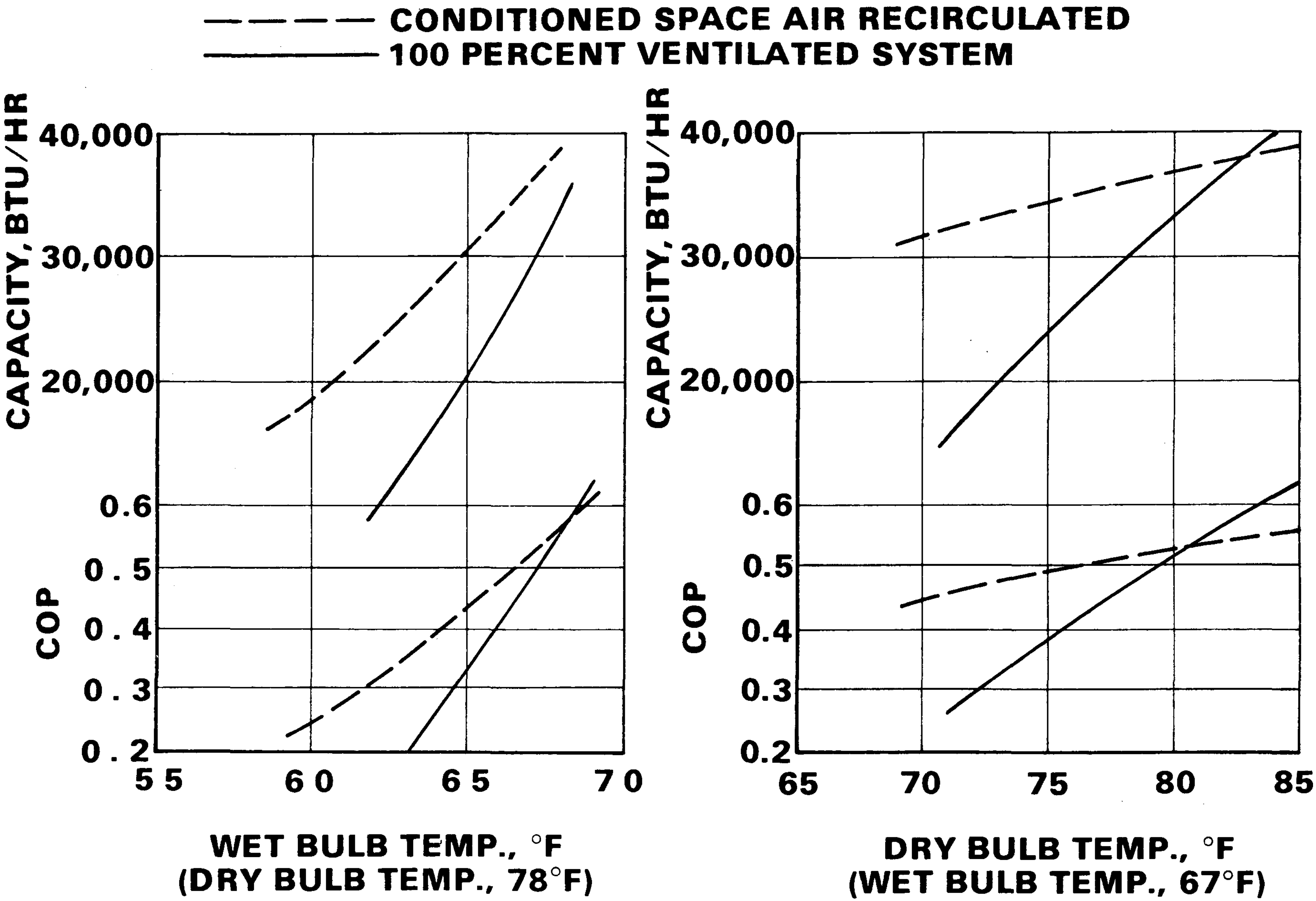

PERFORMANCE AND CAPACITY VS. INSIDE CONDITIONS

Increases in inside wet bulb or dry bulb temperatures will increase capacity and COP as shown in these illustrations.

This type of off-design performance prediction must be used cautiously because a change in only one parameter is likely never to occur in actual operation. For example, an increase in outside wet bulb temperature will most likely be accompanied by an increase in indoor wet bulb temperature due to increased latent loads from infiltration. The net result may be no change in either capacity or COP. This is another reason why performance evaluations cannot properly be made without an integrated system-load-climate model.

The subsystem performance predictions are discussed in detail in Appendix J.

TASK I-10. SUBSYSTEM PRELIMINARY DESIGN

- DESICCANT MATERIAL: 8 TO 10 MESH SILICA GEL
- REGENERATOR MATERIAL: 24 MESH GALVANIZED STEEL SCREEN
- DRUM: ZINC CLAD PERFORATED STEEL PLATE (45 PERCENT OPEN AREA)
- DRUMS SUPPORTED FROM CENTRAL CONCENTRIC SHAFTS
- SEALS: SILICONE RUBBER SLIDING SEAL (BRY-AIR DESIGN)
- DRIVE: MOTOR-GEARBOX-CHAIN-CENTER SHAFT
- SOLAR HEAT EXCHANGER: FINNED TUBE CONSTRUCTION

  CROSS FLOW CONFIGURATION, 8 PASSES

  2 MODULES
- ENCLOSURE: MILD STEEL FRAME
- CONTROL BY MEANS OF VARIABLE SPEED FANS AND DRUMS

TASK I-10. SUBSYSTEM PRELIMINARY DESIGN

The preliminary layout for the desiccant subsystem has been completed, and is included in Appendix K with discussions of alternatives that were investigated.

The silica gel desiccant and steel screen regenerator matrix are enclosed in perforated drums made of zinc-clad steel. The two concentric drums rotate in opposite directions on central shafts. In the prototype unit, two variable-speed gearmotors will drive the two drums.

Stationary partitions in the center of the inner drum, in the annulus between the two drums, and outside the outer drum will form manifolds to direct the air streams. Seals between the drums and the partitions will be flat silicone rubber strips.

The solar heat exchanger will be located in the desorbing air stream in the annulus between the two drums. Standard finned tube construction will be used. In the interest of economy, the heat exchanger will be constructed as two rectangular cores manifolded together.

The enclosure, frame, and ductwork have been designed to be compatible with standard HVAC construction techniques. Dunham-Bush has been consulted concerning design details.

Capacity control will be accomplished by means of variable-speed fans. This will allow parasitic power to be significantly reduced at part-load conditions. In addition, variable-speed desiccant drum drives would provide some increases in COP during part-load operation, but this would require separate desiccant and regenerator drum drive motors, which may be eliminated from production units to minimize complexity.

Technical Progress Report

DEVELOPMENT OF A SOLAR DESICCANT DEHUMIDIFIER

Volume 2: Detailed Technical Information

78-14957-2

March 31, 1978

Prepared by

M.E. Gunderson
K.C. Hwang
S.M. Railing

Approved by

Rousseau

J. Rousseau

Prepared for

Department of Energy
Contract EG-77-C-03-1591

GARRETT

AIRESEARCH MANUFACTURING COMPANY
OF CALIFORNIA

FOREWORD

This volume contains eleven appendixes; in each appendix, part of the work conducted by AiResearch on the solar desiccant dehumidifier project is discussed in detail. With the exception of Appendix A, which documents Task I-0, management, and Appendix K, which documents Task I-10, subsystem preliminary design, the appendixes represent final reports for the particular tasks.

CONTENTS

APPENDIX A

TASK 1-0. MANAGEMENT

INTRODUCTION

AiResearch progress to date on the solar desiccant dehumidifier contract has been close to original plans in terms of expenditure and scheduling. Details of the progress are given below. Also included are accounts of other management activities.

COOLING WORKSHOP

A paper entitled "Preliminary Design of a Solar Desiccant Air Conditioner" was presented at the Third Workshop on the Use of Solar Energy for the Cooling of Buildings, February 15, 16, and 17, 1978, in San Francisco. This paper summarizes the progress of this contract and discusses expected performance. The essence of this paper is given in Appendixes I and J of this report, which document Task 1-4, subsystem computer model, and Task 1-5, subsystem performance map, respectively.

SERI ROUND-TABLE DISCUSSION

AiResearch participated in a round-table discussion of desiccant systems at the SERI facility in Golden, Colorado. The meeting was held on November 16, 1977 and was attended by all current DOE contractors involved in the development of desiccant systems and also by technical personnel from various organizations with interest in this field. Discussions centered on four major topics: materials, modeling, hardware, and system concepts. A brief summary of the discussions and the AiResearch position are presented in Appendix B, as part of the state-of-the-art survey of Task 1-1, review of the literature.

REVIEW MEETING

On February 23, 1978, a meeting was held at AiResearch in Torrance, with representatives from DOE, Brookhaven National Laboratory (BNL), and Planning Research Corporation (PRC) to discuss the status of this contract and the course of future work. The attendees are listed in Table A-1.

TABLE A-1

REVIEW MEETING ATTENDANCE
FEBRUARY 23, 1978 - AIRESEARCH, TORRANCE

AiResearch	U.S. DOE	BNL	PRC
R. A. Fischer M. E. Gunderson K. C. Hwang G. H. McDonald J. Paden J. A. Turnquist J. Rousseau	R. Le Chevalier H. C. Rooks	J. W. Andrews P. C. Auh E. Kush	W. Scholten

Details of the work completed to date were discussed at length. Of particular interest were Task 1-3, candidate cooling subsystems; Task 1-4, subsystem computer model; Task 1-5, subsystem performance map; and Task 1-10, subsystem preliminary design. The coupling of the desiccant system to conventional cooling subsystems received a great deal of attention. It was generally agreed that the most important uses for the desiccant system may be as a dehumidifier in applications where latent loads are high. DOE representatives indicated that standardized residence and climate models would be provided to replace those developed in Task 1-2.

EXPENDITURES AND COMMITMENTS

The total funding level for all three phases of the solar desiccant program is $681,694. The Phase I budget is $112,600 (excluding G&A and fee), to be spent during the first twelve months of the program. Figure A-1 shows projected and actual expenditures for Phase I. In the first two months after the contract effective date, expenditures occurred more slowly than projected; the subsequent four months have shown a slightly higher rate of spending than originally expected. The net result is that the total expenditure is quite close to the projection as of the end of March. It now appears that future expenditures will closely follow the projection.

PROGRAM STATUS

Figure A-2 illustrates the progress of Phase I of the program. Tasks 1-1, 1-2, 1-3, 1-4, and 1-5 are shown as finished, and are documented in this report in other appendixes. The major effort at this time is in Task 1-10, subsystem preliminary design. A layout has been completed for the desiccant subsystem; this progress is documented in Appendix K. Design details are presently being worked out, and it is expected that the preliminary design will be completed by about the first of May.

Work in Task 1-6, system performance model, has temporarily been stopped pending action from DOE concerning climatic and house models. At the February 23 meeting, DOE representatives indicated that the single-family residence and geographic location models developed by AiResearch in Task 1-2 would be replaced by standardized models. The intent of this change is to make the results of analysis by various contractors more uniform. At this time, no information has been received from DOE on the standardized models. Task 1-6 has therefore been postponed. Since Tasks 1-7, 1-8, and 1-9 depend upon the results of Task 1-6, work on these tasks has also been postponed.

Preliminary discussions have been held with representatives of Dunham-Bush concerning Task 1-11, commercialization, and Task 1-12, cost effectiveness studies. Information was obtained for guidance in Task 1-10 to ensure that construction techniques and materials used in the preliminary design would be compatible with standard air conditioning equipment manufacturing practices and installation methods. The bulk of the work in Tasks 1-11 and 1-12 will be conducted later, as scheduled.

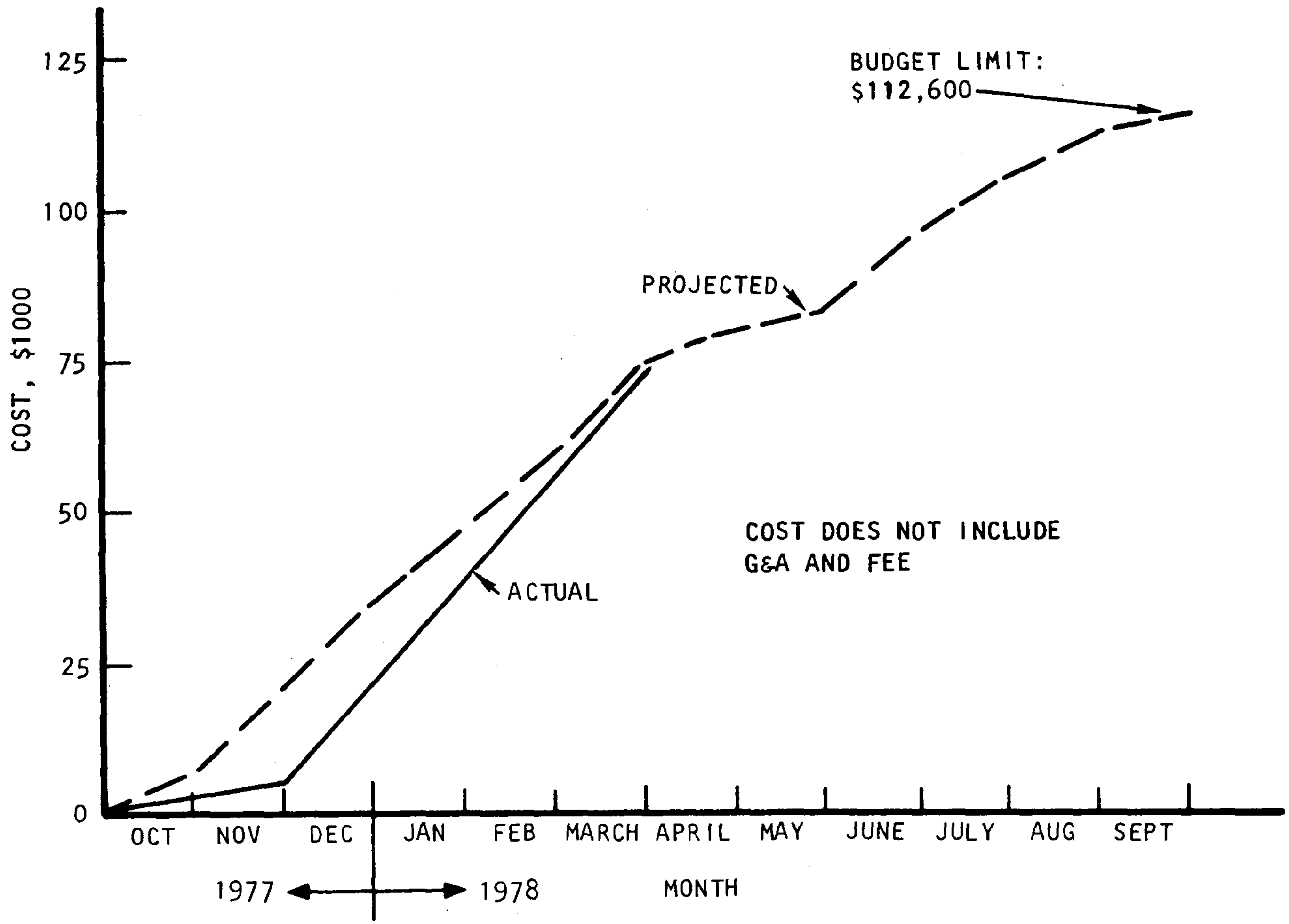

Figure A-1. Phase I Expenditures and Commitments

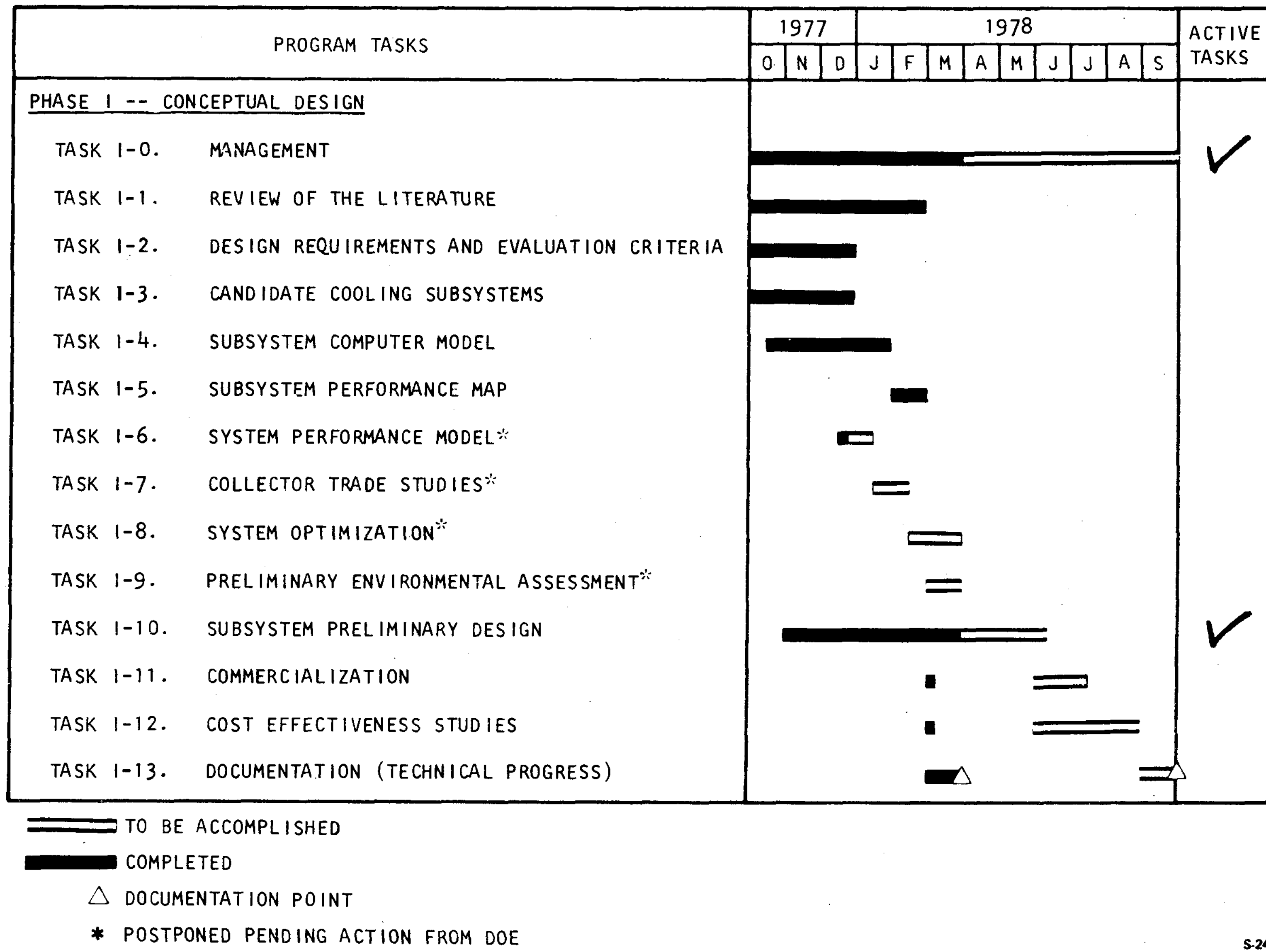

S-24761

Figure A-2. Phase I Program Schedule

Work in Task 1-13, documentation, has lead to the generation of this first technical progress report.

ACCELERATED PROGRAM SCHEDULE

The present contract comprises three phases covering a period of 3 years. Current funding is for the total program. A revised program schedule has been prepared which keeps the scope of the contract unchanged, but completes all tasks within 2 years. This shortened schedule should better serve the purposes of DOE and AiResearch because the results of the program will be available 1 year earlier. This will advance the time at which the final examination of desiccant system viability can be made, and will also shorten the time required to bring the finished product onto the market.

However, the accelerated schedule, submitted to DOE in December, has not been approved. For reference, the original letter proposal from AiResearch to DOE (AiResearch No. CJDM:7450-1222) is reproduced on the following pages. The schedules that were submitted with this letter are presented in Figures A-3 and A-4. In anticipation that approval is forthcoming, work in the active tasks is proceeding at a pace consistent with the new schedule.

SUBCONTRACTING WITH STEPHEN FITCH

Mr. Stephen Fitch, president and chief engineer of Bry-Air, Inc., Sunbury, Ohio, has been made a subcontractor in support of this program. Bry-Air has been marketing desiccant wheels using granular silica gel for a number of years, and it is felt that AiResearch and DOE will profit significantly by transfusion of this technology into the present program.

AiResearch personnel travelled to Sunbury in February 1978 to talk with Mr. Fitch. The primary subjects considered were sealing materials and techniques. Other subjects included drive systems and silica gel expansion and fracturing. In addition, AiResearch was allowed to inspect the Solaron desiccant system, constructed and tested by Bry-Air, and to observe Bry-Air manufacturing operations.

The information gained is expected to save considerable development time. In the future, it is tentatively planned to have Mr. Fitch visit AiResearch, Torrance, California to evaluate the AiResearch preliminary design. This should occur during May.

AIRESEARCH MANUFACTURING COMPANY OF CALIFORNIA
A DIVISION OF THE GARRETT CORPORATION
2525 WEST 190TH STREET • TORRANCE, CALIFORNIA 90509

bcc: R.A. Fischer n/e
J. Rousseau n/e
J. Turnquist w/e
File w/e
Chrono

In Reply Refer To:
CJDM:7450-1222

December 22, 1977

Department of Energy
San Francisco Operations Office
1333 Broadway
Oakland, California 94612

Attention: Contracting Officer

Via: The Garrett Corporation
Los Angeles, California
Attention: Mr. R. Keppler

Subject: Contract No. EG-77-C-03-1591

Enclosure: (1) Figure 1, Revised Program Schedule
(2) Figure 2, Original Program Schedule

Gentlemen:

In the interest of expendiency and program effectiveness it is proposed to accelerate the performance of the desiccant dehumidifier contract without changing the scope or contract value. The revised program schedule is shown in Figure 1; for comparison the original schedule is shown in Figure 2.

The revised program covers a period of two years as compared with the three-year schedule proposed originally. Note that none of the critical path tasks have been changed by more than two weeks, including:

Tasks	I-4	Subsystem computer model
	I-8	Subsystem preliminary design
	II-3	Subsystem detailed design
	III-1	Dehumidifier fabrication
	III-3	Dehumidifier testing
	III-5	Solar System Testing

Some overlap exists between the program phases and also between some of the tasks; however, the overlap shown is normal in programs of this type and no problems are anticipated.

It is believed that with the two-year schedule, program data will be available at a more opportune time with respect to the overall DOE solar cooling effort.

In the event further information is desired regarding this proposal, please contact Mr. R. Keppler, The Garrett Corporation, Los Angeles, or the undersigned.

Very truly yours,

AIRESEARCH MANUFACTURING COMPANY OF CALIFORNIA
A Division of The Garrett Corporation

John D. McPherson

John D. McPherson, Contracts
Environmental and Energy Systems

JDM:rjd

Enclosure (Figure 1 & 2)

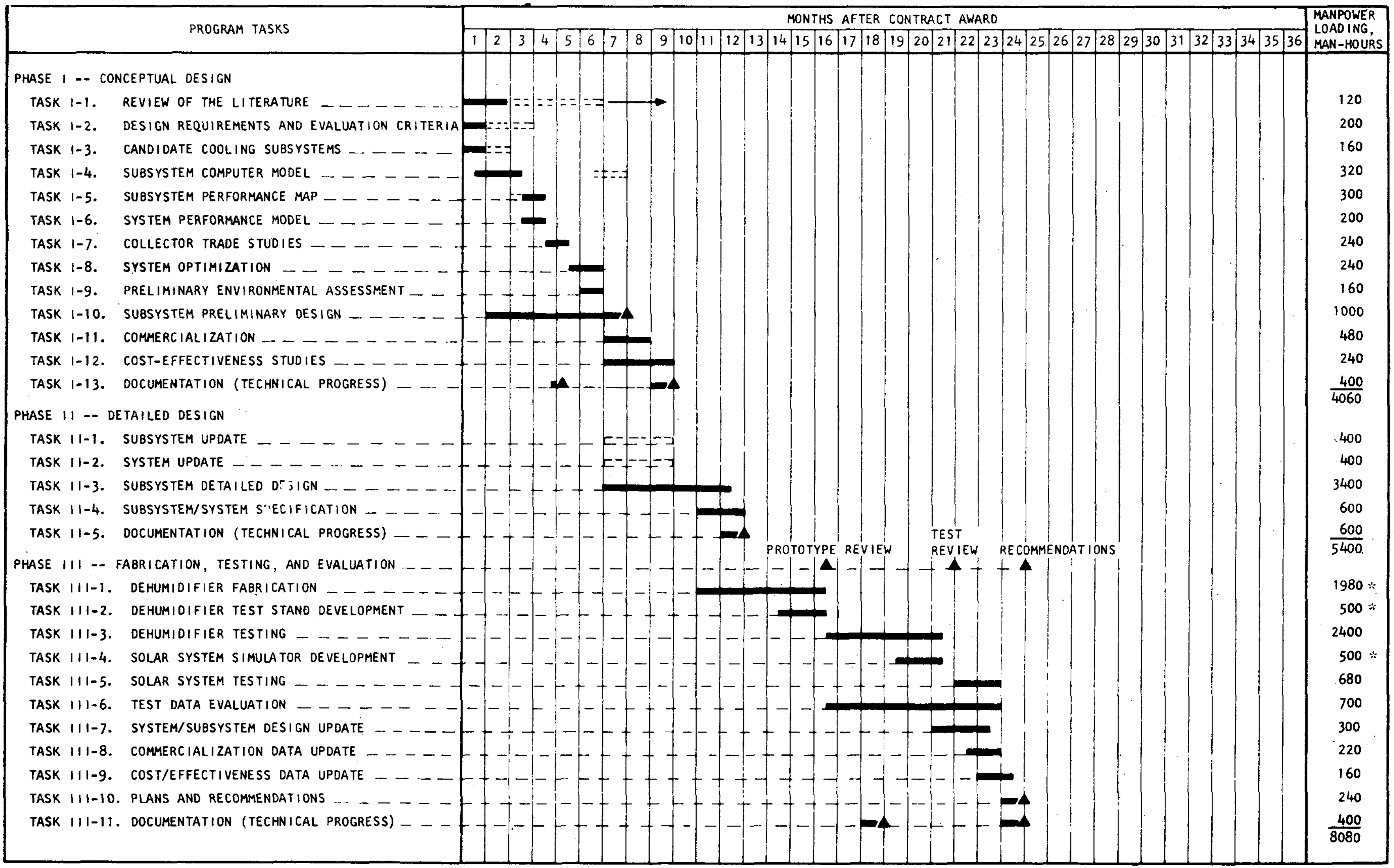

*DOES NOT INCLUDE HARDWARE

S-15997-A

Figure A-3. Proposed 2-year Program Schedule (Figure 1 from CJDM: 7450-1222)

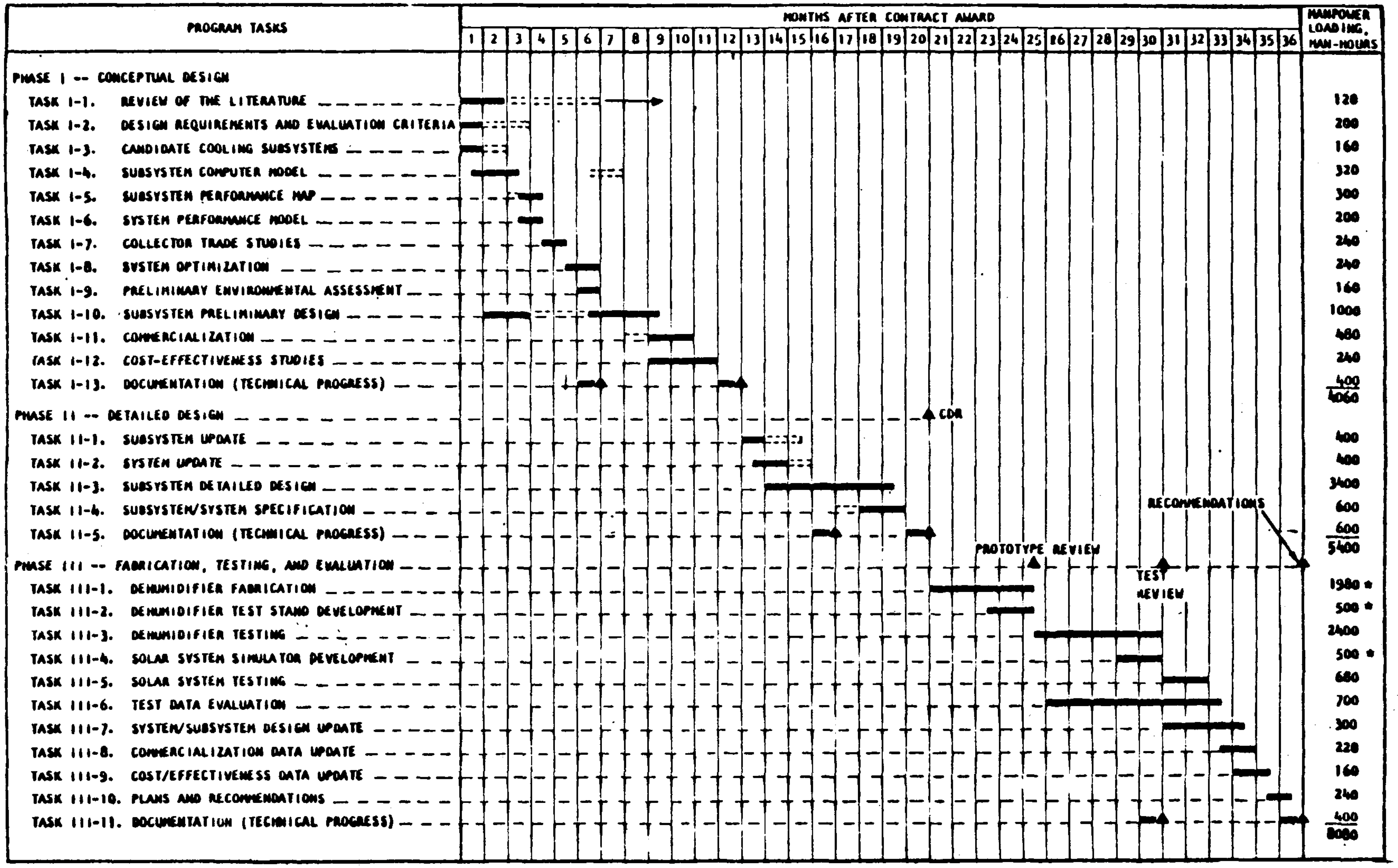

*DOES NOT INCLUDE HARDWARE

Figure A-4. Original 3-year Program Schedule (Figure 2 from CJDM: 7450-1222)

APPENDIX B

TASK I-1. REVIEW OF THE LITERATURE: STATE-OF-THE-ART SURVEY AND SERI MEETING HIGHLIGHTS

INTRODUCTION

The four major contributors to the state-of-the-art in solar desiccant cooling systems are documented in this appendix. A list of the references cited is included at the end of this appendix. Uncited references are listed in the bibliography. The major contributors are:

- Institute of Gas Technology (IGT)
- Center for the Environment and Man (CEM)
- Division of Mechanical Engineering, Commonwealth Scientific and Industrial Research Organization (CSIRO)
- Solaron

A comprehensive state-of-the-art review was conducted at the SERI facility in Golden, Colorado in November 1977. This meeting is also documented in this appendix.

IGT SYSTEM

The solar desiccant cooling system constructed by the Institute of Gas Technology is intended to function primarily as a gas-fired air conditioning system. It was required to be competitive on both energy consumption and economic bases with conventional gas furnace-vapor compression heating and air conditioning systems. Reviewing the development of the system in the literature, the role of solar energy input appears to have changed in intent from a supplemental energy supply to partially effect the gas demand to the primary energy input, with gas being the supplemental input. In fact, the original Munters environmental control (MEC) unit was designed to operate on gas alone. Had this not been the case, some changes may have been made to the unit, particularly the choice of desiccant. In its present configuration, demonstration systems installed by IGT consist of a MEC unit; Owens-Illinois evacuated glass tube collectors; two 500-gallon hot water storage tanks; and the associated plumbing, instrumentation, and controls.

The system is designed to operate in both 100-percent fresh air makeup and recirculating modes. In the fresh air mode, outside air is dehumidified by the desiccant wheel, cooled by the heat exchanger wheel, humidified, and then supplied to the cooled space. Return air from the cooled space is humidified, and then heated by the heat exchanger wheel, the solar heat transfer coils, and, as needed, by the gas burner. The hot return air is used to regenerate the desiccant wheel, and is exhausted to the atmosphere. The recirculation mode is shown in Figure B-1 (taken from Reference B-1). Return air is dehumidified by the desiccant wheel, cooled by the heat exchanger, humidified, and then supplied to the conditioned space. Outside air is humidified and then heated by the heat exchanger wheel, the solar heat transfer coils, and, as needed,

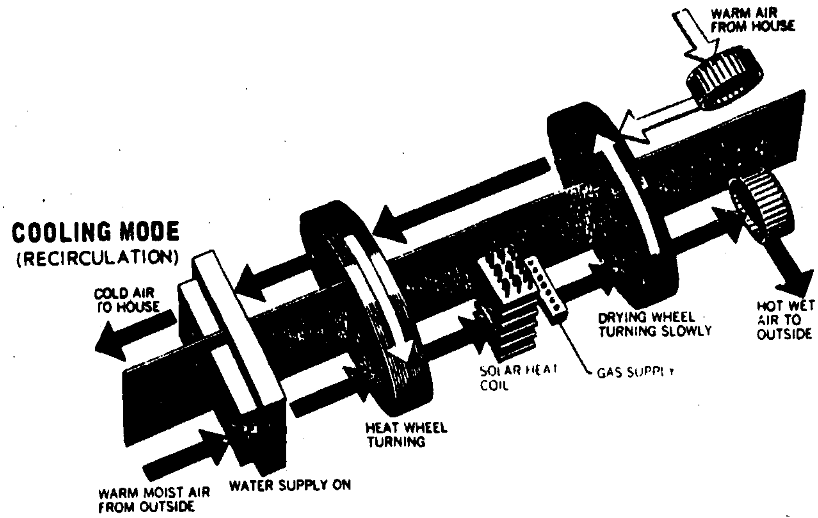

Figure B-1. IGT System Flow Schematic (Taken from Reference B-1)

by the gas burner. The hot outside air is used to regenerate the desiccant wheel and is exhausted back to the atmosphere. Apparently, the installed units have been operated for the most part in the recirculation mode. Figure B-2 (taken from Reference B-1) shows the MEC equipment package. The desiccant wheel is made of 1-mil-thick asbestos substrate impregnated with about 50 percent molecular sieve material. The substrate is corrugated and rolled around the hub of the wheel to form a large number of axial flow passages. The choice of molecular sieve as the desiccant material is most likely a result of the original intent for the unit to be entirely gas-fired. To drive off significant amounts of water requires temperatures in excess of 200°F, which approaches the practical limit of flat-plate solar collector performance. The Owens-Illinois evacuated tube collectors are capable of somewhat higher output temperatures (230°F) at reasonable collection efficiencies than are average flat-plate collectors, but the cost is somewhat higher, and therefore the MEC unit cannot be considered to be a feasible solar unit.

The use of asbestos as the substrate may pose some health problems because all of the air supplied to the conditioned space passes over the desiccant wheel. The IGT authors anticipated questions about this problem, and mention in one of their papers that less asbestos fibre will probably be introduced to the air stream than would be found in the air along a California freeway from automobile brake linings. No data are provided to substantiate this claim, and it does not seem clear that this would establish that the asbestos substrate does not pose a potential hazard. In view of the problems that have recently arisen with seemingly innocent applications of asbestos, it would be advisable to use some other substrate material.

The IGT system has been under study since 1967, and was in operation by 1974. Comprehensive operating data are not available at the present time; it is anticipated that a final report will be released by IGT, but there is no date set at this time. A COP of 0.73 is indicated as being typical of operation in the recirculation mode, and about a possible 10-percent improvement is suggested by reducing seal leakage, for a resultant COP of 0.8. This performance is obtained with all the regeneration energy supplied by the gas burners.

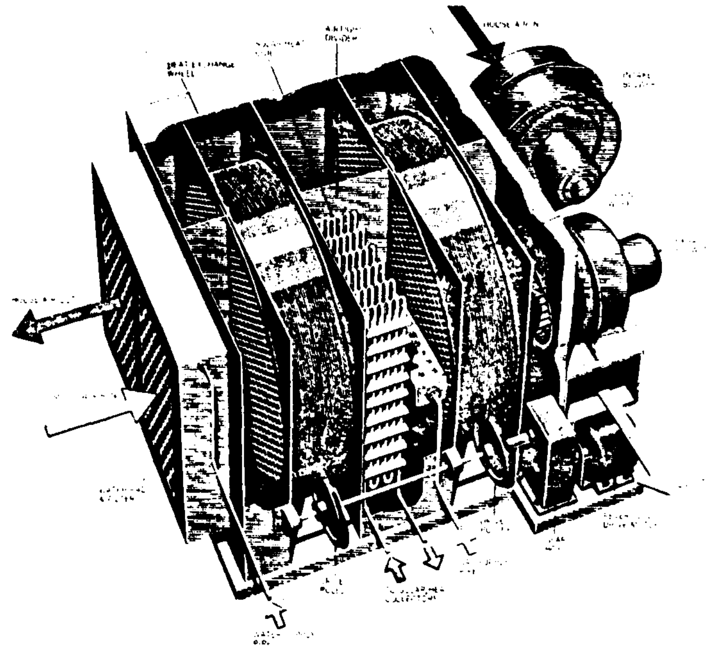

Figure B-2. MEC/IGT System Equipment Package (Taken from Reference B-2)

CEM SYSTEM

The desiccant system proposed by the Center for the Environment and Man (CEM) is intended to function as a solar-powered system. For this reason, it differs significantly from the IGT system in ways that are intended to yield adequate performance with lower desorbing temperatures, at the expense of some additional complication.

Figure B-3 (taken from Reference B-2) shows the operation of the CEM system. Room air is drawn into the unit, where it is heated by the hot side of a regenerative heat exchanger. The air then passes through four rotary desiccant beds, each one being followed by a heat exchanger that cools the stream to nearly the original temperature. The room air then passes over the cold side of the regenerative heat exchanger, is humidified, and is returned to the conditioned space. On the other side of the desiccant beds, outside air is heated by solar energy input by heat exchangers located upstream of each desiccant bed. The desorbing air is then exhausted back to the atmosphere.

The use of multiple desiccant wheels is an attempt to approach the thermodynamically ideal adsorption process, which would be an isothermal one. This would involve an infinite number of desiccant beds and intercoolers; each bed would be of vanishingly small thickness and each intercooler would return the air to its initial temperature. This is desirable because the loading capacity of desiccant materials decreases as the drybulb temperature of the airstream increases. A practical number of desiccant stages and cooling must be chosen, which is, of course, much less than infinite. Four 2-in.-thick desiccant wheels were chosen by CEM.

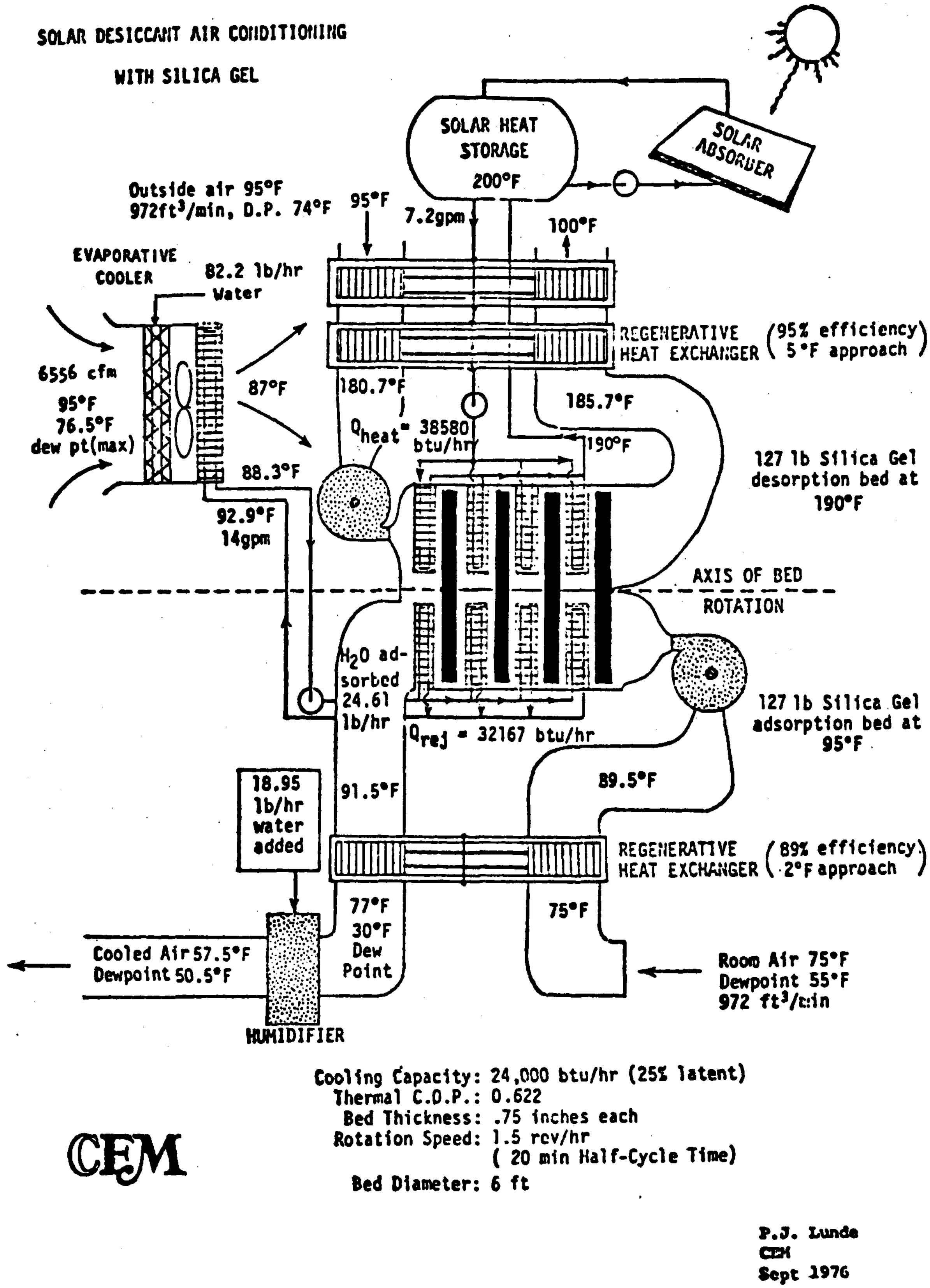

Figure B-3. CEM System (Taken from Reference B-2)

A considerable problem exists with the concept of multiple desiccant wheels. The sliding seals (both circumferential and radial) have apparently not been perfected in the CEM unit, and seal leakage accounts for a large portion of system losses. Seal wear also has not been reduced to acceptable limits, and wear increases leakage and maintenance problems. Of course, multiple wheels compound these problems because the number of seals is increased.

Silica gel was chosen as the adsorbent material primarily because it desorbs readily at temperatures between 150° and 200°F, which is within the performance range of most flat-plate collectors.

A one-quarter-scale system has been constructed by CEM. No performance data or any indication of the capacity of this system have appeared in the literature, although it has been stated that considerable problems with seals have yet to be solved. A larger system is to be constructed by CEM, but again no capacity has been indicated. At this time development work on the CEM unit has been stopped primarily because of the problems mentioned above.

In the CEM literature, it is shown that the performance of other air conditioning equipment (absorption systems, in particular) improves significantly if the air is dehumidified by some other means, thereby allowing the evaporator temperature of the chiller to be increased. The performance of solar-powered absorption chillers can be improved by using an adsorption dehumidifier in conjunction with a chiller.

CSIRO SYSTEM

The desiccant solar air conditioning system investigated by R.V. Dunkle and others at the Division of Mechanical Engineering, Commonwealth Scientific and Industrial Research Organization (CSIRO), Highett, Victoria, Australia, has received considerable attention. Rotary regenerators, packed column humidifiers, solar collectors, energy storage methods, and desiccant dehumidifiers have all been investigated analytically and experimentally over a period of more than 25 years, and have been reported in the literature since 1964. Mr. Dunkle appears to have stopped his investigation of a desiccant system (just short of actually building one) in favor of simpler evaporative coolers, which can be widely used in Australia.

Mr. Dunkle's proposed desiccant system is similar to both the IGT and CEM systems in that the room air is returned after being dehumidified, cooled by a regenerator, and then evaporatively cooled. The system is shown schematically and on a psychrometric chart in Figure B-4 (taken from Reference B-3). A description of the system, taken from Reference B-3, is as follows.

The operation of the system is described for specific conditions typical of a severe day in Darwin when outside conditions are 95°F dry bulb and 82°F wet bulb, while inside conditions are maintained at 77°F and 65 percent relative humidity (68.5° wet bulb temperature). A continuous supply of 200 cfm of outside air for ventilation is assumed, corresponding to a heat load of 12,000 Btu/hr on the system. The peak building load, other than fresh air, is taken to be 18,000 Btu/hr, while the mean building load is 10,000 Btu/hr over a 24-hr period.

CSIRO

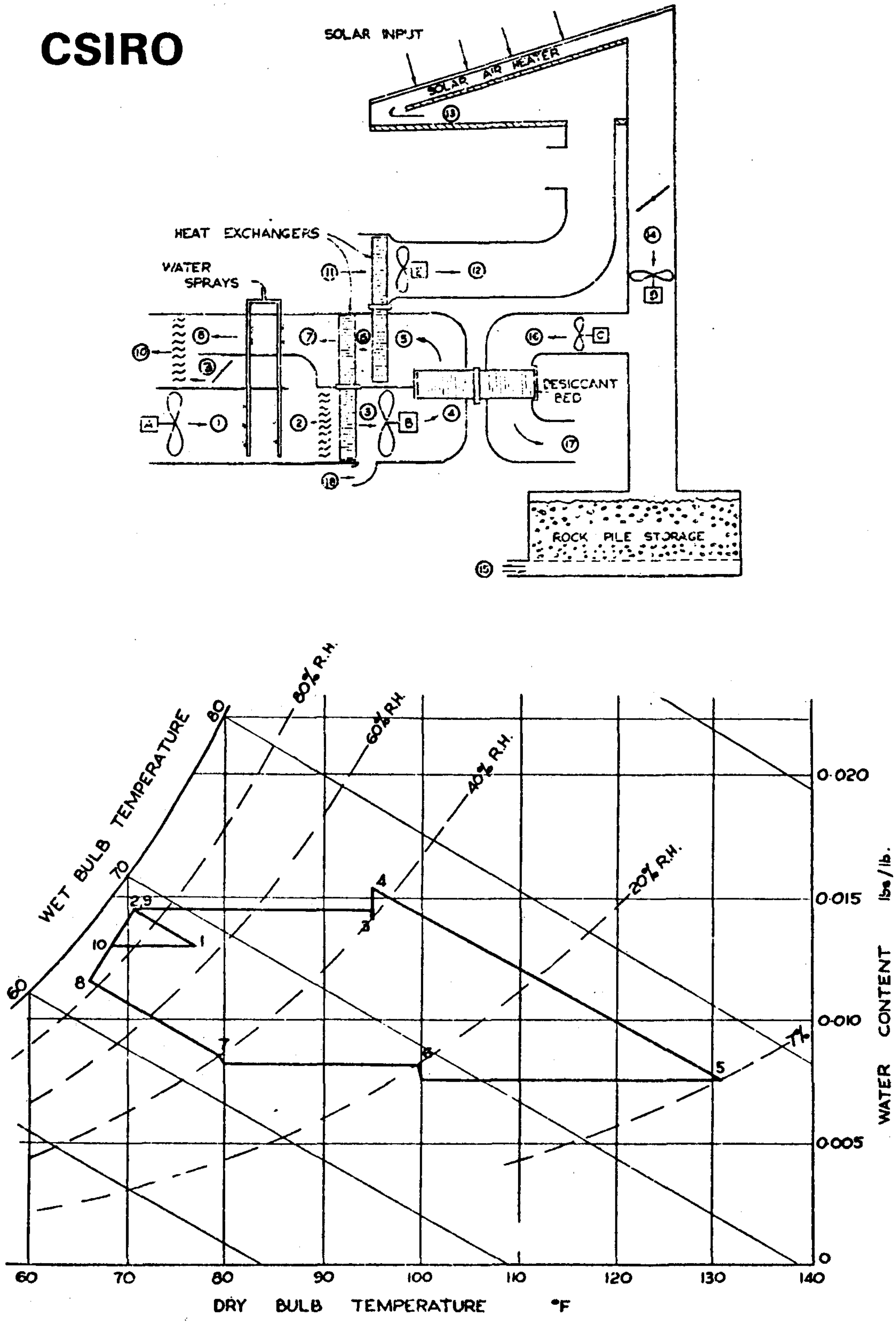

Figure B-4. CSIRO System (Taken from Reference B-3)

Air is drawn from the room at a rate of 1800 cfm and delivered to the first evaporative cooler, which is assumed to have a humidifying effectiveness of 80 percent. The air leaves this cooler at 70.5°F and 90 percent relative humidity. Part of this air stream, 1000 cfm, is diverted to point 9 via a bypass duct controlled by a damper. This bypass air stream then mixes with the cool air at state 8 returning from the dehumidification loop. The resultant mixture at 68.3°F, statepoint 10, is delivered to the room. The temperature rise of air through the room is 8.7°F under these conditions.

In this cycle, no latent heat was included in the room load. If a latent heat load occurs in the building, statepoint 10 must be slightly lowered to maintain the desired conditions, which is accomplished by reducing the bypass ratio by means of the control damper. The recirculation and mixing feature of the bypass system results in a larger enthalpy and humidity rise of the conditioned air when passing through the building, and reduces the quantity of air circulated through dehumidification loop. Consequently, the size and power consumption of the equipment is reduced. The bypass feature enables humidity control to be achieved; the larger the bypass ratio, the higher the resultant humidity in the building and the smaller the quantity of air which must be circulated through the dehumidification system. One of the major advantages of the bypass system is that the effectiveness of the evaporative coolers, or air washers, has little effect on the overall system performance; the only significant effect is a change in the bypass air ratio to maintain the desired conditions. For example, if the two evaporative coolers are reduced from 80 to 60 percent humidifying effectiveness, an increase in the bypass air rate from 1000 to 1800 cfm will maintain the building at the original condition. The evaporative cooler in the return air from the dehumidification system could be eliminated completely by further increasing the bypass ratio; however, this results in undesirably high air circulation rates.

The remainder of the air leaving the evaporative cooler passes through the spray eliminator and enters the first regenerative heat exchanger at state 2. This 800-cfm air stream flows through this heat exchanger counter to the air stream returning from the humidifier and is heated to roughly ambient temperature, 95°F. The effectiveness of each of the rotary heat generators in this cycle is assumed to be 80 percent with equal air rates through both sides, a conservative figure on the basis of experimental units tested in the laboratory. The exchanger is assumed to have leakage and carry-over equal to 5 percent of the airflow per side; as a result, the water content of the air decreases slightly between points 2 and 3. Fresh outside air, amounting to 200 cfm, is drawn into the system at the suction of fan B, mixed with the air at state 3, and delivered by fan B to the desiccant bed at state 4.

The air passes through the desiccant bed and in the process is dehumidified and heated, leaving at state 5 at 130° to 135°F. This hot dry air then passes through the second heat exchanger, counter to an outside air stream, and is cooled to state 6, which is about 5°F above ambient. The water content is raised somewhat in this process due to carry-over of outside air. This cooling process actually constitutes the heat rejection stage of the reversed thermodynamic cycle.

The warm dry air at state 6 leaving this exchanger passes back through the first heat exchanger, where it is cooled to about 80°F, the water content rising slightly to state 7. The air stream then passes through the second evaporative cooler, also of 80 percent humidifying effectiveness, and is cooled to state 8, about 65°F. This cool air is mixed with the bypass air at state 9 to form the mixture at state 10, which is delivered to the building.

The CSIRO system proposed is designed for use with silica gel as the adsorbent. Due to a lack of data on silica gel performance at the time, CSIRO undertook the development of an absorbent model. This has been documented in References B-4 through B-7. Because of the level of detail required to develop this model, it is not discussed in this report.

SOLARON SYSTEM

Very little documentation is available on the Solaron desiccant system. The heart of the unit is a two-wheel dehumidifier constructed by Bry-Air, Inc. of Sunbury, Ohio. Bry-Air has been marketing industrial dehumidifiers for many years, and the Solaron unit is a modified production unit.

The Solaron desiccant wheel consists of two horizontal disks, made of perforated metal, filled with silica gel. The disks rotate about a vertical axis. Conditioned airflow passes through one semicircular portion of each disk, and regeneration air passes through the other semicircle. The two counterflow disks are connected in parallel in the development unit; it is assumed that an appropriate number of disks could be paralleled to obtain a desired capacity.

Figure B-5, taken from Reference B-8, shows the Solaron system layout. In this figure, the desiccant wheels are shown as one unit instead of multiple parallel units. An air collector/rock bed storage system is shown, with an auxiliary heater to supplement the solar input when insolation and storage are low.

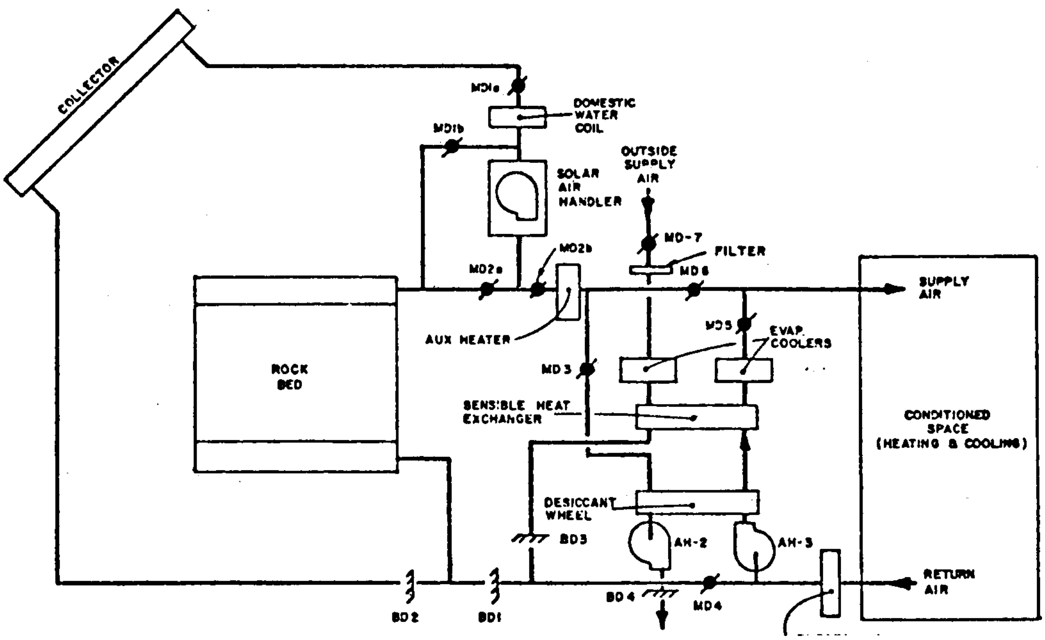

Figure B-5. Solaron Desiccant System (From Reference B-8)

SERI MEETING HIGHLIGHTS

A meeting was held on November 16, 1977 at the SERI facility in Golden, Colorado for the purpose of reviewing in detail the state-of-the-art of desiccant systems. The meeting was in the form of a round-table discussion with five DOE contractors in attendance. In addition, technical personnel from various organizations interested in desiccant systems participated in the discussions. The discussions were broken into four major subjects: (1) materials, (2) modeling, (3) hardware, and (4) system concepts. Highlights of the discussions are summarized below and the AiResearch position is presented.

Materials

The materials discussions were concerned mainly with the relative merits of natural and artificial zeolites and silica gel, including the equilibrium and dynamic properties of these materials. Lithium chloride as a desiccant material for an air conditioner operating in an on-off fashion through the years is unacceptable because of its deliquescent properties. It is unlikely that alternate basic materials will be developed in the near future. The following pertinent comments were noted regarding molecular sieves and silica gel.

(a) In terms of performance in the conditions prevalent in a desiccant air conditioner, there is not much difference between molecular sieves and silica gel. This statement from D. I. Tchernev of MIT is supported by AiResearch preliminary analysis.

(b) Molecular sieves may be more stable than silica gel; however, in certain environments molecular sieve may be poisoned due to atmospheric contaminants (smog).

(c) Silica gel is subject to physical breakdown due to thermal shock if liquid entrained water is present. This is not a problem in the type of systems considered.

(d) Silica gel life under cycling condition may be limiting. Bry-Air has had silica gel wheels in the field for 6 years operating at 4 cycles per hour. Considering the duty cycle of a desiccant air conditioner, it is expected that silica gel would last for 25 to 30 years.

(e) Molecular sieves could be developed with better properties for the duty cycle considered here. This would involve a material development program.

(f) Silica gel on a Teflon membrane is currently under development at ITT.

(g) Minimg and processing of natural zeolites was abandoned by the chemical industry in favor of artificial zeolites for economic reasons.

(h) Silica gel or molecular sieve on an asbestos substrate may present a health hazard.

(i) Equilibrium and dynamic data. Many participants deplored the lack of basic data, particularly dynamic data. With respect to materials, AiResearch has conducted extensive testing of molecular sieves and silica gel and has developed equilibrium and mass transfer data to be used in conjunction with a sophisticated computer model. These data have been checked out experimentally in the design of full-sized beds for various applications. A description of the computer model is contained in NASA CR-112098 ("A Transient Performance Method for CO_2 Removal with Regenerable Adsorbents," Hwang, K.C., October, 1972). The experimental data are presented in NASA CR-2277 ("Development of Design Information for Molecular-Sieve Type Regenerative CO_2-Removal Systems," R.M. Wright et. al., July 1973). Both reports were furnished to Mr. Ben Shelpuk of SERI.

The data available on both silica gel and molecular sieve are deemed adequate for the accurate modeling of the desiccant system. AiResearch does not feel that additional data are required for the design of the system. Although these sophisticated design tools are available, in the design of any sorbent bed (especially in the sizes considered here), other factors such as flow distribution across the face of the bed, seal leakage, and heat losses often will overshadow the results of the sorbent bed analysis. Only through testing of the complete subsystem can the particular bed be fully characterized.

With respect to materials, the AiResearch approach is as follows. Silica gel performance was compared to molecular sieve and found to be similar using average values for air temperatures at the face of the desorbing bed. Since the price of silica gel is about one-half that of the molecular sieve, silica gel was selected as the baseline. Also, when the subsystem computer program is fully checked out, the relative merits of silica gel and the molecular sieve will be evaluated again prior to final selection.

Modeling

Two aspects of modeling were discussed: sorbent bed modeling and system modeling. These are discussed below.

1. Sorbent Bed Modeling

Some of the participants were satisfied with the accuracy of these models and some were not, primarily because of the apparent lack of basic sorbent data. Modeling of the desiccant bed has been discussed above. Computer codes are available at AiResearch for this purpose. Currently, the sorbent bed model is used as the basis for the development of a subsystem model, including the rotary regenerator and the solar heater. The model will predict transient performance of discrete portions of the sorbent and regenerators around the axis of rotation. This subsystem model will be used for:

(a) Comparative evaluation of silica gel and molecular sieve

(b) Subsystem configuration studies, including airflow patterns, cooling air and heating airflows, and adsorbing and desorbing airflows.

(c) Sorbent bed and regenerator optimization in terms of weight and rotational speed.

(d) Performance characterization of the subsystem in terms of desorption temperature and residence and ambient air wet and dry bulb temperatures.

2. System Modeling

TRANSYST appears to be the accepted standard. An overall solar system model is available at AiResearch to predict the performance of the system on an hourly basis through the year. This model is similar in function to TRANSYST and was compared to TRANSYST by ERDA consultants under Contract NAS8-32091; the answers from both programs were found to be very similar. AiResearch will use its own basic program for overall system modeling.

With respect to building models, a simple model has been developed to model sensible and latent load on a typical 1700 sq ft residence. Unless directed otherwise, this model will be used. Should a standard residence model be made available, it will be incorporated in the overall AiResearch program.

Three locations have been selected for system performance evaluation; New York, NY; Lake Charles, La.; and Phoenix, Arizona. Design year weather data are available for these three locations from Contract NAS8-32091.

Hardware

Hardware problems discussed included in the following:

(a) High regenerator effectiveness is essential for reasonable system performance.

(b) Rotary regenerators are the obvious choice for high efficiency.

(c) Hygroscopic properties of the regenerator material are extremely important.

(d) Low pressure drop design is a must to minimize parasitic power.

(e) High efficiency motors, pumps, and blowers are essential to minimize auxiliary power. This kind of equipment may not be available commercially in the sizes of interest for a 3-ton system.

AiResearch recognizes these problems and careful attention will be given to them, particularly in designing for low pressure drop and low auxiliary power requirements.

System Concepts

The more pertinent system topics discussed included:

(a) Comfort criteria should be used for desiccant system control with possible operation at higher dry bulb and lower wet bulb temperatures than the ARI standards (78°F DB and 67°F WB).

(b) Control schemes are not well understood and hardware for control implementation may not be well understood. The best overall control scheme may involve flow control through the desiccant system, desiccant wheel speed control to match desorbing stream temperature, control on residence wet bulb rather than dry bulb, or other approaches to be identified.

(c) Parasitic power should be accounted for in overall evaluation.

(d) Auxiliary power for operation when solar thermal energy is not available must be minimized because of low basic COP.

(e) Optimum use of a desiccant system may be as a dehumidifier in conjunction with a Rankine or absorption air conditioner operated at higher evaporator temperature.

(f) Realistic evaluation must be done on a seasonal basis rather than design point performance.

(g) Evaluation of a cooling system must include heating requirements so as to apportion the cost of collectors and storage subsystems to the heating and cooling loads. In most areas of the country, the collector will be sized by heating requirements.

(h) Commercialization studies must be performed early to determine the eventual applicability of this type of system.

REFERENCES

B-1. Rush, William F., Adsorption Phenomena as Applied to Solar Cooling, Proceedings of the Second Workshop on the use of Solar Energy for the Cooling of Buildings, August 4 to 6, 1975.

B-2. Lunde, Peter J., Solar Desiccant Air Conditioning, Center for the Environment and Man, Inc., August 1977.

B-3. Dunkle, R.V., "A method of Solar Air Conditioning," Mechanical and Chemical Engineering Transactions of the Institution of Engineers, Australia, Vol. MC 1, No. 1, 1965.

B-4. Dunkle, R. V. and D. J. Close, "Use of Adsorbent Beds for Energy Storage in Drying or Heating Systems," Solar Energy, Vol. 19, 1977.

B-5. Close, D. J. and T. L. Pryor, "The Behavior of Absorbent Energy Storage Beds," Solar Energy, Vol. 18, 1976.

B-6. Johnston, R. C. R., "Regenerative Evaporative Air Conditioning with Dehumidification," Australian Refrigeration, Air Conditioning, and Heating, Vol. 21, No. 2, 1967.

B-7. Close, D. J. and R. V. Dunkle, Energy Storage Using Desiccant Beds.

B-8. Desiccant Systems Analysis, notes of Solaron Corporation accompanying presentation at SERI Meeting, November 1977, Golden, Colorado.

BIBLIOGRAPHY

Close, D. J., and R. V., Dunkle, Open Cycle Solar Energy Cooling Systems, Proceedings of the Annual Engineering Conference of the Institution of Engineers, Australia, May 1976.

Wellesley-Miller, Sean, A. Retrofittable Solar Dehumidifier, Proceedings of the Second Workshop on the use of Solar Energy for the Cooling of Buildings, August 4 to 6, 1975.

Kelsey, Patricia A.,"Solar Cooling-Heating Attainable with Liquid Desiccant A/C System," Air Conditioning, Heating, and Refrigeration News, September 26, 1977.

Tchernev, D. I., Solar Energy Application of Natural Zeolites, Proceedings of the Second Workshop on the Use of Solar Energy for the Cooling of Buildings, August 4 to 6, 1976.

APPENDIX C

TASK I-1. REVIEW OF THE LITERATURE: ADSORBENT SURVEY

INTRODUCTION

AiResearch investigation of the various sorbents available for use in the solar desiccant dehumidifer is documented in this appendix. Although dozens of natural and synthetic sorbents are available that could conceivably be used, only silica gel and molecular sieve are serious contenders. Activated alumina and lithium chloride also have been researched, but they have been found to be noncompetitive. The results of this investigation are discussed in terms of the physical structure and adsorption phenomena, particle size considerations, hardness, and cost. References are listed at the end of the appendix.

PHYSICAL STRUCTURE AND ADSORPTION PHENOMENA

The adsorption phenomena of water onto a desiccant can be explained by fairly simple structural models. Some inequities arise which do not fit the general pattern, but the most important parameters to this project can be approximated with reasonable accuracy. These include equilibrium capacity, diffusion rate constants, and molecular selectivity. For a detailed discussion, see References C-1 through C-3. In summary, silica gel and molecular sieve can be expected to have approximately equal performance parameters, except that silica gel will have a larger equilibrium capacity. The molecular selectivity that can be adjusted with molecular sieve presents no advantage in this application. Alumina and lithium chloride have inferior performance.

Silica Gel

Silica gel is a porous, granular, amorphous form of silica synthesized from the chemical reaction between sulfuric acid and sodium silicate. The internal structure of silica gel is composed of a vast network of interconnected pores that attract and hold water, alcohols, hydrocarbons, and other molecules by the process of physical adsorption and capillary condensation. Silica gel adsorption characteristics result from its huge surface area due to the highly porous nature of the particle. Standard grades of silica gel exhibit an internal surface area of approximately 800 sq m/gm. All of this area is available for the removal of adsorbates.

Because of this very large surface area, silica gel has a very large equilibrium capacity. The equilibrium water capacity of silica gel and other desiccants is shown in Figure C-1 as a function of relative humidity. Whenever the relative humidity of the adsorbate stream is greater than about 35 percent, silica gel capacity exceeds the capacity of the other desiccants. Figure C-1 presents capacity as a function of relative humidity. While this yields a convenient plot, it is only an approximation since equilibrium capacity depends on other factors, principally temperature. The curves shown therefore should not be used for design calculations. The typical relationships are useful for discussion purposes, however, over the range of temperature encountered in this project

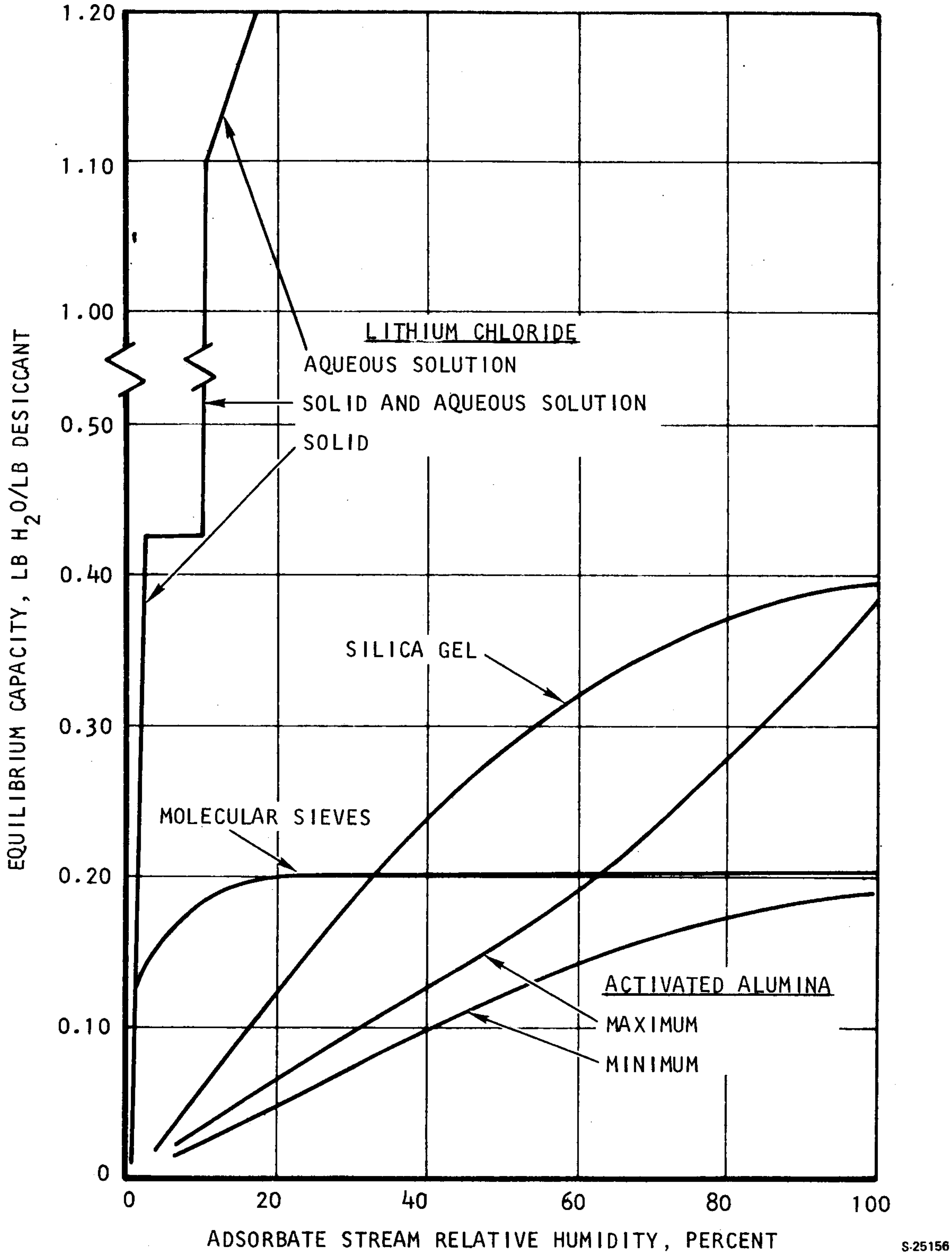

Figure C-1. Equilibrium Water Capacity of Various Desiccants

Silica gel has an effective pore diameter of about 22 Å. This is substantially larger than a water molecule, which is about 3.2 Å in diameter. Water molecules therefore encounter very little resistance as they migrate from the free stream to the solid surface.

Molecular Sieves

Within the past two decades, a new family of adsorbents has become available to the process industries. This new material is known by the somewhat misleading name of molecular sieves. The molecular sieves are crystalline, hydrated metal aluminosilicates. The commercially important types are made synthetically, but their structure is similar enough to certain naturally occurring minerals to be classified as zeolites.

Although the crystalline structures of some of the molecular sieves are quite different (two types, A and X are most important), their significance as commercial adsorbents depends on the fact that in each, the crystals contain interconnecting cavities of uniform size, separated by narrower openings, or pores, of equal uniformity. When formed, this crystalline network is full of water, but with moderate heating the moisture can be driven from the cavities without changing the crystalline structure. This leaves cavities with their combined surface area and pore volume available for adsorption of water or other materials. The process of evacuation and refilling the cavities may be repeated indefinitely under favorable conditions.

The major advantage to the use of molecular sieves over silica gel and other more conventional adsorbents is the ability to control pore size to obtain selective adsorption of one component from a stream of several components. This effect shows up in the analytical adsorption model by providing a means of adjusting the particle diffusion rate constant, D_i. The significance of D_i in diffusion rate prediction is discussed later in this appendix.

As an example of the selective adsorption that can be achieved by adjusting D_i, consider the process of separating oxygen and nitrogen from dry air. If dry air is passed through a 4 Å molecular sieve, oxygen is preferentially adsorbed and nitrogen-rich air passes out of the bed. If dry air is passed through a 5 Å molecular sieve, nitrogen is preferentially adsorbed and oxygen-rich air is produced. However, if water had been present in either case, it would be preferentially adsorbed at the exclusion of either nitrogen or oxygen. This complete reversal in the process illustrates the importance of selecting the correct pore diameter for the intended process. The fact that water is preferentially adsorbed by molecular sieve at the exclusion of almost all other molecules means that the selectivity is not an advantage in this application.

Molecular sieve has a smaller surface area then silica gel. This is reflected in the lower equilibrium capacity, shown in Figure C-1. Maximum capacity is reached at low relative humidity, however, which is an advantage in applications requiring a low dewpoint output.

Activated Alumina

Activated alumina and alumina gel are porous forms of aluminum oxide with between 200 and 400 sq m/gm surface area. Various forms are made by thermal treatment of hydrated alumina, and then impregnating with calcium chloride, cobaltous chloride, and other materials.

The primary use for aluminas is in water removal from oils and closed-circuit fluids such as refrigerants. Extremely low dewpoints are possible in applications such as these. The equilibrium water capacity range of activated alumina is shown in Figure C-1. The actual characteristics of a particular grade of alumina are influenced by additives that customize the material for particular applications.

The desorption temperatures of aluminas are between 300° and 600°F, with 350°F stated as a practical minimum. Below this temperature, a reasonable working capacity cannot be established. For this reason, alumina is not a reasonable desiccant for solar applications unless concentrating collectors are used.

Lithium Chloride

Lithium chloride has many uses as an industrial desiccant. However, it exhibits deliquescence at room temperatures which makes it unusable as a solid adsorbent (see Figure C-1). The equilibrium state at any relative humidity above about 10 percent includes some aqueous solution. In this desiccant system, it might be possible to avoid deliquesence by lengthening the desorption cycle to such an extent that the bed would be almost completey regenerated. The adsorption cycle would be comparatively short. This would result in poor thermodynamic performance, however, and deliquesence would still be a problem when the unit was shut down.

PARTICLE SIZE CONSIDERATIONS

The mass transfer and pressure drop models that lead to the selection of desiccant particle sizes are discussed below. Analytical model development and calculations are not given in these areas. More detail is presented in References C-4 through C-7.

Mass Transfer Differential Model

For purposes of constructing a model of the mass diffusion from a flowing gas stream into a sorbent bed, some simplifying assumptions are made. These include:

(a) Bed properties do not vary in the direction perpendicular to mass transfer.

(b) Temperature gradients in the pellet interior are negligible.

(c) Adsorption occurs by the diffusion of an adsorbate (water in this case) through the boundary layer at the exterior surface of an adsorbent particle (the desiccant), condensing at the surface and then diffusing into the interior of the particle. Desorption occurs in the reverse fashion.

(d) Adsorbent pellets can be represented by spheres for mass transfer calculations

Under these restrictions, a differential control volume analysis of the diffusion of component i through a solid of arbitrary geometry yields the following form of the continuity equation:

$$\frac{\partial W_i}{\partial t} = \frac{D_i}{\rho_s} \nabla^2 W_i \qquad \text{(C-1)}$$

where W_i is the mass loading of the adsorbate i in the adsorbent

D_i is a diffusion rate constant for adsorbate i through the adsorbent

ρ_s is the density of the solid adsorbent

Equation C-1 is commonly referred to as Ficks Second Law of Diffusion. The assumption of no gas phase mixture transport through the solid control volume listed in (c) above allows this simplified version of the general continuity equation to be used.

Since it is assumed that the pellets are spherical, the Laplacian operator of the scalar W_i can be expanded as follows:

$$\frac{\partial W_i}{\partial t} = \frac{D_i}{\rho_s}\left[\frac{1}{r^2}\frac{\partial}{\partial r}\left(r^2\frac{\partial W_i}{\partial r}\right) + \frac{1}{r^2 \sin\theta}\frac{\partial}{\partial\theta}\left(\sin\theta\frac{\partial W_i}{\partial\theta}\right) + \frac{1}{r^2\sin^2\theta}\frac{\partial^2 W_i}{\partial\phi^2}\right] \qquad \text{(C-2)}$$

Since the mass loading can be assumed constant with respect to angular position, the derivatives with respect to θ and ϕ are zero, and C-2 becomes

$$\frac{\partial W_i}{\partial t} = \frac{D_i}{\rho_s}\frac{1}{r^2}\frac{\partial}{\partial r}\left(r^2\frac{\partial W_i}{\partial r}\right) \qquad \text{(C-3)}$$

Equation C-3 is subject to the boundary conditions

$$\frac{\partial W_i}{\partial r} = 0 \text{ at } r = 0 \qquad \text{(C-4)}$$

$$-\rho_s D_i \frac{\partial W_i}{\partial r} = M_i K_g (P_{i_{sat}} - PX_i) \text{ at } r = r_s \qquad \text{(C-5)}$$

where M_i is the molecular weight of component i

K_g is the mass transfer coefficient between the bulk stream and the surface of the adsorbent

$P_{i_{sat}}$ is the saturation pressure of component i

P is the total pressure of the bulk stream

X_i is the mole fraction of component i in the bulk stream

r_s is the outside radius of the adsorbent bead

From equations C-3 and C-5, it is clear that the important parameters influencing the performance of a particular adsorbate - adsorbent combination are r_s, K_g, and D_i.

For water adsorption on silica gel or molecular seive, the radius of the particle (r_s) becomes a significant impediment above r_s = 0.063 in., approximately. This corresponds to the average particle size in 8 to 10 mesh material. Larger particles exhibit significant decreases in mass transfer rate, but smaller particles do not improve the transfer rate significantly.

The surface mass transfer coefficient K_g has been experimentally determined by AiResearch in a variety of programs. For the range of particle sizes under consideration in this project, K_g equals approximately 6.5 x 10^{-3} lb-moles/hr-ft^2- mm Hg.

The diffusion rate constant D_i can be predicted by analytical methods based upon the theoretical interaction between an adsorbate molecule and an adsorbent pore. This analytical procedure has been well substantiated by experimental results for several adsorbate-adsorbent pairs, and it is possible to predict values for D_i as a function of pore diameter and mean molecular size. It is this prediction capability that most influences adsorbent selection when it is desired to selectively adsorb one material in the presence of others. For adsorption of water from moist air, both silica gel and molecular seive have a D_i of about 2.0 x 10^{-5} ft^2/hr. This is valid for molecular seive materials with effective pore diameters greater than about 3 Å.

In a wide range of prior programs, AiResearch has conducted experimental mass transfer investigations on adsorbent materials. The data gathered in these programs has lead to the successful design of systems (principally in the area of spacecraft life-support), and has established a firm basis for the use of analytical models for performance prediction. For this reason Equations C-3 through C-5 can be applied with reasonable certainty. For a discussion of experimental investigation and examples of the use of the analytical models, see References C-8 and C-9.

Pressure Drop

Pressure drop across the desiccant bed and regenerator matrix is important to the energy conservation characteristics of the solar desiccant subsystem. If care is not taken to minimize pressure drop, it is likely that more electricity will be required to operate the system fans than would be consumed by a conventional Rankine air conditioner. Low pressure drop is therefore critical to the viability of the solar desiccant system.

Several correlations are available for the prediction of pressure drop as fluids flow through granular material. One of the most reliable was developed by Lexa, and taken from Reference C-10. Under the assumption that compressibility factors are negligible, the pressure differential across a granular bed is given by:

$$\Delta P = \frac{2\, f_m G^2 L (1-\epsilon)^{3-n}}{D_p g_c \rho \phi_s^{\,3-n} \epsilon^3} \tag{C-6}$$

where ΔP is the pressure drop, lb_f/ft^2

L is the bed depth, ft

g_c is a dimensional constant, 32.174 $ft\text{-}lbm/lb_f\text{-}sec^2$

D_p is the average particle diameter in feet, assuming spherical particles having the same volume as the actual particles

ϵ is the fractional void volume, dimensionless

n is an empirical exponent, dimensionless

ϕ_s is the shape factor of the particles, defined as the ratio of the area of a sphere equivalent to the volume of the particle, to the actual surface of the particle, dimensionless

G is the superficial mass velocity based on an empty chamber cross-section, $lb/sec\text{-}ft^2$

ρ is the fluid density, lbm/ft^3

and f_m is a modified friction factor, dimensionless

n and f_m are functions of a modified Reynolds number, N'_{Re}, as shown in Figure C-2. N'_{Re} is defined as:

$$N'_{Re} = \frac{D_p G}{\mu} \tag{C-7}$$

where μ is the fluid viscosity, lbm/ft-sec.

For nonspherical particles,

$$D_p = \frac{6(1-\epsilon)}{\phi_s S} \tag{C-8}$$

where S is the specific surface, or area of particle surface per unit volume of bed, ft^2/ft^3.

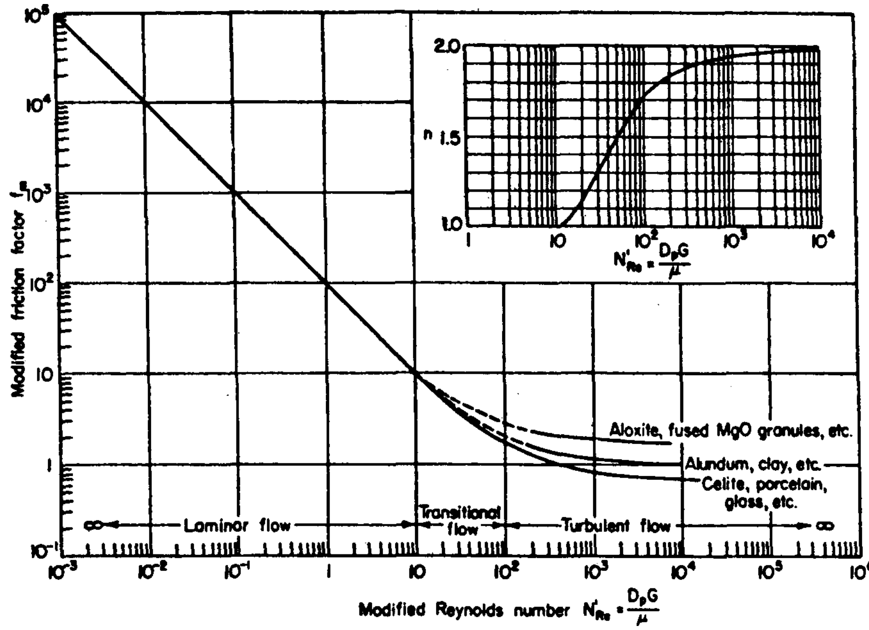

Figure C-2. Modified Friction Factor, f_m, and Exponent, n, as Functions of Modified Reynolds Number, N'_{Re}. From Reference C-10.

The shape factor has been tabulated for a variety of materials in Reference C-8. For jagged crushed glass, ϕ_s = 0.065; for rounded sand, ϕ_s = 0.83; for angular sand, ϕ_s = 0.73. Molecular seive material is nearly spherical, and ϕ_s = 0.95 (approximately). Granular silica gel has ϕ_s = 0.7 (approximately).

The relationship of equation C-6 can be used with the subsystem computer model to predict fan power consumption (based on particle size and shape), bed size, and airflow rates.

HARDNESS

Hardness has been variously defined as resistance to local penetration, scratching, machining, wear and abrasion, and yielding. The multiplicity of definitions, and corresponding multiplicity of hardness measuring instruments, together with the lack of a fundamental definition indicates that hardness may not be a fundamental property of a material, but rather a composite one including yield strength, work hardening, tensile strength, modulus of elasticity, and perhaps others. However, it is felt that a relative indication of hardness among the desiccant materials under consideration provides an indication of relative structural integrity.

"Scratch hardness" is measured on the Mohs scale of minerals, which is so arranged that each mineral will scratch the mineral of the next lower number. Table C-1 shows the ten Mohs scale standards, and the hardness of some desiccant materials. For a more detailed discussion, see Reference C-11.

Molecular seive, with a hardness of about 3, powders easily when handled; a can of this material usually contains a significant amount of dust when first opened after shipping. During differential bed testing at AiResearch, a process used to determined mass transfer characteristics, glass tubes filled with desiccant were alternately subjected to flowing gas streams, and then weighed. Laboratory personnel consistently noted a cloud of dust from the tube when the gas stream was first turned on after the gentle handling required to remove the tube and weigh it. This indicates that a significant amount of the bed material could be lost over a long period of service.

TABLE C-1

HARDNESS OF DESICCANTS RELATIVE TO THE MOHS SCALE STANDARDS

Desiccant	Hardness Number	Scale Standard
	1	Talc
	2	Gypsum
Type A molecular sieve	3	Calc-spar
	4	Fluorospar
Granular silica gel	5	Apatite
	6	Feldspar
	7	Quartz
	8	Topaz
Activated alumina	9	Sapphire
	10	Diamond

Molecular seive material is produced initially as a fine powder, which is then mixed with clay or organic binders and formed into spheres or pellets. The structural properties of the particles are therefore dependent on the properties of the binder material; it is therefore possible that stronger particles could be formulated with different binders. However, only commercially available materials have been considered here.

Silica gel is somewhat harder than molecular seive, having a Mohs rating of 5. No powdering problems like those associated with molecular seive have been observed at AiResearch as long as the material is not subject to severe tumbling or grinding motion. Silica gel will fracture if contacted by liquid water due to thermal stresses within the granules caused by very rapid water adsorption. This should not be a problem with this system because water droplets will not be entrained in the airstreams during normal operation.

Activated alumina is significantly harder than the other materials considered. Indeed, corundum and emery, which are composed chiefly of alumina crystals, have been used for centuries as good natural abrasives, and have only recently been replaced by manufactured substitutes. Although it is likely that alumina would be much less likely to powder than some other materials, any dust that did form could be very damaging to bearings and seals.

No hardness data have been found for lithium chloride (LiCl), which has been suggested as a desiccant. Lithium chloride is deliquescent, however, and if allowed to contact air at normal temperatures and humidity, enough water will be adsorbed to form a saturated aqueous solution, which, of course, has no structural integrity. For this reason, lithium chloride is not a practical desiccant for this application.

COST

Cost estimates have been received for silica gel, molecular sieve, and activated alumina desiccants. These costs were based on 1000-lb lots. Somewhat lower costs should be expected for production sized orders, but these estimates provide a consistent basis for comparison of the various materials. Estimates for larger quantities will be obtained for commercialization studies in Task I-11 and cost effectiveness studies in Task I-12. Cost estimates are shown in Table C-2.

TABLE C-2

DESICCANT COST ESTIMATES

Material	Price, $/lb
Granular silica gel, 8 to 10 mesh	1.10
Molecular sieve pellets, 8 to 10 mesh, 80 percent zeolite, 20 percent binder	1.75
Molecular sieve paper, asbestos substrate	26.25*
Granular activated alumina, 8 to 10 mesh	0.90

*Based on price of active zeolite material, and not on bulk weight of zeolite and substrate.

REFERENCES

C-1. Activated and Catalytic Aluminas, Aluminum Company of America, 1969.

C-2. Davison Silica Gels, W. R. Grace and Co., Davison Chemical Division.

C-3. Davison Molecular Sieves, W. R. Grace and Co., Davison Chemical Division.

C-4. Welty, J. R., Wicks, C. E., and R. E. Wilson, Fundamentals of Momentum, Heat and Mass Transfer, John Wiley and Sons, 1969.

C-5. Hwang, K. C., S9960 Transient Performance Prediction for CO_2 Removal by Composite Sorbent Bed, AiResearch Manufacturing Company, NAS 1-8559, 1969.

C-6. Arpaci, V. S., Conduction Heat Transfer, Addison-Wesley, 1966.

C-7. Kays, W. M., Convective Heat and Mass Transfer, McGraw-Hill, 1966.

C-8. Hwang, K. C., A Transient Performance Method for CO_2 Removal with Regenerable Adsorbents, NASA CR-112098, Oct. 1972.

C-9. Wright, R. M., et. al., Development of Design Information for Molecular Sieve Type Regenerative CO_2 Removal Systems, NASA CR-2277, July 1973.

C-10. Perry, John, H., et. al., Chemical Engineers' Handbook, McGraw-Hill, 1963.

C-11. Baumeister, Theodore (Editor), Standard Handbook for Mechanical Engineers, McGraw-Hill, 1967.

APPENDIX D

TASK I-2. DESIGN REQUIREMENTS AND EVALUATION CRITERIA: GEOGRAPHIC LOCATIONS

AiResearch has available design year climatic and solar data for ten locations in the United States (New York City, Santa Monica, Omaha, Washington D.C., Cleveland, Columbia, Madison, Phoenix, Lake Charles, and Los Angeles). These data were generated by Beckman, Duffie, and Associates for AiResearch under Contract NAS8-32091. From these locations, New York City; Lake Charles, Louisiana; and Phoenix, Arizona were chosen for system evaluation.

New York City was chosen as being representative of the Boston-Washington megalopolis. This area includes a large amount of the population of the United States, and also has a large market for air conditioning. The summer weather is typically quite warm and humid.

Lake Charles is a worst-case climate in terms of high humidity levels, which is a condition in which the solar desiccant system should perform very well. This humid climate exists in most of the Southeast United States, particularly near the Gulf Coast and Southern Atlantic Coast.

Phoenix is representative of desert areas where sensible loads are extreme and ambient humidity is low. The normal climate is such that simple evaporative coolers are successfully used for cooling. Evaporative systems are almost always full fresh-air makeup systems, whereas the solar desiccant system will recirculate the conditioned air.

The relationship of these three locations to the rest of the United States can be seen in part in Figures D-1 and D-2. Lines of constant average July dry bulb and wet bulb temperatures indicate the general nature of the climate. Figures D-1 and D-2 are taken from the Handbook of Air-Conditioning, Heating, and Ventilating, The Industrial Press, New York, N.Y., 1959, Clifford Strock, editor.

Following workshop discussions and the program review held at AiResearch in mid-February, the decision was made to use weather data which will be applied by DOE for New York, Phoenix, and Apolachicola. The data tapes to be provided by DOE will also include the residence loads for these three locations.

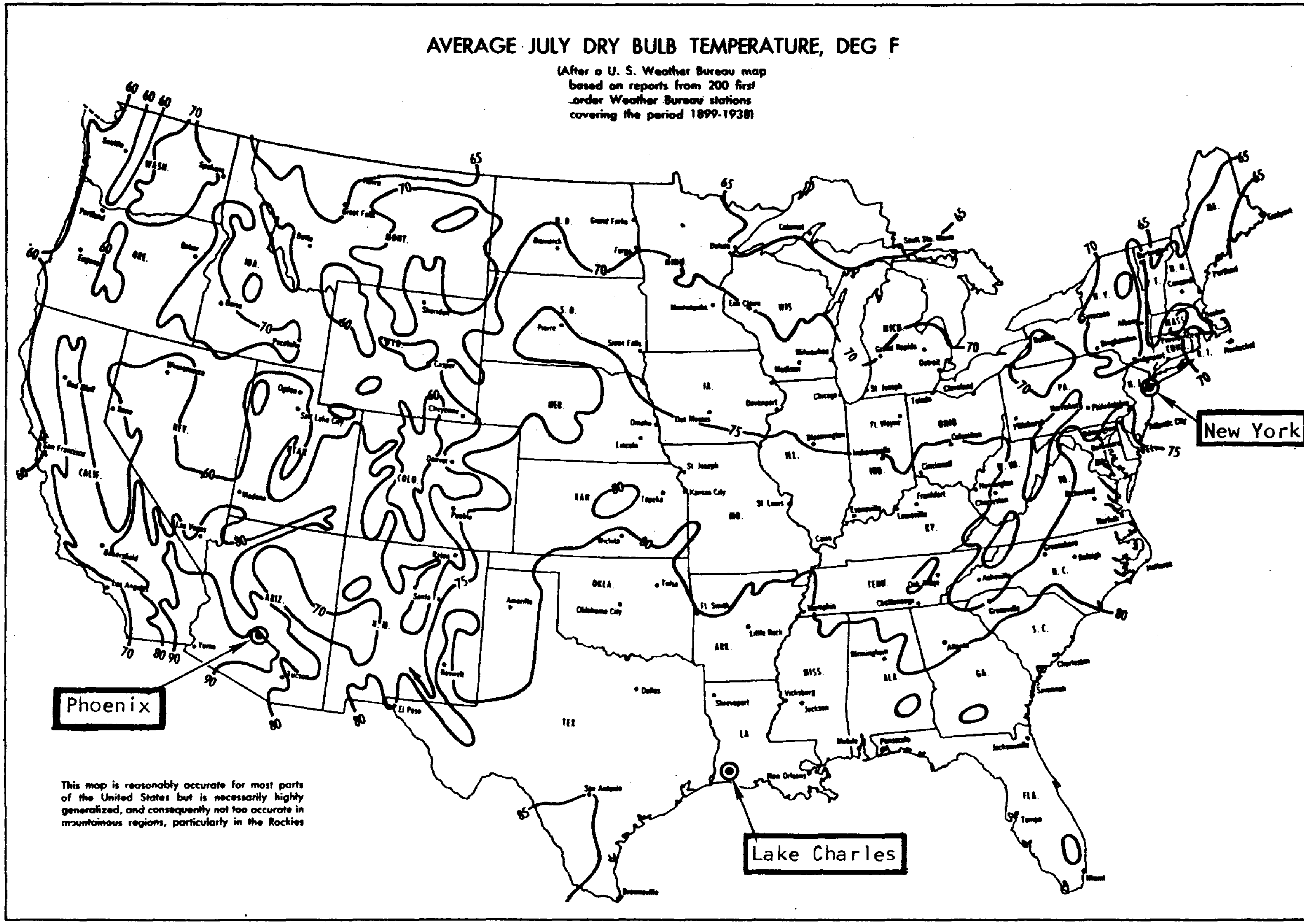

Figure D-1. Dry Bulb Temperatures for the United States (From Handbook of Air Conditioning, Heating, and Ventilating, 1959)

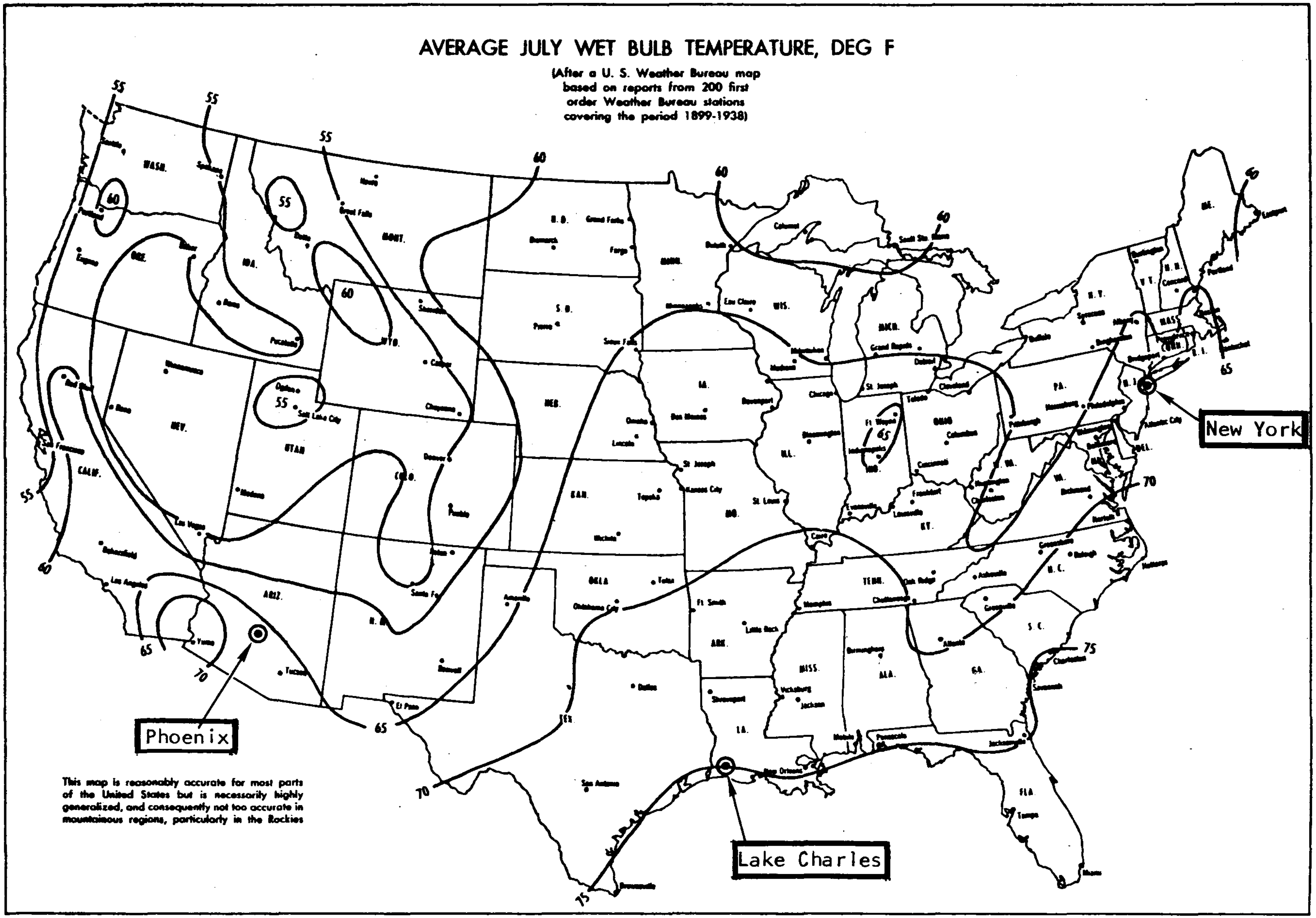

Figure D-2. Wet Bulb Temperatures for the United States (From Handbook of Air Conditioning, Heating, and Ventilating, 1959)

APPENDIX E

TASK 1-2. DESIGN REQUIREMENTS AND EVALUATION CRITERIA: SINGLE-FAMILY HOUSE MODEL

INTRODUCTION

A typical split-level single-family house has been selected as the design load for the subsystem and system. The characteristics of the house will become part of the system computer performance model. The model will reflect cooling and heating requirements as functions of (1) internally generated latent and sensible time-dependent loads, (2) time-dependent solar loads, and (3) latent and sensible loads from outside as a function of climatic conditions. Drawings of the model residence are shown in Figure E-1.

Design-point cooling laods were calculated using ASHRAE 2-1/2 percent Summer design temperatures. These design-point loads will be used only to size the equipment not related to solar energy collection and storage. Since a design period that will reflect the energy storage requirements must be established for a given locality, variable storage parameters will be included in the system model.

For simplicity, one house model will be used for all three locations. This will not make the model less useful than it would be if the building parameters were customized for each location because (1) although there are some regional variations in materials and architecture, a frame construction house such as the one selected is representative of buildings in all parts of the United States, and (2) most important, basic improvements in current construction practice are required to decrease the energy consumption in all buildings, regardless of location. The most significant of these improvements are to increase insulation, reduce infiltration and excessive ventilation, and control solar loads on fenestration to either lower cooling loads or augment heating loads, as required.

The improvement of building construction to minimize energy consumption is discussed in ASHRAE Standard 90-75. This standard is written so as to address general values of minimum insulation thermal resistance, maximum air leakage, etc.; it does not specify or suggest particular materials or techniques. With the exception of interior lighting requirements, the standard can be quite easily met using common materials and reasonably good workmanship. The house model that has been developed is of conventional construction and materials, and exceeds ASHRAE 90-75 in all respects. Conservation in construction is essential to the success of a solar home conditioning system. Whereas a conventional heating and cooling system can be over-sized to accommodate poor construction, it may not be possible to build a solar system large enough to compensate for these problems because solar collection and storage capacity are limited by the physical size of the building.

HOUSE MODEL DESIGN

The design of the house shown in Figure E-1 is shown only in enough detail to allow its use at a part of the system mode. No details are

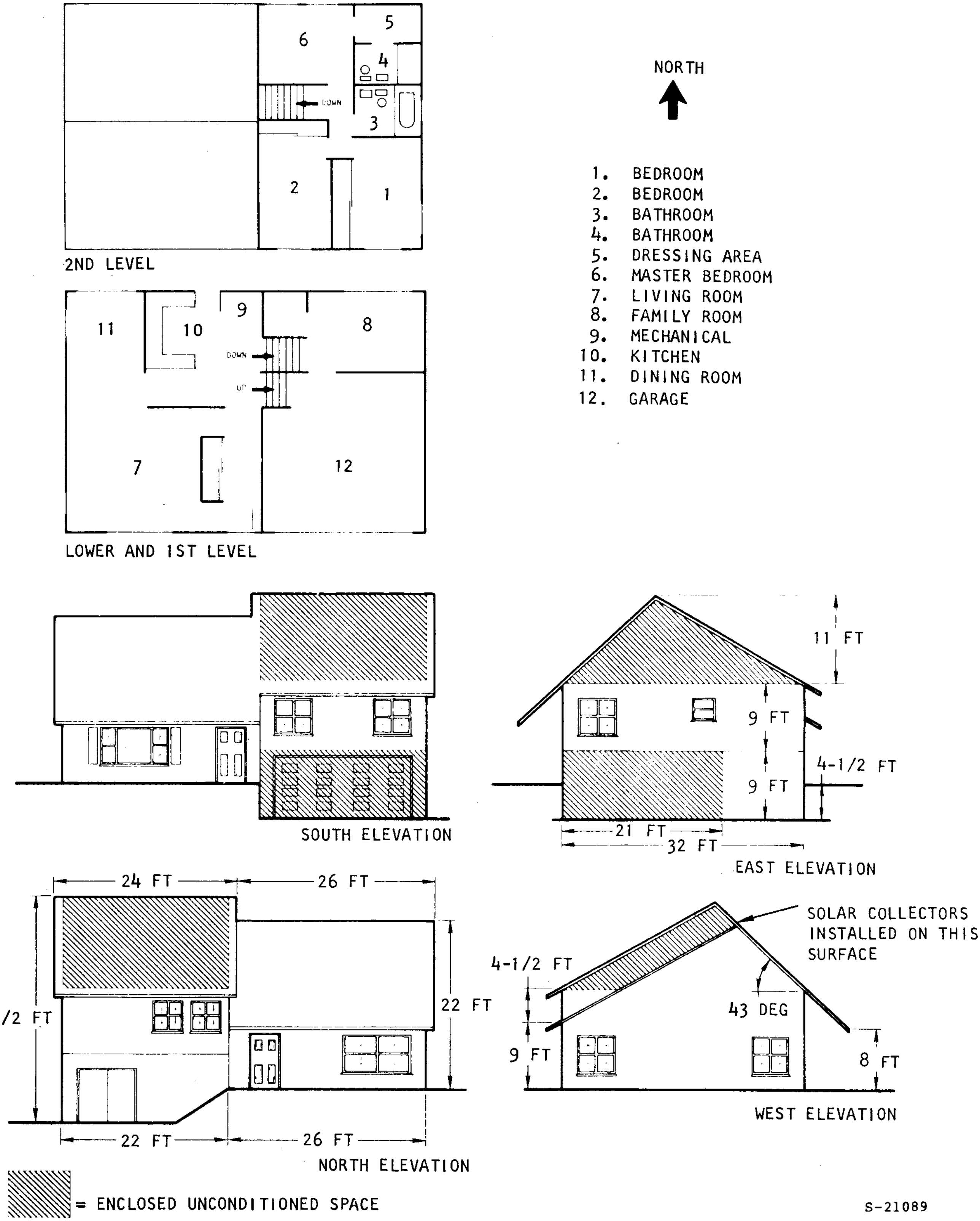

Figure E-1. Layout of Single-Family House Selected for Solar Desiccant Dehumidifier included that are not pertinent to this use. The general construction details are as follows:

> Arrangement--1-1/2 story split level, 3-bedrooms. Bottom floor comprises garage and partial basement.
>
> Solar Collector Array--North-facing roof provides sufficient area for approximately 800 sq ft of unshaded collectors.
>
> Unconditioned Enclosed Spaces--Garage and attic space above second story.

The general dimensions are listed in Table E-1. House construction details are presented in Table E-2. Where applicable, ASHRAE Standard 90-75 values are included for comparison.

The energy gain or loss through a surface is given by

$$Q = UA\ (T_o - T_i)$$

where Q is the energy loss or gain, Btu/hr

U is the heat transfer coefficient, Btu/hr-ft^2-°F

A is the area of the surface, ft^2

T_o is the outside temperature, °F

T_i is the inside temperature, °F

To compute loads through surfaces between the conditioned space and an unconditioned space, the temperature difference is commonly taken as one-half the difference between the outside and the conditioned space.

INTERNAL LOADS

A reliable number for internal loads is difficult to estimate. Latent and sensible loads from appliances, cooking, bathing, and the occupants all contribute to the load, but it is difficult to predict the total effect at a particular time. Generally, for a structure as large as a house with a normal-size family, the occupant load is negligible unless large gatherings such as parties or meetings are very common. Load profiles for typical occupant, appliance, and lighting loads are shown in Figure E-2. An estimate of the average sensible load imposed by common appliances is shown in Table E-3.

SOLAR LOADS THROUGH FENESTRATION

A simplified method for estimating solar heating is the ASHRAE solar heat gain factor procedure. Solar heat gain factors (SHGF) are tabulated for various latitudes, directions, and times of day and year. A shading coefficient (SC) is selected for the particular fenestration, and the following relationship is used to calculate solar heat gain (SHG):

$$SHG = SC \times SHGF \times Area$$

TABLE E-1

GENERAL DIMENSIONS

House Structure	Area, sq ft
Floor area	1775 conditioned space 462 unconditioned space (garage)
Exterior* walls	1609
Windows	256
Exterior* wood doors	49
Exterior* glass door	56
Garage door	144
Interior** door	20
Interior** walls	310
Second story ceiling	704
Second story roof	858
Cathedral roof/ceiling	988
Garage ceiling	462
Floor over crawl space	832

*Exterior refers to structure between the conditioned space and outdoors.

**Interior refers to structure between the unheated space (garage) and conditioned space.

TABLE E-2

CONSTRUCTION DETAILS

Structure	Construction	Heat Transfer Coefficient (U), Btu/hr-ft^2-^{o}F
Exterior walls	Wood siding and building paper on 25/32 in. insulation board sheathing outside. 2 by 4 studs on 18-in. centers. Gypsum lath with 1/2-in. sand aggregate plaster inside. Wall filled with R-11 insulation.	U = 0.065 ASHRAE maximum U (including windows and doors) = 0.235
Windows	Triple pane glazing with 1/2-in. air spaces. Sash made of wood, with 80 percent glazing area.	U = 0.342
Exterior and interior wood doors	Solid wood 2-in. thick doors with storm doors.	U = 0.24
Exterior glass door	Triple pane glazing with 1/2-in. air spaces. Aluminum frame, 95 percent glazing area.	U = 0.36
Interior walls	1/2-in. plywood on garage side. 2 by 4 studs on 18-in. centers. Gypsum lath with 1/2-in. sand aggregate plaster inside. Wall filled with R-11 insulation.	U = 0.0746 ASHRAE maximum U (including door) = 0.235
Second story ceiling	2 by 6 stringers on 18-in. centers. No top surface. Gypsum lath with 1/2-in. sand aggregate plaster inside. Spaces between stringers filled with R-22 insulation.	U = 0.0423 ASHRAE maximum U (for roof and ceiling combination) = 0.05
Second story roof	2 by 6 rafters on 18-in. centers. No bottom surface. Asphalt shingles and building paper on 25/32-in. wood sheathing.	U = 0.4405
Cathedral roof/ceiling	Asphalt shingles and building paper on 25/32-in. wood sheathing outside. 2 by 6 rafters on 18-in. centers. Insulation board lath and 1/2-in. sand aggregate plaster inside. On south-facing roof, solar collector panels will be installed.	U = 0.0388 ASHRAE maximum U = 0.05 Note: No insulation value is assumed for the solar collector or for any decorative interior treatment such as false beams, etc.
Garage ceiling	Linoleum and felt on 5/8-in. plywood and 25/32-in. subfloor on top. 2 by 8 joists on 18-in. centers. 3/8-in. sheet rock on bottom. Spaces between stringers filled with R-22 insulation.	U = 0.0423 ASHRAE maximum U = 0.08 for New York City and 0.28 for Lake Charles and Phoenix.
Floor over crawl space	Linoleum and felt on 5/8-in. plywood and 25/32-in. subfloor on top. 2 by 8 joists on 18-in. centers. R-11 insulation between joists.	U = 0.0681 ASHRAE maximum U = 0.08 for New York City and 0.28 for Lake Charles and Phoenix.

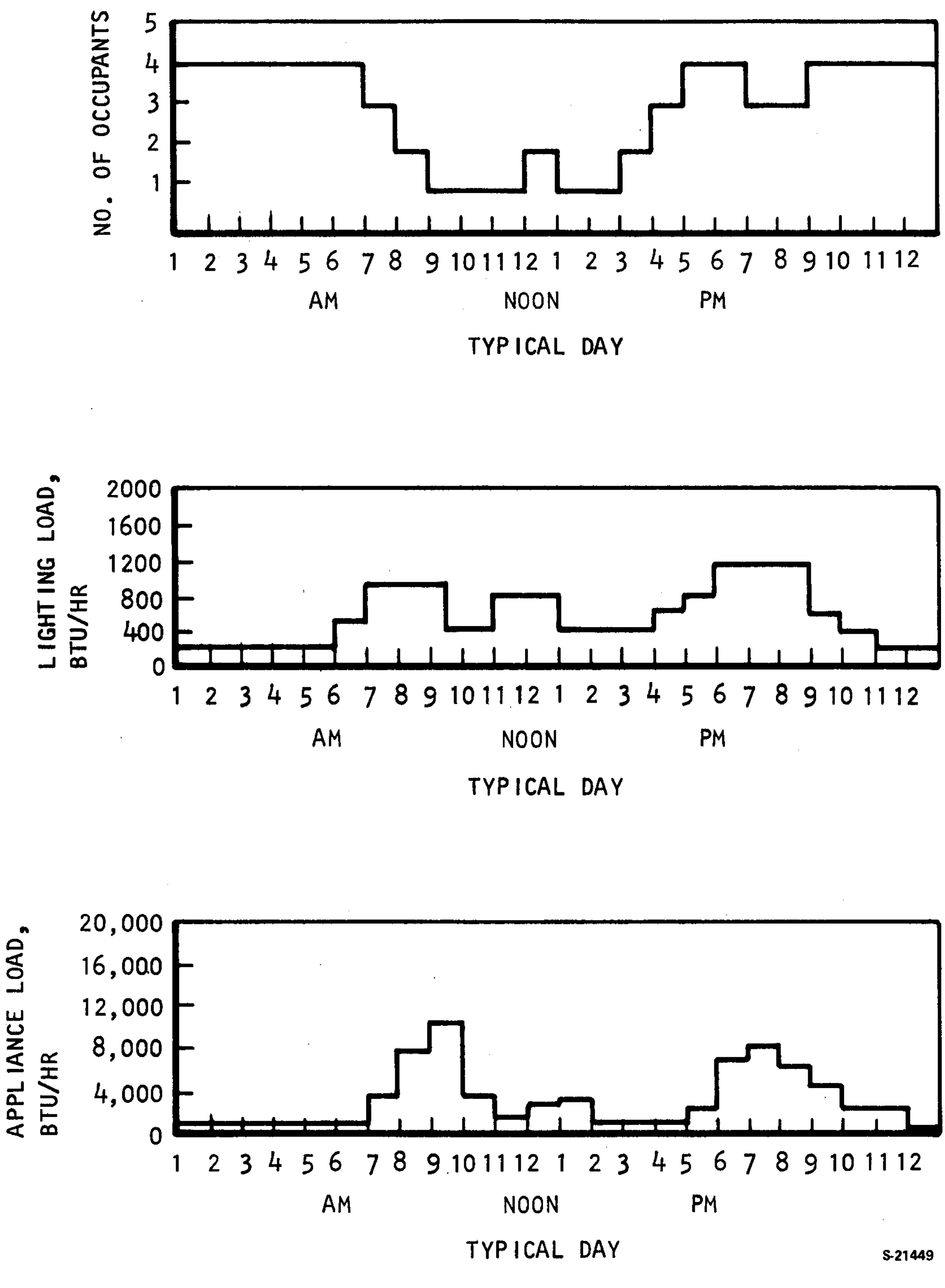

Figure E-2. Occupancy, Lighting, and Appliance Load Profile

TABLE E-3

APPROXIMATE SENSIBLE LOADS IMPOSED BY
AVERAGE HOUSEHOLD APPLIANCES

Appliance	Sensible Load, Btu/hr
Water heater	820
Clothes dryer	190
Clothes washer	40
Range	450
Refrigerator	560
Freezer	590
Color TV	190
Dishwasher	140
Miscellaneous	470
Lights	570
Total	4020

Afternoon solar loads for the house model at 2 pm on July 21 are given in Table E-4. This represents the approximate maximum solar load on the house, and was used to calculate the design point cooling loads.

TABLE E-4

SOLAR LOADS THROUGH FENESTRATION

Location	Solar Heat Gain Factor (SHGF), Btu/ft^2-hr	Shading Coefficient (SC)	Area, ft^2	Direction Surface Facing	Solar Heat Gain (SHG), Btu/hr^2
Phoenix or Lake Charles	37	0.72	133	North	3543
	35	0.72	34	East	857
	148	0.72	50	West	5328
	53	0.72	95	South	3625
Total					13,353
New York City	35	0.61	133	North	2840
	35	0.61	34	East	728
	146	0.61	50	West	4453
	80	0.61	95	South	4636
Total					12,655

LATENT LOADS

Because of the many variables involved in calculating a latent load, the ASHRAE rule-of-thumb will be used, which states that the latent load is approximately 30 percent of the sensible load, excluding infiltration and ventilation. This factor is commonly used in residential design calculations.

INFILTRATION AND VENTILATION

In ASHRAE 90-75, the maximum allowable infiltration limits are stated in terms of cfm per window edge length or door area. Obviously, the significance of the infiltration for a given set of windows and doors depends on the volume of the closed space. While excessive infiltration is to be eliminated, it is not desirable to eliminate fresh air makeup altogether. One-half air change per hour is commonly taken as the minimum desirable makeup in a residence.

For the house model described above, application of ASHRAE 90-75 indicates a maximum infiltration of 214 cfm. Since the volume of the conditioned space is approximately 19,800 cu ft, this rate amounts to 0.65 air changes per hour. By slightly improving workmanship, it is arbitrarily assumed that this can be reduced by 23 percent, to 165 cfm, which is one-half air change per hour.

DESIGN POINT COOLING LOAD

The design point cooling loads and the ASHRAE design temperatures used to estimate these cooling loads are shown in Table E-5.

TABLE E-5

DESIGN POINT COOLING LOADS

	New York City	Phoenix	Lake Charles
Inside design temperature			
Dry bulb, °F	78	78	78
Wet bulb, °F	67	67	67
Outside design temperature			
Dry bulb, °F	91	106	93
Wet bulb, °F	76	76	79
Cooling loads			
Sensible, Btu/hr	24,200	32,000	25,600
Latent, Btu/hr	9,900	8,900	12,000
Total, Btu/hr	34,100	40,900	37,600
Total, tons	2.84	3.41	3.13
Sensible heat factor (SHF)*	0.71	0.78	0.68

$$*SHF = \frac{\text{Sensible Load}}{\text{Total Load}}$$

DOE COOLING LOADS

As mentioned in Appendix D, the decision was made by DOE to supply standardized cooling loads together with weather data to all desiccant system contractors. Development of the system model has been postponed until these data are made available.

APPENDIX F

TASK 1-2. DESIGN REQUIREMENTS AND EVALUATION CRITERIA: ECONOMIC MODEL

INTRODUCTION

The economic model described in this appendix has been structured to predict the costs to consumers associated with the design, acquisition, and operation of a solar-energy-powered air conditioning system. Although the particular application is the solar desiccant system, the method of evaluation is valid for analyzing any project that involves capital expenditures, fuel or electricity consumption, maintenance costs, and tax incentives over a number of years. This versatility is important because the absolute costs of a solar system are not useful alone, and they must be compared to the costs of other viable alternatives for accomplishing the same task.

A number of tradeoffs involving system initial cost and operating costs (primarily supplemental energy) require an economic model for proper evaluation and system optimization. Typical optimizations required for system design are:

- Solar collector area versus supplemental energy
- Heat exchanger effectiveness versus solar collector area or supplemental energy
- Thermal energy storage capacity versus supplemental energy
- Solar-powered air conditioner cycle efficiency versus solar collector area or supplemental energy
- System performance versus solar collector area or supplemental energy

Supplemental energy may consist of electrical power, natural gas, fuel oil, or propane. Evaluation of different solar collector designs and their operating parameters is also significant.

This analysis is restricted to an examination of direct receipts and disbursements by the purchases of a solar cooling system; social costs or benefits from external economies or diseconomies, such as air pollution from fossil fuel, are not included. The analysis is limited to private costs because these are the most relevant factors in the widespread adoption or rejection of solar energy systems, and private decision-making does not generally include social costs or social benefits.

Further inequities may arise when making recommendations based on an analysis involving fuel prices. For example, natural gas is a superior fuel in many respects to oil or coal because it does not produce pollution problems, is easy to handle, and does not require refinement before end use. Based on its desirability, it seems that it should be priced at least as high as an equivalent fuel value of oil or coal. Since artificial price controls have kept gas prices lower than other fuel prices, this desirable fuel is being rapidly depleted. A purely economic analysis, then, will give little credit to a system that conserves natural gas, when indeed this should be of prime importance. The subject of fuel cost prediction will be treated later.

A particularly important subject that may be the deciding factor in economic feasibility at the present time is tax credits and other artificial incentives or penalties designed to motivate a consumer to use or not to use a particular energy option. At current energy prices, this factor may be essential for the economic viability of a solar project. Tax programs vary from one location to another, but are generally in the form of investment income tax credits (based on initial capital expenditures) and property tax exemptions for solar equipment. These programs are still in their infancy in most locations, and substantial changes will probably occur in the near future.

Additional factors that influence decisions by the consumer and are not treated in this economic analysis are psycho-social factors such as personal "duty" (as to country), anxiety from energy shortages and the effects on future generations, and "novelty"; the prediction of these would be a complex exercise in pyschology. The "duty" and "anxiety" factors arise because a consumer feels that it is his duty to select a home air conditioning system that would save fuel. In the recent history of the United States, it has become apparent that efforts to convince the public to conserve have been almost totally ignored. The public, in general, seems to be suspicious of claims of fuel shortages, and hence this factor should not help sell solar systems until the present infrequent acute energy shortages become chronic. The "novelty" factor may indeed influence decisions to install solar equipment, even in opposition to adverse economic predictions.

Equipment first costs, operating costs, time-dependent accounting, energy cost forecasts, interest rate determination, tax credits, and artificial incentives reviewed below provide a composite economic model. Also reviewed are thermodynamic model evaluations. The model will yield the results necessary to determine economic feasibility.

THERMODYNAMIC MODEL

These evaluations require an adequate thermodynamic model that describes the operating environment and resulting performance over a yearly climatic cycle. In Task I-6, AiResearch will develop a thermodynamic model that provides detailed cycle analysis as a function of the system load and instantaneous solar and climatic conditions. This model also will integrate daily performance over the course of a year. In this way, yearly supplemental energy requirements will be determined for specific system configurations. By varying the solar collector area, for example, the resulting impact on yearly supplemental energy consumption can be directly determined. Similarly, other tradeoffs such as heat exchanger effectiveness or thermal energy storage capacity can be readily determined.

EQUIPMENT FIRST COSTS

The economic model must translate the engineering parameters into relative costs. AiResearch has worked closely with Dunham-Bush and others for some time on a wide variety of contracts to develop manufacturing cost data, with cost buildups at the user level, for the novel types of equipment required for solar heating and cooling systems. Under the present program, estimates will be made of the cost of the solar dehumidifier in volume production. Also, the cost of the collectors and storage unit will be determined using manufacturer's data.

OPERATING COSTS

In this case, the operating costs are represented primarily by the supplemental energy (electrical, natural gas, fuel oil, or propane) required for a system functioning over the course of the yearly cycle. Maintenance costs will be estimated for the proposed equipment once the equipment designs have been finalized. Replacement of desiccant, lubrication of machinery, seal replacement, and adjustment and cleaning of filters and humidifiers are the most obvious items that will require attention, although there may be other significant items in the final design.

TIME-DEPENDENT ACCOUNTING

The method of accounting for receipts and disbursements over the life of an air conditioning system is described below. Several different methods are available for comparing systems on a life-cycle cost basis. These include the following:

(a) <u>Payback Method</u>--The number of years required to repay the original investment. This method has serious drawbacks because it does not account for the time value of money, or the benefit derived after the date of payback. For these reasons, it is generally not an acceptable method, except for preliminary studies.

(b) <u>Present Worth Method (Sometimes Called Net Present Value)</u>--The present worth of future benefits and costs are discounted at the appropriate cost of capital plus the cost of the initial investment. The result is a single dollar value that can be compared directly with alternate systems. The system offering the required level of service at the most attractive net present worth is the economic choice.

(c) <u>Internal Rate of Return (Sometimes Called Prospective Rate of Return)</u>--This is the interest rate that equates the present value of future returns to the initial investment cost.

(d) <u>Benefit-Cost Ratio</u>--The benefit-cost ratio is the ratio of economic benefit to the initial investment cost. In this study, the numerator of the ratio is the present worth of future returns discounted at the appropriate cost of capital, and the denominator is the initial investment cost. In this way, the data are consistent with the net present worth method.

(e) <u>Equivalent Uniform Annual Cost</u>--This is the future benefits and costs plus a portion of initial investment cost, expressed as an equivalent uniform yearly cash flow.

Methods (b), (d), and (e) above properly account for the time value of money, and account for the benefits and costs throughout the system lifetime. Although differing in the method of presentation, all yield equivalent results. Therefore, the selection of methods is based largely on the end use of the data obtained. The net present worth method allows the direct comparison of a single dollar value for each system. The internal rate of return method yields an equivalent interest rate on the investment. If different levels of service are provided by alternate systems with substantially different initial investments, this method generates a single interest rate value that can be compared directly for each system. By contrast, the net present worth method in this case would yield results with substantial dollar differences, but without visibility to the different initial investments. The benefit-cost ratio is essentially another presentation method for the data used in the net present worth method. It is used often in Government programs, where it offers an easily understood ratio of what is achieved for a given initial cost. In industry, a comparable concept is the profitability index.

To compare amounts of money that are assumed to have certain values at particular times in the life of a project, it is necessary to "shift" all dollar amounts to a common time. A method of facilitating this shifting involves the definition of six compound interest formulas that are functions of the real interest rate and the number of years over which the shift is made. These factors are listed and defined in Table F-1. Generally, the single present worth formula--P(F, i, n)--and the uniform present worth formula--P(A, i, n)--are the most commonly used in present worth analysis. For example, at ten percent the present value of $100 spent at the end of each of 10 years is:

$$P = A \cdot P(A,\ 10\%,\ 10) = (\$100)\ \frac{(1 + 0.1)^{10} - 1}{0.1(1 + 0.1)^{10}} = \$614.46 \qquad \text{(F-1)}$$

It is assumed that the present time is when n = 0, and a disbursement is assumed to occur at the end of the interest period. During the actual life of a project, financial transactions may actually occur throughout the entire year. However, it is usually not possible to pinpoint dates exactly, as most amounts and their timing are estimates, with insufficient accuracy to warrant accounting periods less than one year in length. Also, as long as the life of a project is significantly longer than the accounting period (for example, a 20-year life with annual accounting), the shifting of a transaction by less than one period has a small effect on the final result. For the case where two alternatives show final answers that are almost identical, it may be desirable to examine the sensitivity of the estimates to the timing of transactions within the accounting period. Very likely, however, the uncertainty in estimating the magnitudes of the various costs will be the predominant factor influencing accuracy.

The present worth method makes use of compound interest formulas to shift all future receipts and expenditures back to the present time. Uniform annual amounts can be shifted with the uniform present worth formula to yield a single present worth for the series. Future single amounts can be shifted with the single present worth formula. Salvage value of the equipment, if any, is

TABLE F-1

COMPOUND INTEREST FORMULAS

Standard Nomenclaure	Use When	Notation	Algebraic Form
Single Compound Amount Formula	Given P; to find F	F(P, i, n)	$F = P\left[(1+i)^n\right]$
Single Present Worth Formula	Given F; to find P	P(F, i, n)	$P = F\left[\frac{1}{(1+i)^n}\right]$
Uniform Compound Amount Formula	Given A; to find F	F(A, i, n)	$F = A\left[\frac{(1+i)^n - 1}{i}\right]$
Uniform Sinking Fund Formula	Given F; to find A	A(F, i, n)	$A = F\left[\frac{i}{(1+i)^n - 1}\right]$
Uniform Capital Recovery Formula	Given P; to find A	A(P, i, n)	$A = P\left[\frac{i(1+i)^n}{(1+i)^n - 1}\right]$
Uniform Present Worth Formula	Given A; to find P	P(A, i, n)	$P = A\left[\frac{(1+i)^n - 1}{i(1+i)^n}\right]$

Where:

P = a present sum of money.
F = a future sum of money, equivalent to P at the end of n periods of time at an interest of i.
i = an interest rate per period of time.
n = number of interest periods.
A = an end-of-period payment (or receipt) in a uniform series of payments (or receipts) over n periods at i interest rate, usually annually.

Source: Gerald W. Smith, Engineering Economy, p. 47.

treated as a future receipt. The present worth of a project is therefore given by:

$$PW = C + \sum_{j=1}^{x} A_j \cdot P\ (A,\ i,\ n)_j + \sum_{k=1}^{y} F_k \cdot P\ (F,\ i,\ n)_k \qquad (F-2)$$

where PW is the present worth of the project

C is the initial capital cost of the project

A_j is the jth uniform annual expenditure or receipt, and

F_k is the future expenditure or receipt

In the above terms, C, A_k, and F_k are taken as positive (+) when they represent a disbursement and negative (-) when they indicate a receipt. In this manner, a larger value for PW indicates a larger amount of money expended over the life of the project.

It is important to choose the correct time period for each value of P (A, i, n) and P (F, i, n) in Equation F-2. When an annual cost A_j does not continue for the entire life of the project, the n_j used to compute P (A, i, $n)_j$ is the number of years that A_j continues. The present worth of A_j will then be based on a present time at the beginning of the first year of the series of expenditures A_j. When this present time does not coincide with the beginning time of the project, if is further necessary to shift this present worth of A_j to the same actual present date used for the rest of the analysis. This is done by multiplying by a single present worth factor P (F, i, n), with n set equal to the number of years from the beginning of the project to the beginning of the A_j series. Similarly, the factors P (F, i, $n)_k$ in Equation F-2 are computed on the basis of the number of years from the beginning of the project to the expenditure.

A major drawback to the present worth method is that the initial expenditure C is hidden because it is combined with the other costs. This does not degrade the validity of the results; however, large one-time expenditures such as capital costs and (for example) future overhaul costs may require that the project owner obtain financing, so these numbers should be examined separately.

The equivalent uniform annual cost method contains the same information as the present worth method, but is expressed as an annual number based on the life of the project and the appropriate interest rate. In terms of the present worth:

$$AC = PW \cdot A(P,\ i,\ n)_1 \qquad (F-3)$$

where AC is the annual cost

The uniform capital recovery factor A (P, i, $n)_1$ is computed with n set equal to the life of the project. Obviously, AC could be calculated directly from the various individual transactions, in the same manner as PW in Equation F-2. However, it is simpler to use Equation F-3 when it is desired to calculate both AC and PW.

The annual cost method has an advantage over the present worth method in that it indicates the costs in the manner in which the consumer is most likely to encounter them (i.e., as a combination of periodic operating expenses and mortgage payments). This is more of a concern to the average homeowner than is the present worth of the system. In this contract, both present worth and annual costs will be calculated.

The internal rate of return method is very useful for businesses that invest money in capital projects and expect to generate revenue as a result of the investment. The rate of return can be calculated from Equation F-1 by trial and error for the case when most of the future transactions A and F are receipts (that is, have the opposite sign as C). The rate of return is the interest rate that yields a value of zero for PW. This would indicate that the future transaction benefits justify the investment of capital as long as the calculated rate of return is equal to or greater than the minimum acceptable rate of return selected by the company for capital projects.

Obviously, the rate of return method has no meaning if all transactions considered are disbursements. Since a home air conditioning system is not a revenue generating venture, it is necessary to assume a conventional baseline system and then calculate the rate of return on the incremental capital cost of a solar desiccant system, offset by the reduced costs of operation. The reductions in the future and annual costs would be taken as receipts. The rate of return is for the increase in capital cost for a solar system over a conventional system, whereas the present worth and annual cost methods are absolute measures without reference to a baseline system. In this project, the rate of return for the incremental solar desiccant system investment will be computed with respect to a conventional baseline air conditioning system.

SELECTION OF AN INTEREST RATE

For the most part, the cost of solar energy is dominated by the cost of the associated capital. In the case of a residential space conditioning system, the annual capital costs of the solar system actually represent the monthly payments over a year for the money borrowed to finance the solar system. Unfortunately, due to the way financial institutions function, it is nearly impossible for homeowners to compare energy cost savings with either the additional mortgage payment associated with adding solar systems to homes, or the annual cost of money one might borrow to retrofit such a system to a residence because inflation distorts the pattern of yearly payments over time. This distortion is a result of the difference between the real interest rate and the nominal interest rate. For example, if the inflation rate is 6 percent and the real interest rate is 3 percent, then the effective nominal interest rate (the rate charged by a bank) is 9 percent. If a consumer borrows $1000 at 9 percent for 30 years, the yearly payment would be $97.34. On the other hand, if there were no inflation and one could borrow at the real interest rate of 3 percent, the yearly payment would be $51.02. In the case of no inflation, the consumer would pay $51.02 in purchasing power during each of the 30 years of the loan. This is very different when inflation is considered because in the first year $97.34 would be paid in purchasing power, but by year 30 this would decrease to $16.95 in first year purchasing power. This is shown in Figure F-1.

This example illustrates why a combination of mortgage payment (which would be based on the real interest rate plus inflation) and projected present day fuel and operating costs should not be used to determine the annual cost or present worth of a solar project. If a bank mortgage payment is used in a life-cycle analysis, all future transactions must be corrected to account for inflation. Since this is not commonly done, answers are badly distorted.

A distinction also must be made between escalation and inflation. In particular, energy costs are expected to escalate in the future, which means that with zero inflation the cost of an energy resource will increase exponentially (i.e., compound) in first-year dollar terms. For the non-zero inflation case, an energy cost will increase according to the sum of the escalation and inflation rates. Escalation and inflation of energy costs are discussed in the next section.

A survey of 20 lending institutions in Southern California during December 1977 yielded an average mortgage rate of 9.5 percent for 30 (or 29-3/4) year terms for first trust deeds on owner-occupied single-family dwellings. Since the annual rate of inflation is now approximately 6.2 percent, the real interest rate is 3.3 percent per annum. These values will be used in this analysis as being typical of the cost of money in the United States and of the inflation rate during the near future.

ENERGY COSTS

The most important factors influencing economic viability of a solar air conditioning system are the energy supply costs that the system is intended to supplant. Unfortunately, these costs are the most difficult of all expenses associated with such a system to predict with certainty. The only prediction that can be made with absolute certainty is that energy prices will rise faster than almost any other commodities, anytime during the forseeable future.

Electric energy will be assumed to be available for $0.04/kwh at the beginning of 1978, and to escalate at 2.5 percent per year in constant dollar terms. When added to the general inflation rate of 6.2 percent per year, this is an 8.7 percent annual escalation in electricity prices.

Similarly, fossil fuel will be assumed to be available for $2.50/10^6 Btu at the beginning of 1978, and to escalate at 5 percent per year in constant dollar terms. Added to the general inflation rate of 6.2 percent per year, the rate becomes 11.2 percent per year. These figures are averages, and obviously must be expected to vary depending on the individual fuel in question. Energy price predictions based on these rates are shown in Figure F-2.

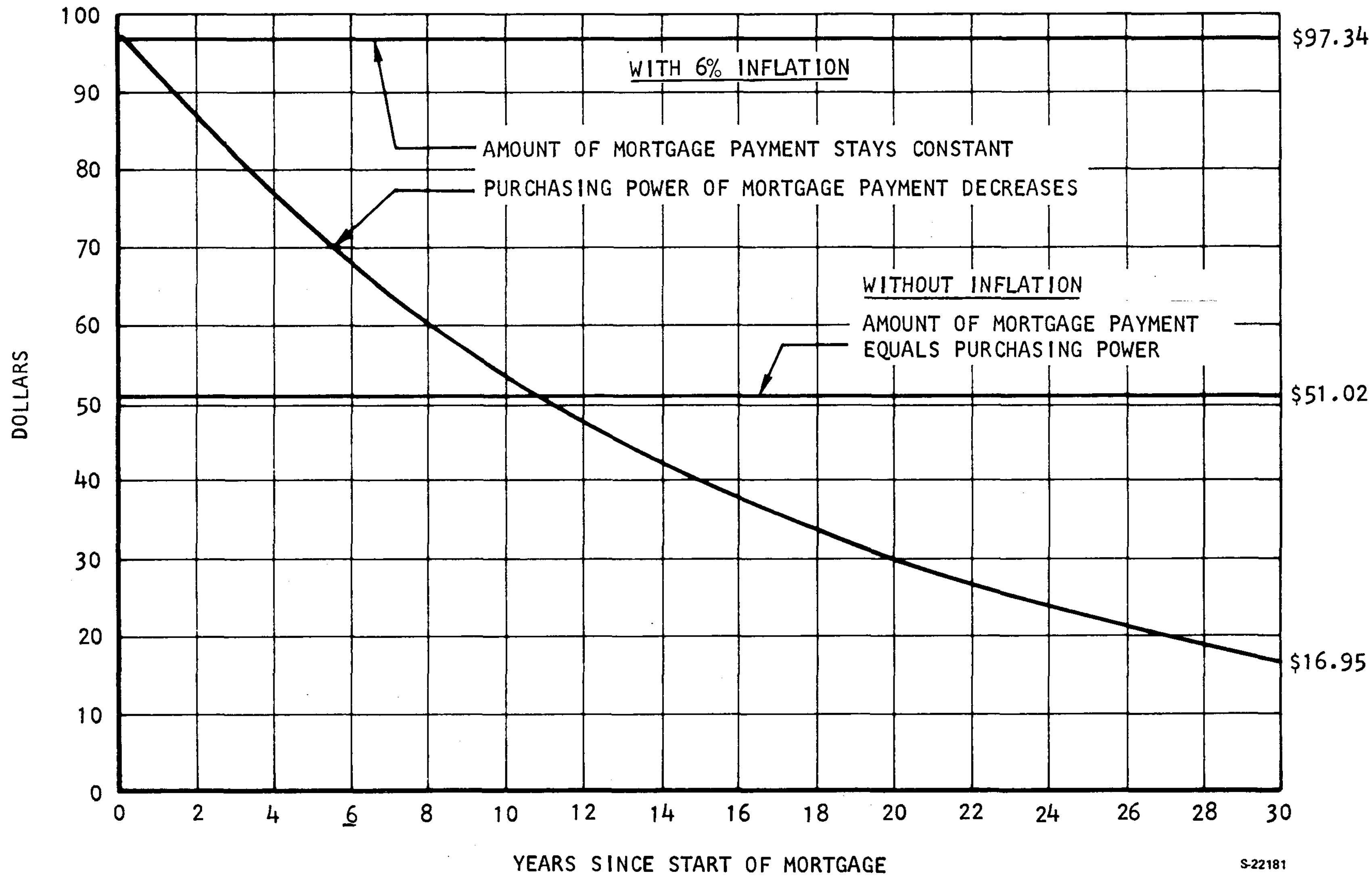

Figure F-1. Financing of Solar Project (Real Interest Rate = 3 Percent, Principal = $1000, Term = 30 Years)

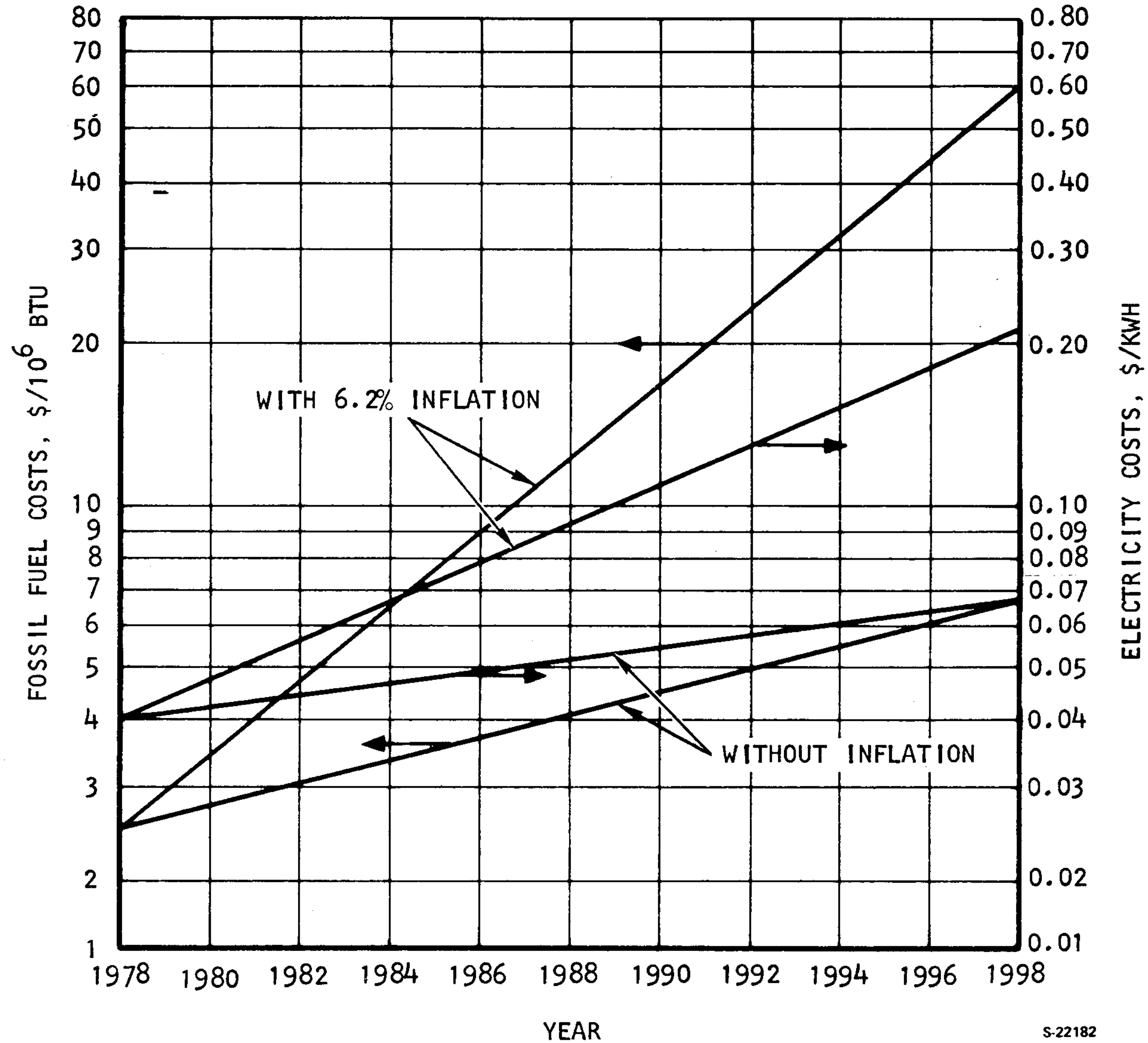

Figure F-2. Projected Energy Costs

Energy supply costs are likely to undergo significant restructuring in the near future. Natural gas is now subject to price controls that keep its price far below that of other fuels, even though it is a superior fuel in many respects to other fossil fuels. Both gas and electricity are delivered to most consumers by utilities whose rate schedules decrease as a consumer's consumption increases, thereby making excess consumption inexspensive. Oil prices are more nearly governed by market influences than are the other energy sources, but have a unique characteristic in that the world oil price is influenced strongly by OPEC. All of these controls and influences keep energy source prices from assuming levels that an open market would dictate. It is assumed (and, incidentially, hoped) that price controls will be relaxed so that energy conservative projects, such as this one, will become economically viable.

ECONOMIC INCENTIVES

A considerable amount of activity has taken place recently in various legislative bodies regarding tax credits and other economic incentives for people who install solar equipment. Many of these efforts have produced worthwhile results, but at the present time the overall picture is quite fragmented. This is unfortunate because in areas that have well-developed programs, they have made the difference between feasibility and nonfeasibility in many cases.

As an example of the influence from such a program, consider the program enacted by the California State Legislature, and administered by the State Franchise Tax Board. An individual installing active solar energy equipment may take a state income tax credit of $3000, or 55 percent of the cost of the installation, whichever is less. If all of the tax credit is not used in one year (i.e., the individual's income tax is reduced to zero), the excess credit may be carried forward to successive years as necessary. This can have a profound effect on the financial picture of such a project because the capital cost is the major obstacle for most people.

Other proposed programs include exemptions from property taxes for the value of the solar equipment and low-cost financing from utilities and Government. Most local programs and any future national program will probably include a combination of these methods.

Because of the nonuniformity of this factor, the influence of economic incentives must be evaluated for each site. For this study, the specific programs in effect for installation in Lake Charles, Phoenix, and New York City will be applied. Information was requested on these programs from the appropriate agencies in January. Responses have been received which indicate that no solar energy legislation has been enacted in Louisiana and New York; programs have, however, been discussed in both state legislatures, and it is possible that they will be enacted shortly.

The State of Arizona has enacted a variety of legislation providing substantial economic incentives. The applicable statutes are summarized in Table F-2; the data were supplied by the Arizona Department of Revenue.

CHAPTER 42 (SALES TAX EXEMPTION FOR ENERGY DEVICES)

ARS Sections 42-1312.01, 42-1409
33rd Legislature, May, 1977, House Bill 2063

Provides an exemption from sales and use tax for solar energy devices. Defines a solar device as a system or series of devices designed primarily to provide heating, cooling or both; produce electrical or mechanical power or both; pump irrigation water; or store solar energy. This exemption is effective as of August 27, 1977 and will expire in 1984.

CHAPTERS 83, 129, 165 (TAX DEDUCTION AND PROPERTY TAX EXEMPTION FOR SOLAR ENERGY DEVICES)

ARS Sections 42-123.01, 43-123.37

Chapter 93	32nd Legislature, May, 1975, Senate Bill 1011
Chapter 129	32nd Legislature, June, 1976, House Bill 2067
Chapter 165	31st Legislature, May, 1974, Senate Bill 1231

Rapid Amortization:

Provides for tax deduction for the installation of solar energy devices whether for residential, commercial, industrial or governmental installations or experimental or demonstration projects. Allows amortization of the cost of the solar energy equipment over 36 months for purposes of reporting income for Arizona state income taxes.

Property Tax Exemption:

Provides for the exemption of installed solar energy devices from the assessed value of the property.

CHAPTER 81 (INCOME TAX CREDIT FOR SOLAR ENERGY DEVICES AND RESIDENTIAL INSULATION)

ARS Sections 43-123.37, 43-128.03, 43-128.04
33rd Legislature, May, 1977, House Bill 2068, incorporates HB 2064

Provides for an income tax credit for installation of residential solar devices. The credit shall be thirty-five percent of the total cost of the installation if the installation takes place during 1978. The percentage of the cost of installation which shall be allowed as a credit shall decrease by five percent each year until the end of 1984. The maximum allowable credit is $1,000.

This act also provides for an income tax credit for installation of insulation and ventilation. The credit shall be equal to twenty-five percent of the total cost with the maximum allowable credit being $100. The credit shall only be available until December 31, 1984.

The 36 month amortization provided in Chapters 93, 129 and 165 (tax deduction and property tax exemption for solar energy devices) if claimed, shall be in lieu of, not in addition to, any other state income tax credit allowed for installation of a solar energy device.

APPENDIX G

TASK 1-2. DESIGN REQUIREMENTS AND EVALUATION CRITERIA: CONVENTIONAL SYSTEM MODELS FOR COMPARISON

INTRODUCTION

An extensive review of the available information concerning solar-powered air conditioning systems has been conducted in partial fulfillment of Task 1-2. This review was concerned with the establishment of baseline data defining the performance, physical characteristics, and cost of systems using (1) the Rankine/reverse-Rankine approach of a solar power plant driving a refrigeration plant, and (2) the $LiBr/H_2O$ absorption system. The baseline data are to be used later in the study for comparison with the solar desiccant dehumidifier operating in an integrated air conditioning system. The findings are summarized briefly below and the most pertinent information discussed, including adsorption system literature, evaluations with solar collectors, and AiResearch investigations. Also, Rankine air conditioner literature is reviewed.

SUMMARY

Air conditioners specifically designed for operation using solar thermal energy are only recently appearing on the commercial market. Most air conditioners installed in experimental solar houses have been conventional electric-driven vapor compression units or adsorption-type coolers. The latter are obsolete Arkla $LiBr/H_2O$ adsorption units modified for this specific application; the modification involves replacing the gas-fired generator with a water-fired unit to accommodate the solar collector subsystem interface. Under NSF sponsorship, Arkla has developed and started marketing a $LiBr/H_2O$ water chiller design incorporating a recirculation pump and a water-cooled adsorber. The anticipated performance of the unit is listed in Table G-1 at the operating conditions noted.

With respect to Rankine-driven refrigeration systems, the data listed in Table G-2 characterize the performance of such systems using state-of-the-art compressor and turbine designs. These values agree fairly well with experimental data obtained on a Barber-Nichols system developed for installation and evaluation in the Honeywell mobile solar laboratory.

TABLE G-1

ESTIMATED PERFORMANCE OF WATER-FIRED ABSORPTION AIR CONDITIONER

Cooling capacity	3 tons
Hot water source temperature	195°F in/185°F out
Chilled air temperature	80°F DB, 67°F WB in/57°F sat. out
Cooling water temperature	85°F in/103°F out
Coefficient of performance	0.65
Electrical consumption	875 watts maximum

TABLE G-2

TYPICAL STATE-OF-ART RANKINE AIR CONDITIONER PERFORMANCE DATA

Hot water inlet temperature	220°F
Evaporator temperature	45°F
Condensing temperature	90°F
Rankine-cycle efficiency	0.11
Vapor-compression cycle COP	6.0
Overall COP	0.65

The conclusions reached by various investigators as to the economic applicability of solar-powered air conditioners are widely conflicting (References G-1, G-2, and G-3)*. Overall system life-cycle cost and pay-back data vary by more than an order of magnitude. The discrepancies between the published data are due to the different assumptions basic to these studies. These assumptions are primarily related to (1) the projected cost of solar collectors, (2) the projected cost of fuel, and (3) the effectiveness of the heat-powered refrigeration system configuration and utilization. It is apparent from these studies that the cost of the solar collector is a decisive factor in determining payback time. Since the size of the collector is directly related to the effectiveness of the refrigeration system, every effort should be made to develop a refrigeration machine designed for maximum efficiency and low fabrication cost. The technology for this is available.

As an example, the solar collector size necessary to power a Rankine-cycle air conditioner can be reduced by 30 percent as the efficiencies of the system compressor and turbine increase from 70 percent to 80 and 85 percent. In itself, this represents a significant factor in the performance of economic studies. It is an objective of the present study program to determine the potential of Rankine-powered air conditioning equipment optimized for operation at the low-temperature heat source attainable from flat-plate solar collectors. The future utilization of solar-powered air conditioners may not be determined from economic factors, but rather may be imposed by legislation aimed solely at resolving the nation's energy dependency.

REVIEW OF ABSORPTION SYSTEM LITERATURE

An excellent treatment of absorption refrigeration systems is presented in Reference G-4. At the time (1957), Servel manufactured lithium bromide/water ($LiBr/H_2O$) air conditioners for residential use. These were atmospheric-steam or water-cooled units. In an effort to eliminate the requirements for cooling towers as ultimate heat sinks for the $LiBr/H_2O$ absorber, much work was

*References are presented at the end of this appendix.

performed in the development of refrigerant-absorbent combinations with improved vapor pressure properties more suitable to the design of air-cooled systems. Such a program, sponsored by the American Gas Association (AGA), is summarized in Reference G-5 (1968); data presented indicate that a LiBr/LiSCN/H_2O fluid system has lower vapor pressure characteristics, and this offers potential for air-cooling the absorber without crystallization.

Absorption-type air conditioners have not penetrated the residential market to any extent. Currently, only Arkla markets a small-tonnage (3-ton) unit that is specifically designed for solar operation. This unit, designated the SOLAIRE 501-WF, uses a LiBr/H_2O cycle, is water cooled, and includes an air chilling coil and blower so that the unit can be directly connected to forced-air ductwork. Data typical for the performance of this unit are given in Table G-3. The coefficient of performance is 0.65 at a condensing water supply temperature of 85°F and at air inlet conditions of 80°F dry bulb, 67°F wet bulb.

ABSORPTION SYSTEM EVALUATIONS WITH SOLAR COLLECTORS

Wisconsin University Tests

An early Arkla 3-ton LiBr/H_2O absorption unit (Model DUCS-2) was tested in conjunction with a flat-plate solar collector at the University of Wisconsin in 1962 (Reference G-7). In this installation, the generator (designed for steam heating) was heated with liquid water from the solar collector. The lower heat transfer coefficient obtained with water resulted in a reduction in capacity from 3 to 2 tons. The absorption system provided cooling with water temperatures at generator inlet as low as 180°F and 85°F cooling water. A coefficient of performance between 0.4 and 0.6 was generally achieved on test.

Marshall Space Flight Center Tests

A water-cooled Arkla LiBr/H_2O system was modified by replacing the gas-fired generator with a water-fired unit compatible for operation with a flat-plate solar collector. This modified unit was designed to provide 3 tons of refrigeration at a COP of 0.65 with water temperatures of 210°F at generator inlet and 85°F at absorber inlet. Such a unit was installed in the NASA Marshall Space Flight Center Solar House for experimental evaluation (Reference G-8). Estimated performance for this version of the Arkla unit is presented in Reference G-1. Figure G-1 (taken from Reference G-1) shows the sensitivity of the cooling capacity of the unit in terms of water temperature at the inlet of the generator and the absorber. For an 85°F cooling water temperature (which represents a normal design value for cooling towers), the capacity of the unit will drop from 3 to 1.5 tons as the generator water inlet temperature drops from 210°F to 180°F.

Arkla Industries

Under NSF sponsorship, Arkla has developed a modification of their basic absorption systems. Several modifications were explored, including direct evaporative cooling of the absorber and condenser. The program is discussed in Reference G-9. The result of these investigations is the Solaire 501-WF unit previously described. The January 1978 list price of this unit is $2070, FOB Evansville, Indiana (Reference G-10).

TABLE G-3

SPECIFICATION DATA FOR
ARKLA MODEL SOLAIRE 501-WF SOLAR ABSORPTION
AIR CONDITIONER
(MODIFIED FROM REFERENCE G-6)

Capacity	3 ton (36,000 Btu/hr)
Energy supply	
Hot water input	55,000 Btu/hr
Hot water inlet temperature	210°F
Hot water flow	1 gal/min
Pressure drop	2 psi
Maximum permissible flow	22 gal/min
Minimum permissible inlet temperature	180°F
Air circuit	
Airflow	1200 cfm
Air inlet drybulb temperature	80°F
Air inlet wetbulb temperature	67°F
Air outlet temperature (saturated)	57°F
Energy sink	
Energy rejection rate	91,000 Btu/hr
Condensing water inlet temperature	85°F
Condensing water flow	10 gal/min
Pressure drop	1.75 psi
Maximum permissible flow	17.5 gal/min
Electrical**	
Voltage	115/230* vac, 60 Hz, single phase
Fan motor power	1/2 hp
Full load current	8.0/4.0* amp
Typical operating power	450 w
Physical	
Operating weight (approx.)	985 lb
Shipping weight (approx.)	1060 lb
Dimensions (approx.)	75 in. high by 55 in. wide by 27 in. deep

*Fan motor can be field-changed between 115 and 230 v operation.
**Cooling tower fan and circulating pumps not included in electrical loads.

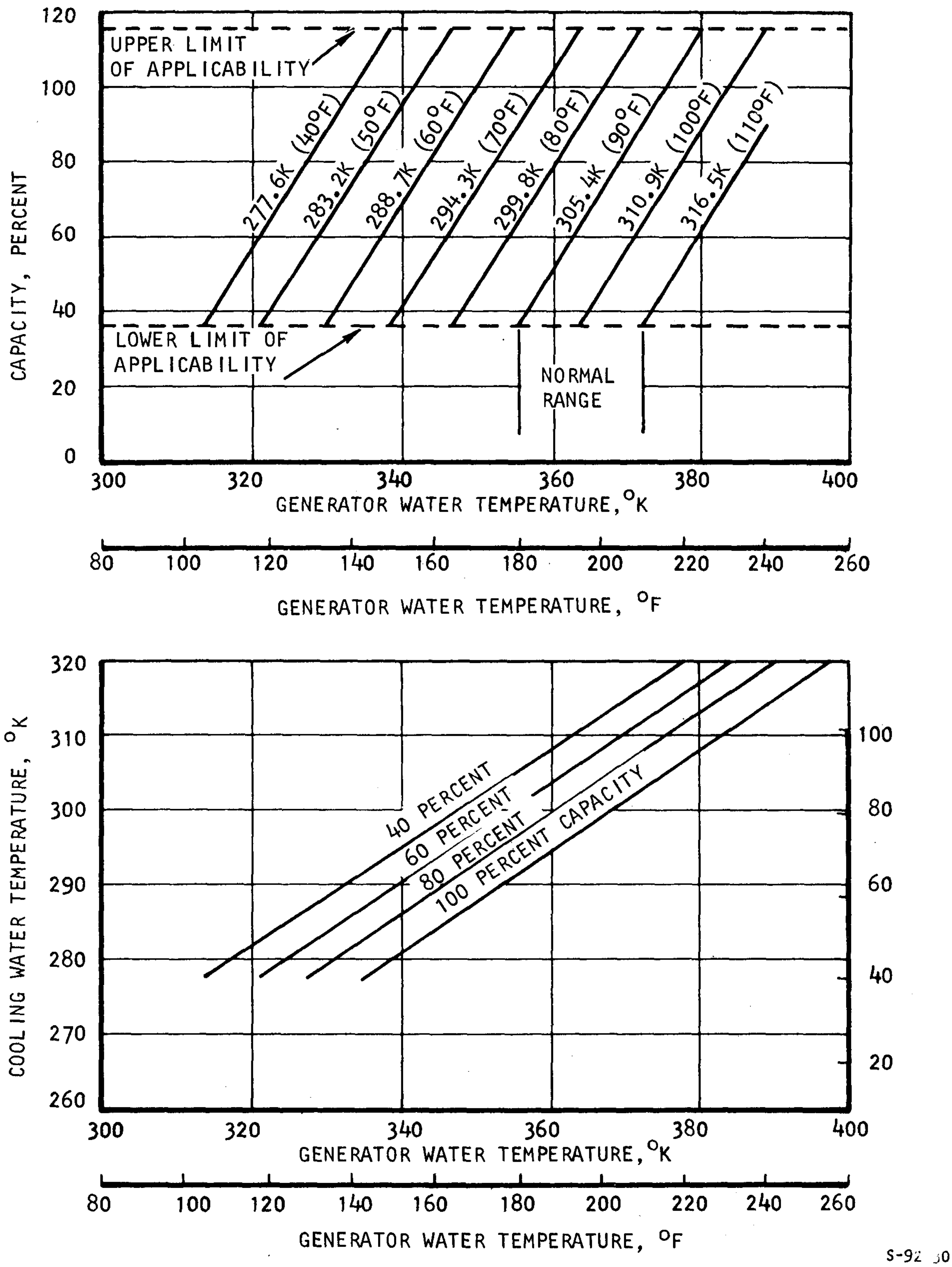

Figure G-1. Performance of Modified Arkla $LiBr/H_2O$ Refrigerator (From Reference G-1)

A computer program was developed by AiResearch to generate parametric LiBr/H_2O absorption system performance data. The system modeled is illustrated in Figure G-2. The program computes cycle COP for fixed values of the following system parameters.

(a) Generator temperature

(b) Absorber temperature

(c) Condenser temperature

(d) Evaporator temperature

(e) Evaporator load

(f) Recuperator effectiveness

(g) Absorber effectiveness

The computation procedure involves iterative material and energy balance calculations until the concentrations of the solution in the absorber and generator are such that the thermodynamic and mass transfer requirements established by the input parameters are satisfied. The pressure drop in each system element is taken into account and pump power is computed. This program was exercised over a range of conditions for fixed values of recuperator effectiveness (0.8) and absorber efficiency (0.6); these values appear realistic for the system considered. The data have been checked against published performance for this type of unit from Carrier, Trane, and Arkla, and good agreement has been established. The data are presented in Figure G-3 as cycle COP (evaporator load/generator heat input) plotted as a function of hot water supply temperature and chilled water temperature. Each plot corresponds to a different condensing water temperature.

Examination of the data indicates that for any combination of absorber-condenser-evaporator temperatures, the attainable COP remains about constant over a wide range of hot water temperatures. However, as the hot water temperature drops below a critical value, the design of a LiBr/H_2O absorption system becomes thermodynamically impossible. Since the computer program is a design program rather than a performance prediction program, the plots of Figure B-3 cannot be used to predict off-design point performance because the concentration of the LiBr/H_2O solution varies for each condition represented by the system temperatures. Referring to Figure G-3, it is apparent that hot water temperatures higher than 220°F are necessary to provide a heat sink temperature consistent with the requirements for a dry cooling tower, which would be a desirable simplification in a home installation. An evaporative cooling tower should reliably provide 85°F cooling water, requiring hot water temperatures over 180°F. It follows that the design of such a system will require relatively high effectiveness heat exchangers for operation. The effects of absorber and recuperator effectiveness on cycle COP for fixed values of system operating temperatures are shown in Figure G-4. The plots

ABSORPTION CYCLE

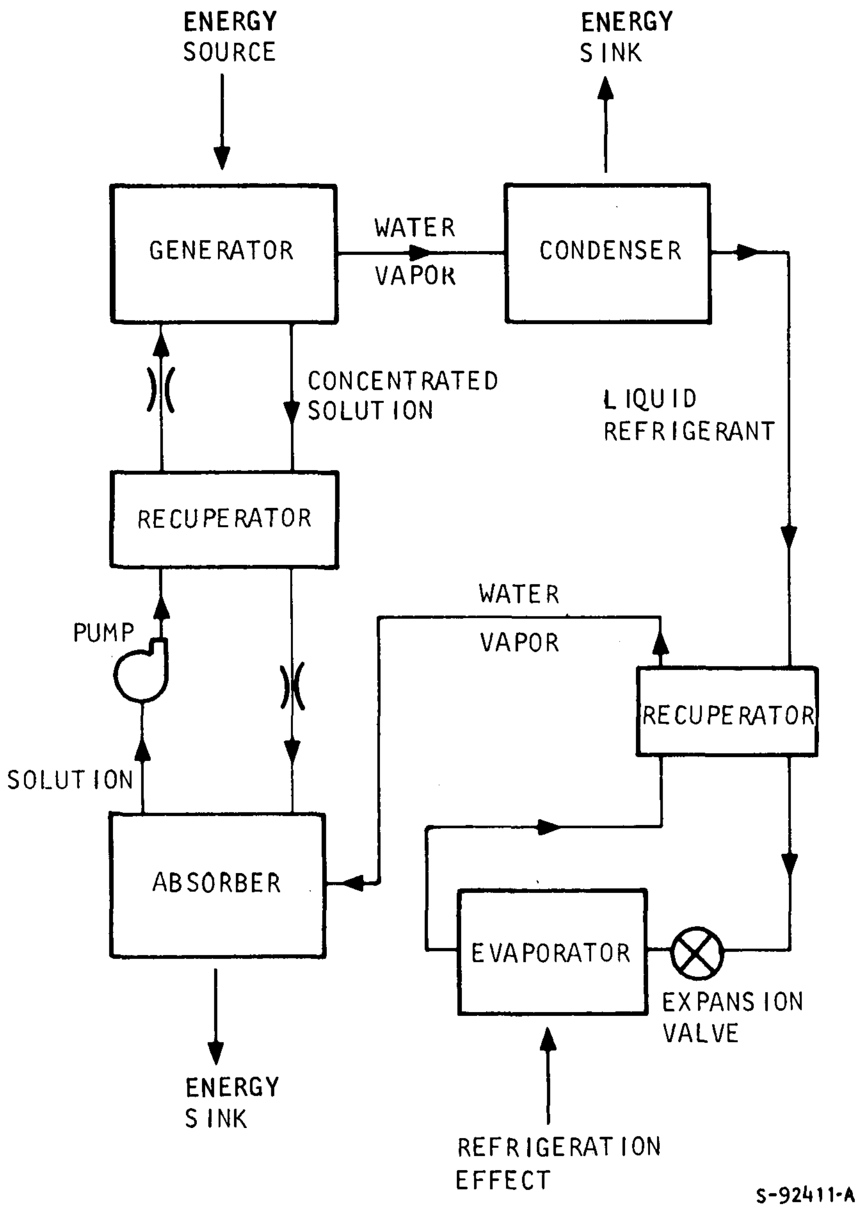

Figure G-2. LiBr/H_2O Absorption System Schematic

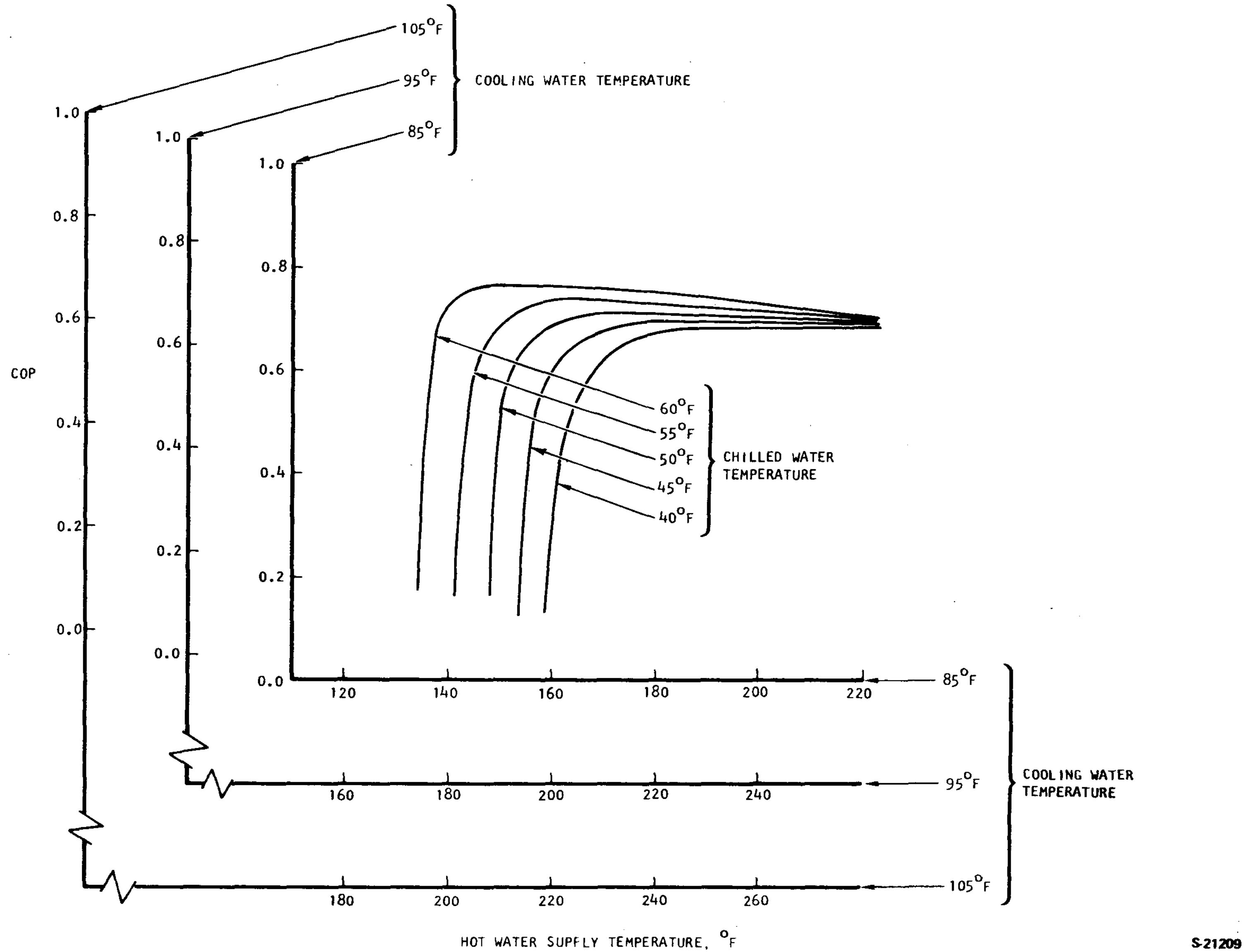

Figure G-3. Single Effect LiBr/H_2O Absorption Chiller Performance From Trane, Carrier, Arkla and AiResearch Performance Predictions

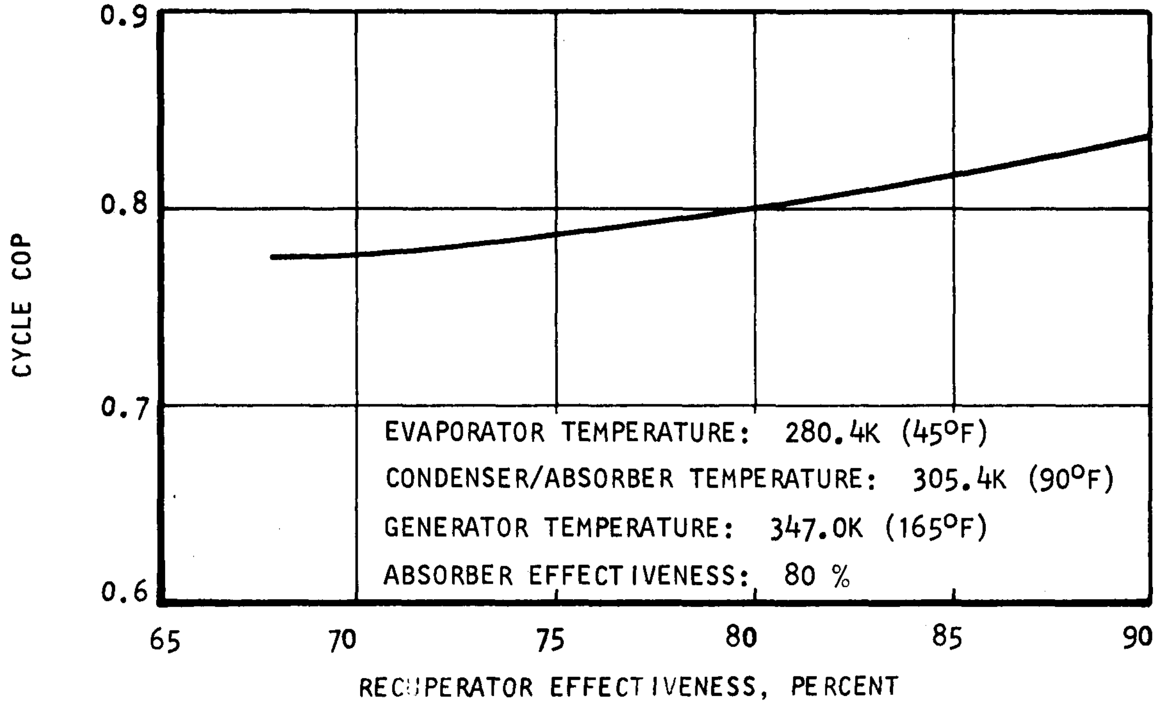

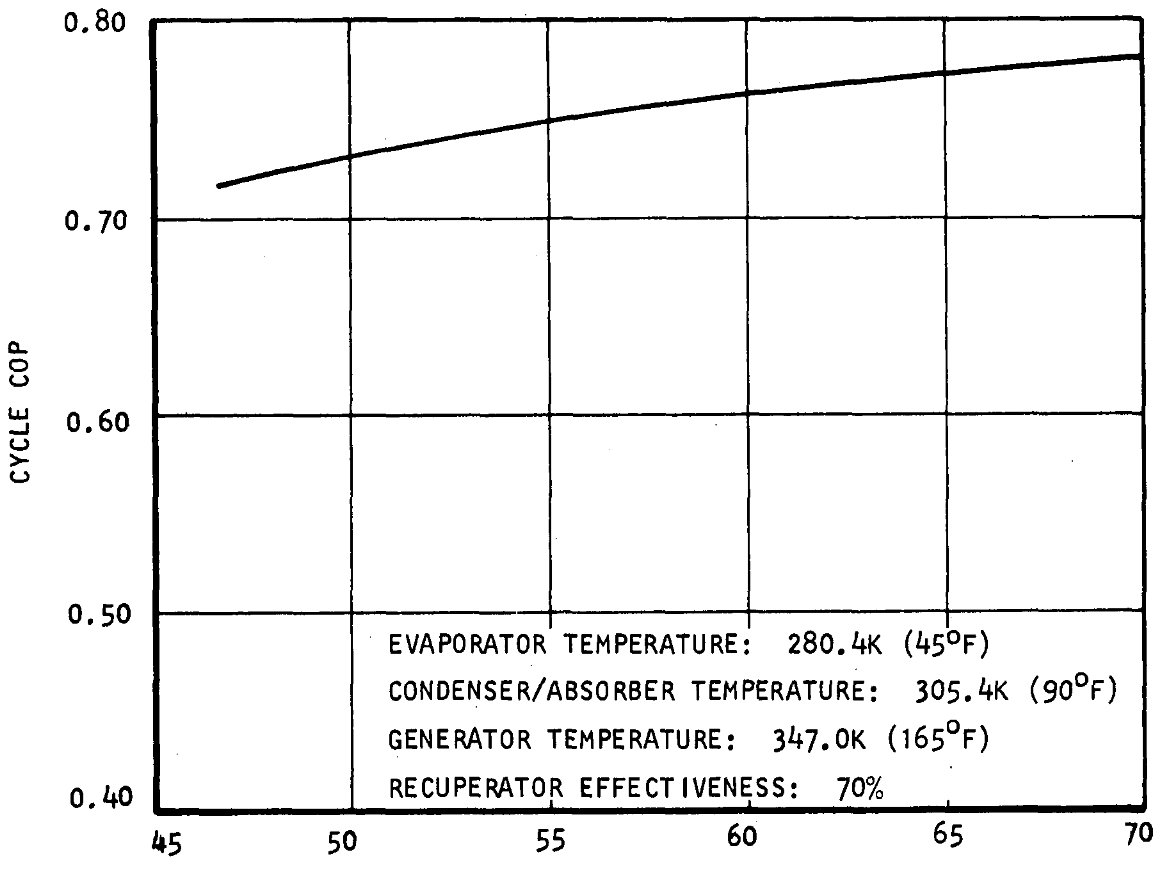

S-92433

Figure G-4. Effect of Absorber and Recuperator Effectiveness on $LiBr/H_2O$ Refrigeration System Performance show a relatively small change in COP as a function of these two parameters. The COP shown includes the effect of pressure drop on system performance. However, these data are somewhat optimistic because heat losses and gains from ambient are not considered in the calculation procedure. Such losses would easily result in a drop in COP as large as 0.1.

REVIEW OF RANKINE AIR CONDITIONER LITERATURE

A thorough review of Rankine-power systems and equipment was published in 1974 by Hittman Associates, Inc. (Reference G-2). This review was conducted under NSF Contract C858. Emphasis was placed on the Rankine power loop, and the air conditioner portion of the overall system was not presented at the same level of detail. Some of the information contained in Reference G-2 is discussed below in the context of the current contract. Also, additional programs covered in the Hittman survey are summarized. Some of the organizations currently active in this field are:

(a) Barber-Nichols Engineering

(b) General Electric Co.

(c) AiResearch Manufacturing Company

Hittman Survey Data

The Rankine power system and equipment data compiled by Curran et al. are summarized in Table G-4 (from Reference G-2). Most of the Rankine engines listed were designed for electrical power generation from relatively high grade thermal energy; also, the power output of these machines far exceeds the requirements of a 3- to 5-ton refrigerant compressor (about 3 kw). However, the data are significant because the efficiencies attained with various types of expanders and liquid pumps are representative of existing design technology. Also, the machines listed are experimental units and in general have not been subjected to extensive developmental efforts aimed at maximizing efficiency. The data show that expander efficiencies between 70 and 80 percent can be achieved with various types of machines (turbine, rotary, and reciprocating) over a relatively wide range of power output.

Cycle efficiency, however, is dependent on the operating temperature levels of the boiler and condenser. Data from Reference G-2 were used in the preparation of Figure G-5. The overall efficiency shown is defined as follows:

$$\text{Overall cycle efficiency} = \frac{\text{net Rankine-cycle power}}{\text{boiler heat input}}$$

where the net Rankine-cycle power is the expander power less the power necessary to drive the loop pumps, fans, and controls. The overall efficiencies of Figure G-5 represents 55 to 65 percent of the Carnot efficiencies corresponding to the source/sink temperature shown, with the higher Carnot approach occurring at the lower boiler temperatures.

TABLE G-4

SUMMARY OF CHARACTERISTICS FOR SMALL RANKINE ENGINES (FROM REFERENCE G-2)

Manufacturer/ No. Designer	Type of Fluid	Type of Expander	Type of Application	Conceptual/ Experimental/ Production C/E/P	Cycle Conditions: Expander Inlet °F/psia	Cycle Conditions: Condenser °F/psia	Rated Power hp	Expander: Efficiency %	Expander: RPM @ Rated Power	Pump: Efficiency %	Pump: Power hp	Condenser Fan Power hp	Actual Overall Cycle Efficiency %	Estimated Service Life Years
1. Aerojet-Liquid Rocket	AEF-78	Turbine	Automobile	E	650/1000	201/35	74.9	69	26,500	60	25.6	9.7	10*	
2. Barber-Nichols	R113	Turbine	Solar Cooling	E	200/57	95/9.5	2.7	75	51,180	50	.1		8.3*	
3. Energy Research	Water	Rotary	Automobile	C	1200/3500	281/50	100.0	76		80			19.1	
4. Fairchild-Hiller	FC75	Turbine	Total Energy Plant	E	428/206	217/14.5	25.34	77.7	20,000				**	
5. Keller	Water	Rotary	Solar Power Plant	C	400/250	160/5	Any	80	1,800	80			16.	20
6. Keller	Water	Rotary	Automobile	C	550/1000	275/45	50-200	80	200-2000	80		0.5	10.	10
7. Kinetics	R113	Rotary	Automobile	E	375/355	200/55	47.0	70	3,500	85	4.0	5-7	***	
8. Kinetics	R114	Rotary	Solar Cooling	E	200/180	80/35	7.5	70	2,500		0.32		10.2	
9. Lear	Water	Turbine	Automobile	E	1100/1100	222/19	82.7	62	65,000		1.77	2.01	17.6	
10. Ormat	MCB	Turbine	Powerpack	P	Variable		3.0	70	20,000				6.0	20
11. Philco-Ford	MIPB	Turbine	Powerpack	E	600/37	374/1	0.13	54					5.0	
12. Steam Engine Systems	Water	Reciprocating	Automobile	E	550/750	228/20	135.0		2,750				**	
13. Scientific Energy Systems	Water	Reciprocating	Automobile	E	1000/1000	230/20	140.0	70	500-2000	80	20	7+	17.2	10-20
14. Sundstrand Aviation	CP-25	Turbine	Total Energy Plant	E	825/195	137/3.4	134.1	70	25,200		30-40		20.0	20
15. Sundstrand Aviation	Dowtherm A	Turbine	Powerpack	E	700/70	255/.5	8.05	72	24,000				17.4	20
16. Thermo Electron	Fluorinol 85	Reciprocating	Automobile	E	600/700	208/34	145.5	70	1,800	80	11.2	13.6	16.0	
17. Thermo Electron	Fluorinol 85	Turbine	Automobile	E	600/700	208/34	145.5	70	30,000	70	11.8	13.6	16.0	
18. Thermo Electron	CP-34	Reciprocating	Powerpack	E	550/500	220/25	5.0	75	3,600	60	0.37	0.25	13.0	
19. Thermo Electron	R114	Reciprocating	Solar Cooling	C	212/265	120/63	3.15	72	1,800		0.33		8.0	
20. United Aircraft	R113	Turbine	Solar Cooling	C	200-375/ 70-340	125/16.8	4.3	80	50,000				++	
21. United Aircraft	R114	Turbine	Solar Cooling	E	250-275/ 250-400	120/63	8.0	70	27,000				++	

* Not given in Reference. Calculated by HAI from data in Reference.

\+ Value assumed for efficiency calculation

** Not given in Reference. Insufficient data for calculation.

*** Final results of current research not yet available.

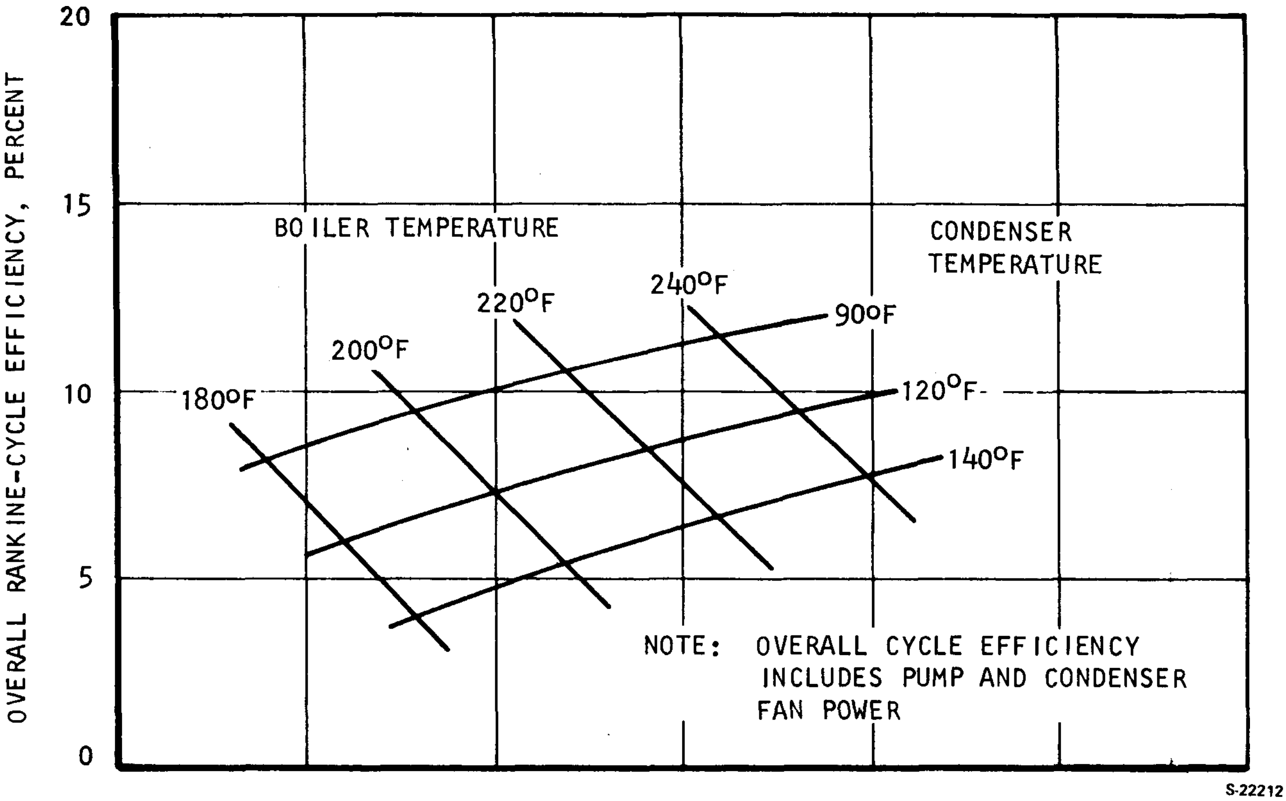

Figure G-5. State-of-the-Art Rankine Engine Efficiencies

Barber-Nichols Investigations (References G-11 and G-12)

Barber-Nichols has developed a solar-powered Rankine-cycle air conditioner for installation and evaluation testing in the Honeywell transportable solar laboratory. This program was conducted under joint sponsorship of NSF (Grant PTP 74-01555) and Honeywell, Inc. A schematic of the solar-powered air conditioner is shown in Figure G-6 (from Reference G-12). A motor-generator is used to supplement the Rankine turbine when solar heat is not adequate to drive the air conditioning compressor. When the turbine output exceeds the requirements of the compressor, electric power can be generated. The system is designed to provide 3 tons of refrigeration with a collector water temperature of 215°F and a condenser water temperature of 85°F.

System overall performance (COP) is shown in Figure G-7 as a function of collector water temperature. The data were obtained prior to installation in the solar laboratory; an overall COP of 0.5 was achieved. Through further development and relatively minor component and system improvements, it is anticipated that the overall COP should be increased significantly (above the 0.6 value at design point). It is significant that the system did operate with collector water temperatures as low as 170°F. This is 45°F below design value. Under this condition system capacity drops from 3 to 1 ton; also, the

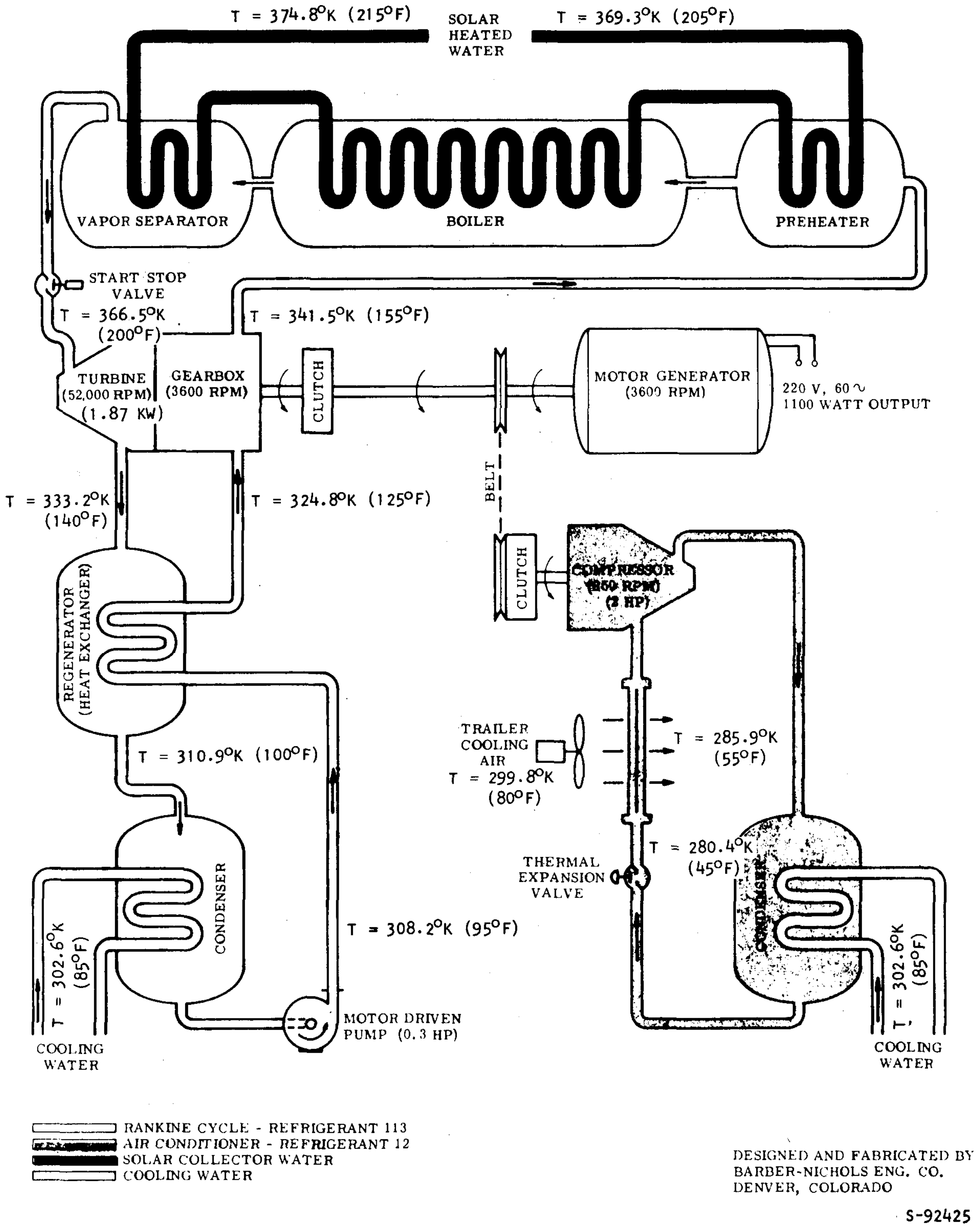

Figure G-6. Barker-Nichols Solar-Powered Rankine-Cycle Air Conditioner (From Reference G-12)

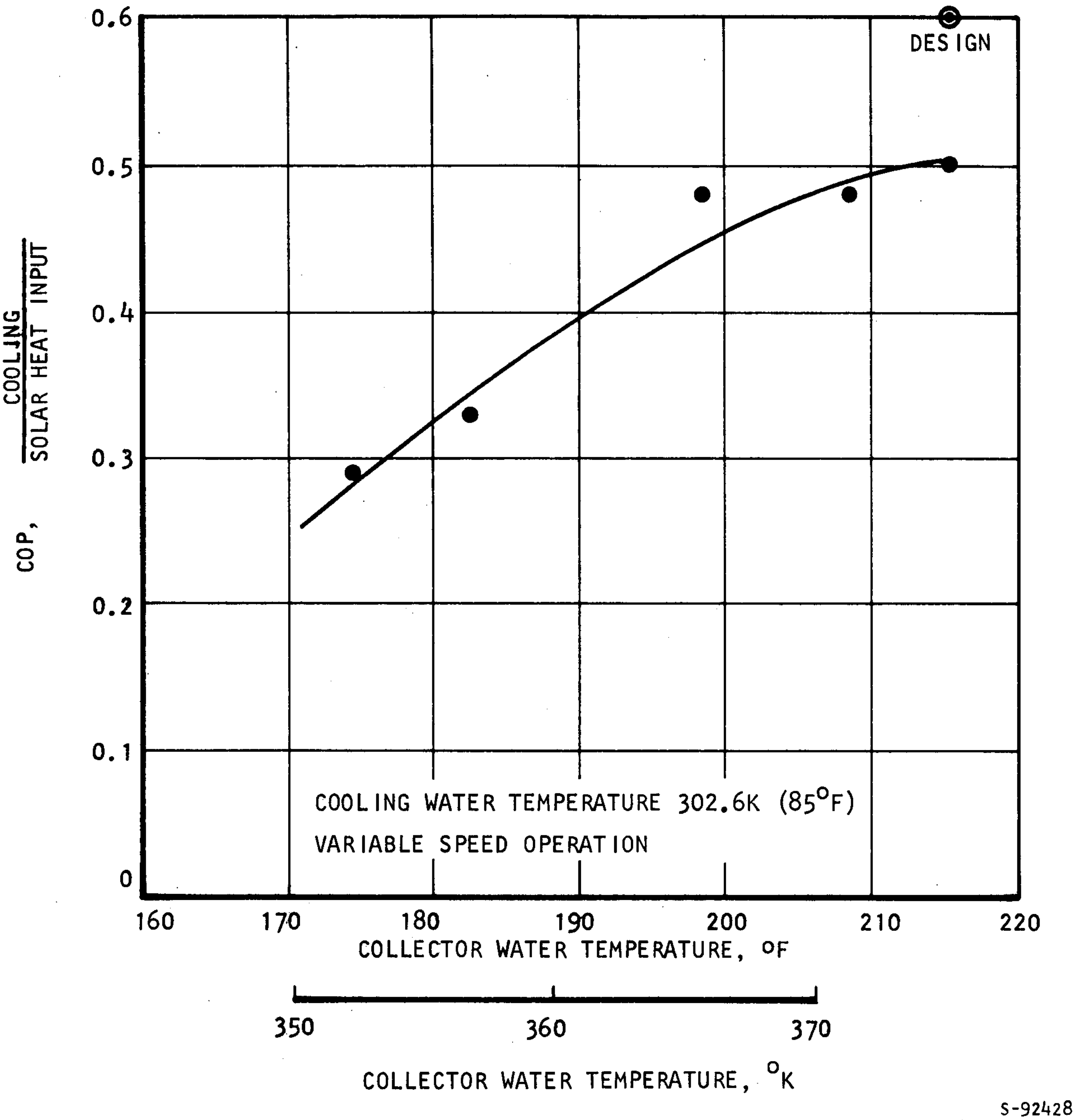

Figure G-7. Barber Nichols System Test Performance (From Reference G-12)

COP decreases from 0.5 to about 0.25. Data presented in Reference G-11 show that a turbine efficiency of 72 percent was achieved; also, the efficiency could be maintained above 65 percent by maintaining turbine speed at design value through the use of the electric motor.

General Electric

General Electric Space Division has been engaged in the development of a multi-vane expander for low-temperature Rankine-cycle application for about 5 years. A 4.85-kw Freon unit is currently in test. Expander efficiencies as high as 75 percent have been achieved, and through development it is anticipated that this value can be increased to 85 percent. Figure G-8 (from Reference G-13) shows the expander configuration and its performance over a range of flow. A 3-ton commercial refrigerant compressor was coupled to a multivane expander and tested over a range of temperatures. The unit has been subjected to 1020 hr of unattended endurance testing. A COP of about 0.5 was achieved, corresponding to the following conditions.

Expander efficiency	= 72 percent
Compressor efficiency	= 60 percent
Condenser efficiency	= 100°F
Expander inlet temperature	= 200°F

The major advantage of a vane expander is the high torque at low speed.

AiResearch Investigations

AiResearch has been engaged in the development of solar-powered Rankine heating and cooling systems for approximately two years under contract from NASA (Contract NAS8-32091). This contract covers the design, development, and testing of 3-, 25-, and 75-ton heating and heating/cooling heat pump systems, and the installation of the equipment in several demonstration facilities. As part of this work, a detailed computer model has been developed to predict system performance. Schematics of the complete installation and the heat pump portion of the 3-ton heating/cooling system are shown in Figures G-9 and G-10, respectively.

The AiResearch-NASA systems are somewhat more complicated than needed for this study because they incorporate heating capability and total system control. However, the cooling performance of the system is not compromised as a result of this extra capability, so the predicted performance in the cooling mode represents state-of-the-art capability in Rankine systems. Cooling COP is shown in Figure G-11 as a function of evaporator temperature, hot water supply temperature, and cooling water temperature.

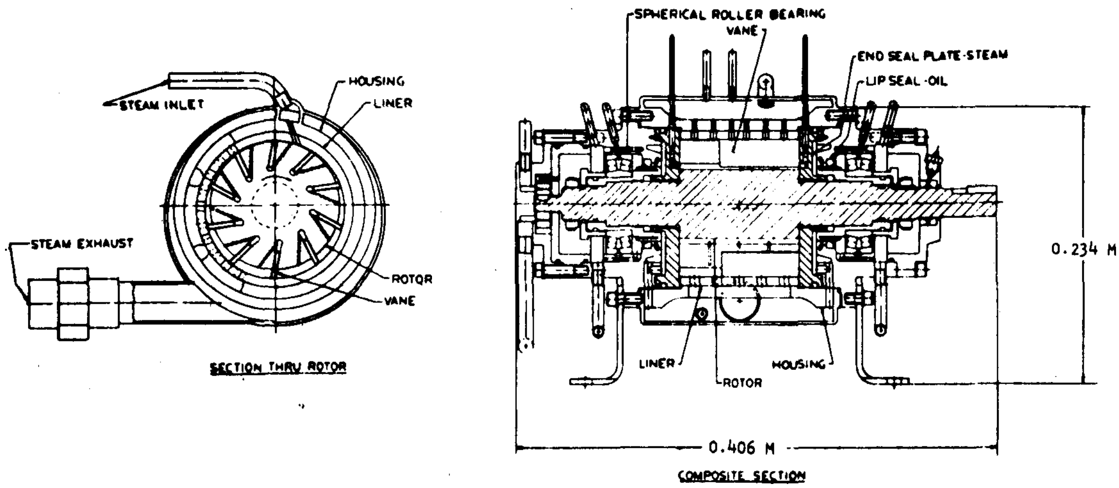

a. CONFIGURATION

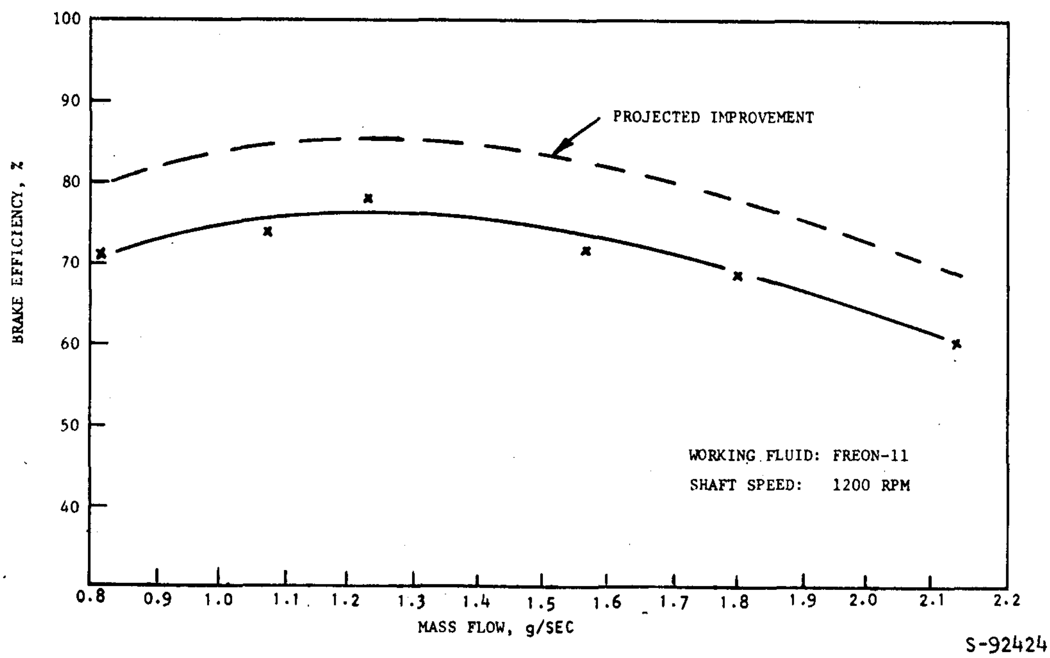

b. PERFORMANCE

Figure G-8. General Electric Multivane Expander (From Reference G-13)

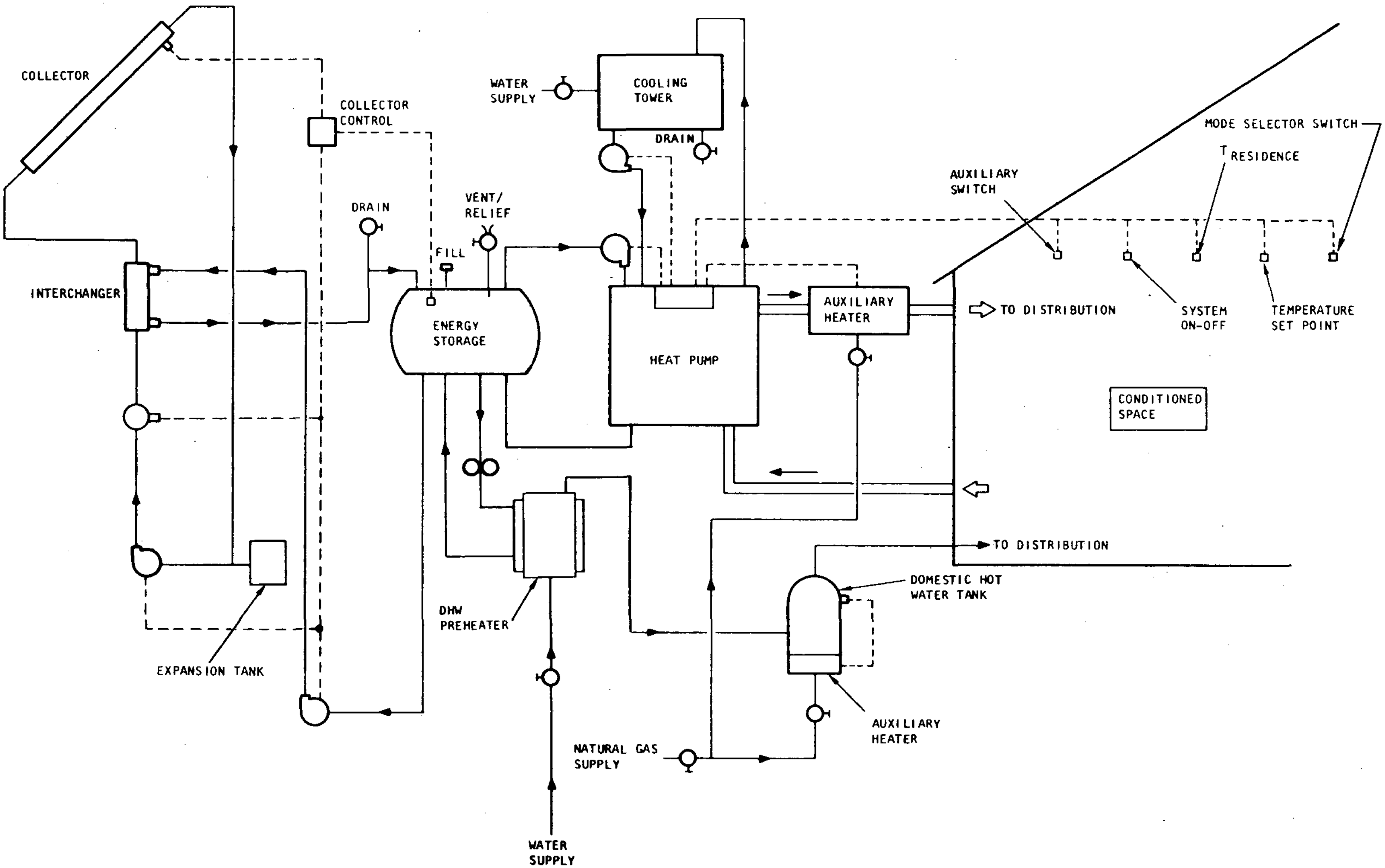

Figure G-9. Single-Family Residence Heating and Cooling System

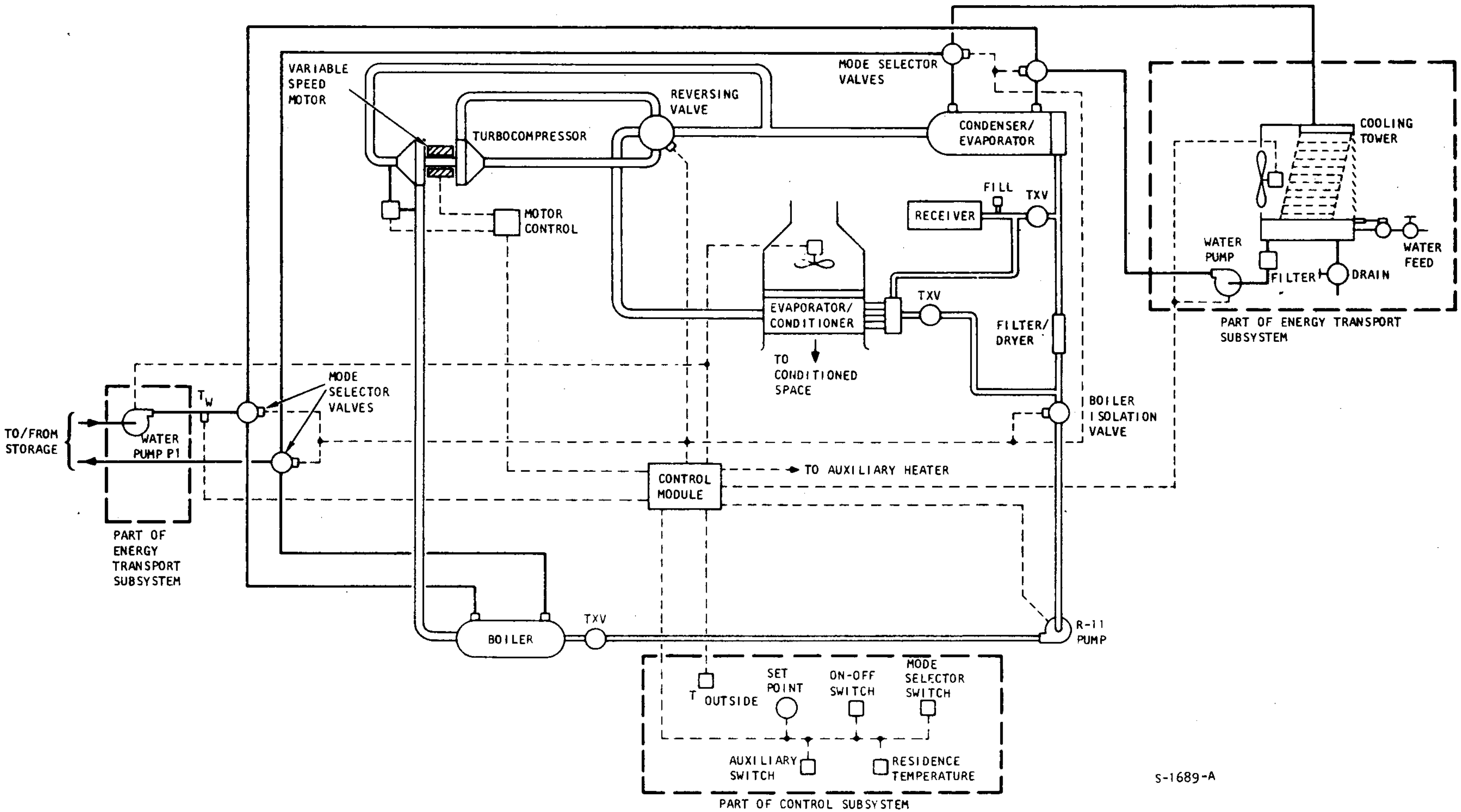

Figure G-10. Single-Family Residence Space Heating and Cooling Subsystem

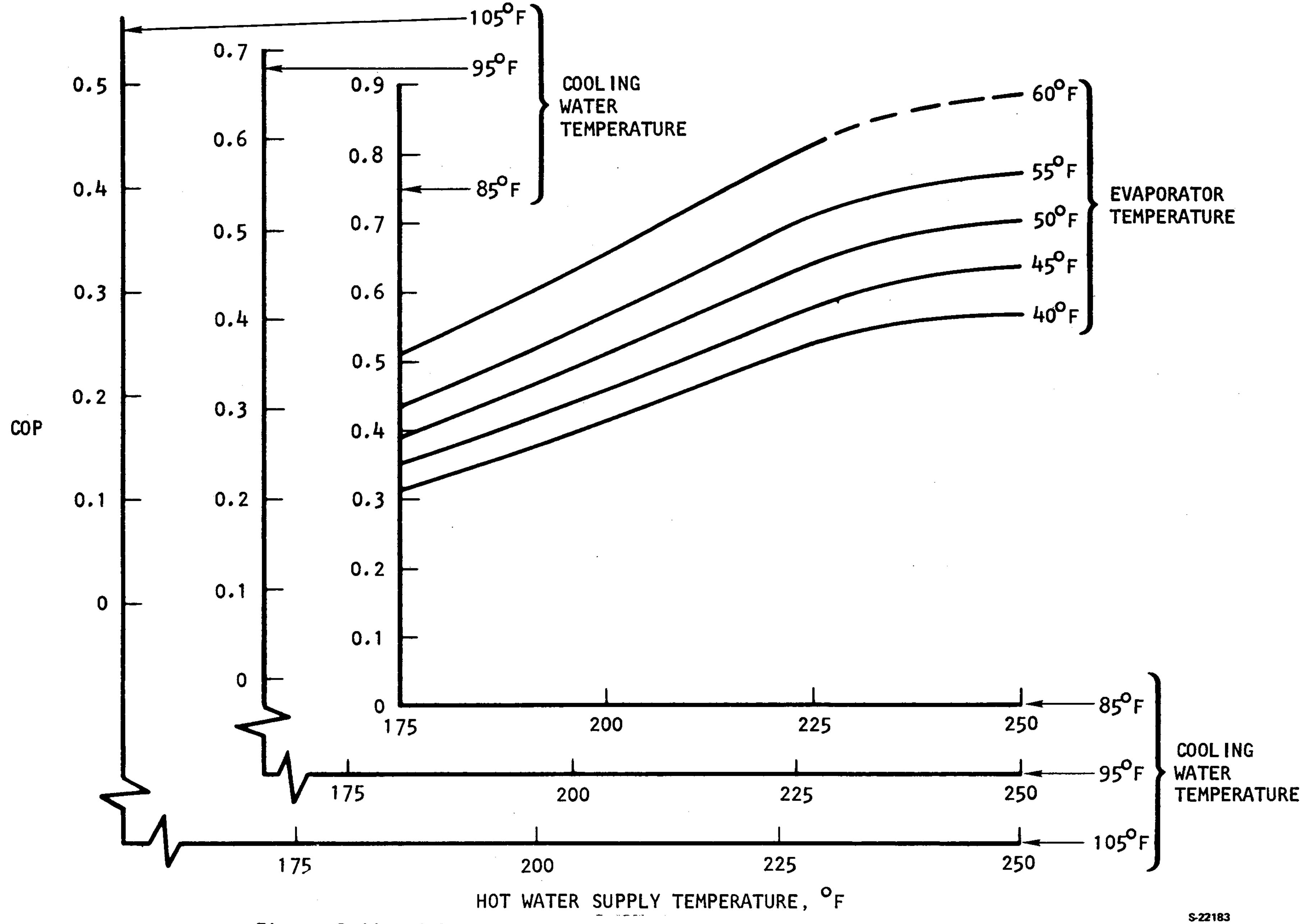

Figure G-11. AiResearch-NASA 3-Ton Rankine Cooling System Performance

REFERENCES

G-1. Solar Heating and Cooling of Buildings, Phase 0, Final Report, NSF/RA/N-74-022C (Appendix Volume), TRW Systems Group, May 1974.

G-2. Curran, H. M. et al., Assessment of the Rankine Cycle for Potential Application to Solar-Power Cooling of Buildings, NSF Contract C858, Final Report HIT-581, Hittman Associates, Inc., Columbia, Maryland, August 1974.

G-3. Solar Heating and Cooling of Buildings, Phase 0, Final Report, NSF RA-N-74-021 A, Volume I, Executive Summary, May 1974.

G-4. Ellington, R. T., Kunst, G., Peck, R. E., and J. F. Reed, The Absorption Cooling Process--A Critical Literature Review, Institute of Gas Technology Research Bulletin 14, August 1975.

G-5. Macriss, R. A., "Physical Properties of Modified LiBr Solutions," Paper Presented at Symposium on Absorption AC Systems, AGA, February 1968.

G-6. Arkla Specifications for Solaire Model Sol-WF, Form SP52T-1, Arkla Industries, Inc., Evansville, Indiana, 1977.

G-7. Chung, R., Duffie J. A., and G. O. G. Lof, "A Study of Solar Air Conditioner," Mech. Eng., Volume 85, August 1963.

G-8. The Development of a Solar-Powered Residential Heating and Cooling System, National Aeronautics and Space Administration, Marshall Space Flight Center, Report M-TU-74-3, May 1974.

G-9. Solar Optimized Absorption Cooling Unit, Research Proposal to the National Science Foundation, 73-22, Arkla Industries, Inc., November 1973.

G-10. Private Communication, Arkla Industries, Inc., January 1978.

G-11. Prigmore, Daryl R., and Robert E. Barber, "A Prototype Solar Powered, Rankine Cycle System Providing Residential Air Conditioning and Electricity," Proceedings of the 9th Intersociety Energy Conversion Engineering Conference, August 1974.

G-12. Design and Test Report for Transportable Solar Laboratory Program, Honeywell Systems and Research Center, Report 2852-41433, October 1974.

G-13. Private Communication, General Electric Company, Energy Systems Programs, Cincinnati, January 1975.

APPENDIX H

TASK I-3. CANDIDATE COOLING SUBSYSTEMS

INTRODUCTION

The solar desiccant dehumidifier is a latent load control device, with sensible cooling capacity added by means of a humidifier. Adding sensible cooling in this manner represents a simple and inexpensive way to complete an air conditioning system, but there are several drawbacks inherent in this approach. First, in most operating conditions, supply airflow rates will be significantly higher than with conventional systems. With careful design, noise and draft problems that could be caused by high airflow can be minimized or eliminated.

The second problem can be more troublesome. There is little flexibility in selecting the relative humidity of the supply air to the space when the sensible cooling is done by adiabatic saturation. Thus, it may be possible to meet the total cooling demand, but the supply air state may not fall on the sensible heat factor line for the process (as drawn on a psychrometric chart), in which case the rate of moisture removal from the space will not match the rate of moisture addition. This is most likely to occur when either the ambient relative humidity is high or the conditioned space internal latent loads are high. To obviate this problem, dry processed air could be bypassed around the humidifier. Of course, the supply air dry bulb temperature would increase if this were done.

A third consideration, one most important in a solar cooling system, is the fact that overall better thermodynamic performance may be achieved with a hybrid dehumidifying-cooling system instead of the simple dehumidifying-humidifying system. Especially in large systems, improvements in COP can represent substantial savings in collector and storage system costs.

In this appendix, the psychrometric processes in which a hybrid can be useful are discussed and the characteristics of cooling subsystems are outlined. Also, examples that illustrate the savings that can be expected with hybrid systems are presented.

PSYCHROMETRIC PROCESSES

In the design of an air conditioning system for a particular space, it is necessary to assume equilibrium design state conditions for the air in the space, and then to evaluate the loads that the air conditioning equipment must meet to maintain the assumed conditions. In most cases, the load will be a mixture of moisture and energy removal from the space. Since the ratio of energy removal associated with condensation of the water to the total energy load is different for each individual application, the supply air conditions must be adjusted to meet both the moisture and energy removal demands. There are several methods in use in the air conditioning industry to express the moisture-to-energy relationship; some are more useful than others, depending on the application. For residential applications such as this project, the sensible heat factor (SHF) is convenient. SHF is defined as follows*:

$$SHF = \frac{\text{Sensible Cooling Load}}{\text{Total Cooling Load}}$$

Figure H-1 illustrates the significance of SHF on a basic psychrometric chart. Return air from a conditioned space is denoted by state R. Lines of SHF = 1.0, 0.8, and 0.5 are drawn through R with the aid of a protractor-style scale on most commercially available psychrometric charts. These lines are only approximately straight because the rectangular coordinates of the psychrometric chart, humidity ratio (pounds of water/pound of dry air), and dry bulb temperature are not linearly related to enthalpy. The straight line approximation is close enough for most air conditioning calculations, however. For simplicity, the condition R is assumed to include ventilation and equipment loads.

Once the SHF line has been drawn, any supply air state that falls on the SHF line will satisfy the design point moisture and energy loads. The designer must select a state on the line that gives reasonable airflows, equipment characteristics, etc.

Figure H-2 shows three possible supply air states--S_1, S_2, and S_3--for the three SHF lines. For purposes of discussion, the three states have the same enthalpy, which results in the same air mass flow rate per ton. Of particular interest are the methods required to process the return air from state R to state S_1, S_2, or S_3.

For the case of SHF = 1.0, no moisture need be removed from the air. State R and state S_1 both have a humidity ratio of W_1. No moisture will condense until the air is cooled to point C_1 at temperature Ts_1 on the saturation curve. If the cooling is done by a coil, the cold-side fluid will have to be, say, 5°F colder than T_1.

When some moisture must be removed, as is the case with SHF = 0.8, the required state S_2 can be formulated by mixing some bypass (uncooled) air from state R with some cooled, dehumidified air at state C_2. Air at C_2 is obtained by cooling state R air at constant moisture to state C_1, and then along the saturation curve to state C_2, which has humidity ratio W_2'. By varying the proportions of state C_2 air and state R air, state S_2 can be located with humidity ratio W_2. In this case, the cooling coil cold-side temperature must be below Ts_2.

The third case, SHF = 0.5, illustrates a situation where the required supply state S_3 cannot be obtained by mixing refrigerated air with return air. Instead, air at state R must be cooled at constant humidity ratio W_1 to state C_1, and then along the saturation curve to C_3 at temperature Ts_3 and humidity ratio W_3. The air can then be reheated to state S_3. This situation

*Only cooling loads are considered here due to the intent of the project. The concept of SHF is also valid for heating applications.

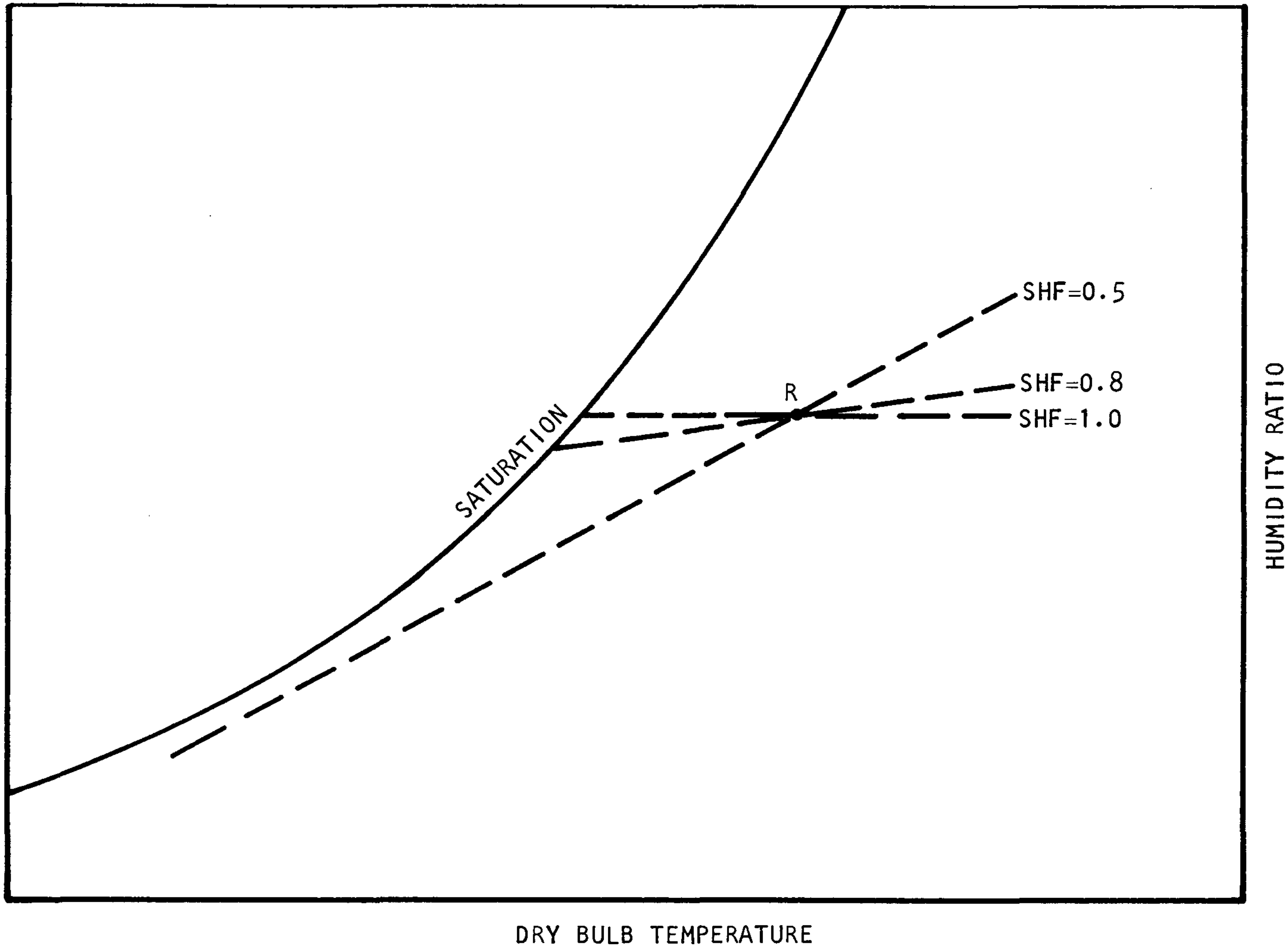

S-25014

Figure H-1. Different Sensible Heat Factor Lines for a
Given Return Air Condition

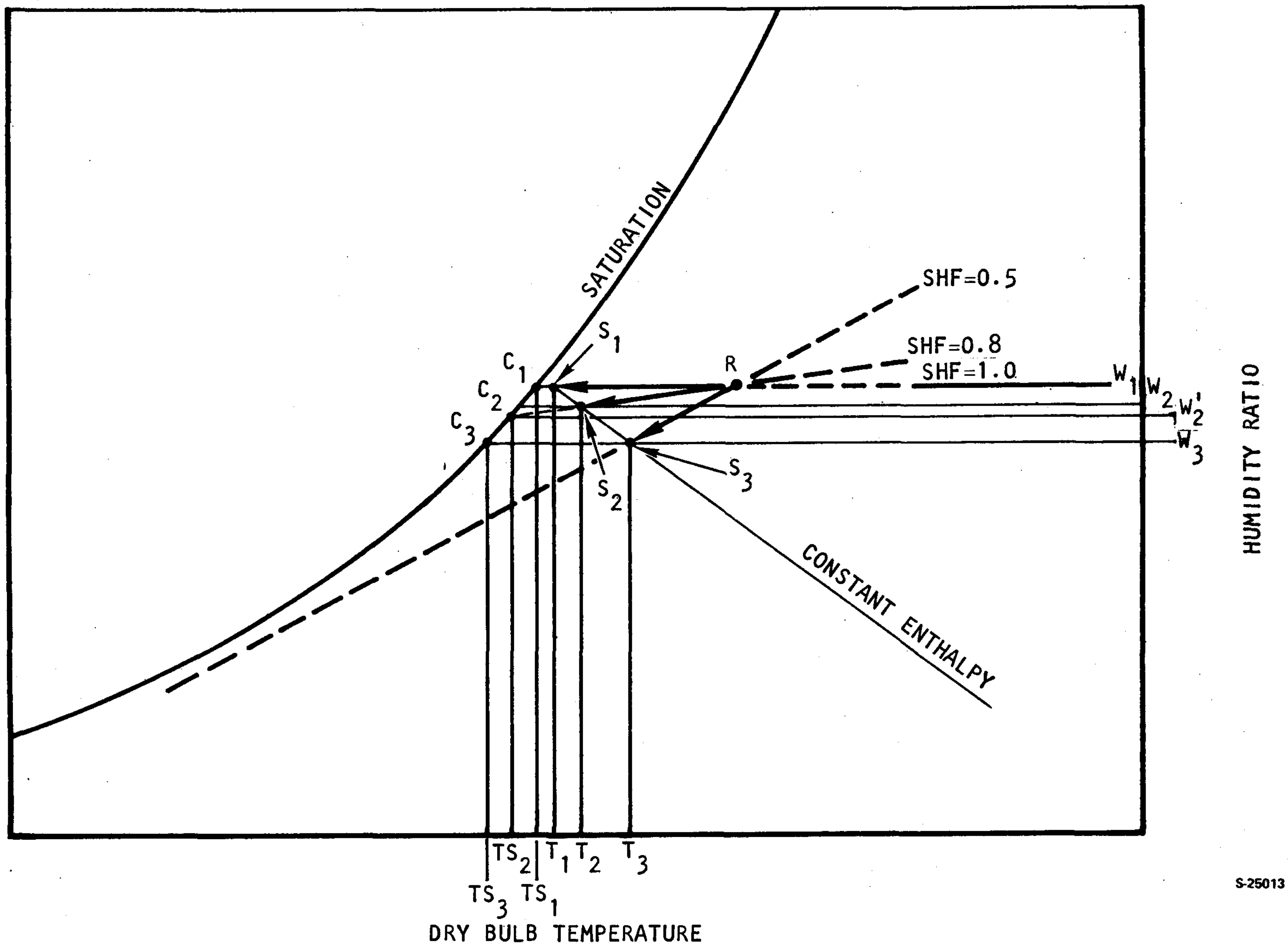

Figure H-2. Cooling Processes for Various Sensible Heat Factors exists whenever the SHF line does not intersect the saturation curve, or whenever the intersection occurs at a very low temperature. As before, the coil cold-side temperature must be below Ts_3.

These three illustrations show that the larger the latent fraction of the load, the lower the temperature at which the cooling must take place. Furthermore, the temperature difference between the coldest air state and the supply air state becomes larger as the SHF becomes smaller. This also is indicative of irreversibility. Because of the low temperatures required to carry out dehumidification by conventional coils, a desiccant system should yield improved thermodynamic performance when used in a hybrid system.

HYBRID SYSTEM CONFIGURATIONS

To maintain the concept of an entirely solar-powered air conditioning system, only solar-powered cooling subsystems will be considered here. A review of such systems is given in Appendix G. Design-point performance for a typical LiBr/H_2O absorption chiller and the AiResearch NASA 3-ton Rankine cooling system are given in Figures H-3 and H-4. These performance predictions will be used as typical in the example applications discussed below. For a discussion of these systems, refer to Appendix G.

A block diagram of a hybrid solar desiccant-conventional cooling system is shown in Figure H-5. The solar desiccant subsystem is shown in series with a cooling subsystem.

EXAMPLES

To illustrate the advantages of hybrid systems, particularly in high latent load applications, two situations are considered. Case A represents a typical residence. Return air is assumed to be 78°F DB, 67°F WB, which is the same as the design point for this project. The SHF is assumed to be 0.8. Case B represents high latent load application, a commercial kitchen. Return air is assumed to be 80°F DB, 70°F WB, and SHF is 0.5. In both Case A and Case B, outside air is taken as 95°F DB, 75°F WB. The solar thermal energy supply temperature is 200°F, and cooling tower water is assumed to be available at 85°F.

Case AI. Residence with Solar Desiccant-Evaporative Cooling System

Case AI is essentially the same as the baseline system of this project. Referring to Figure H-6, return air at state 1 is dehumidified by the desiccant bed to state 2, cooled by the regenerator to state 3, and saturated to state 4. State 4 is the supply air state, falling on the SHF = 0.8 line drawn through state 1, the return air. Outside air, state 5, is humidified to state 6, and then used to cool the regenerator, exhausting at state 7. Supply air, state 4, will be at about 63°F DB, 60.5°F WB. This system will operate with a COP of about 0.52.

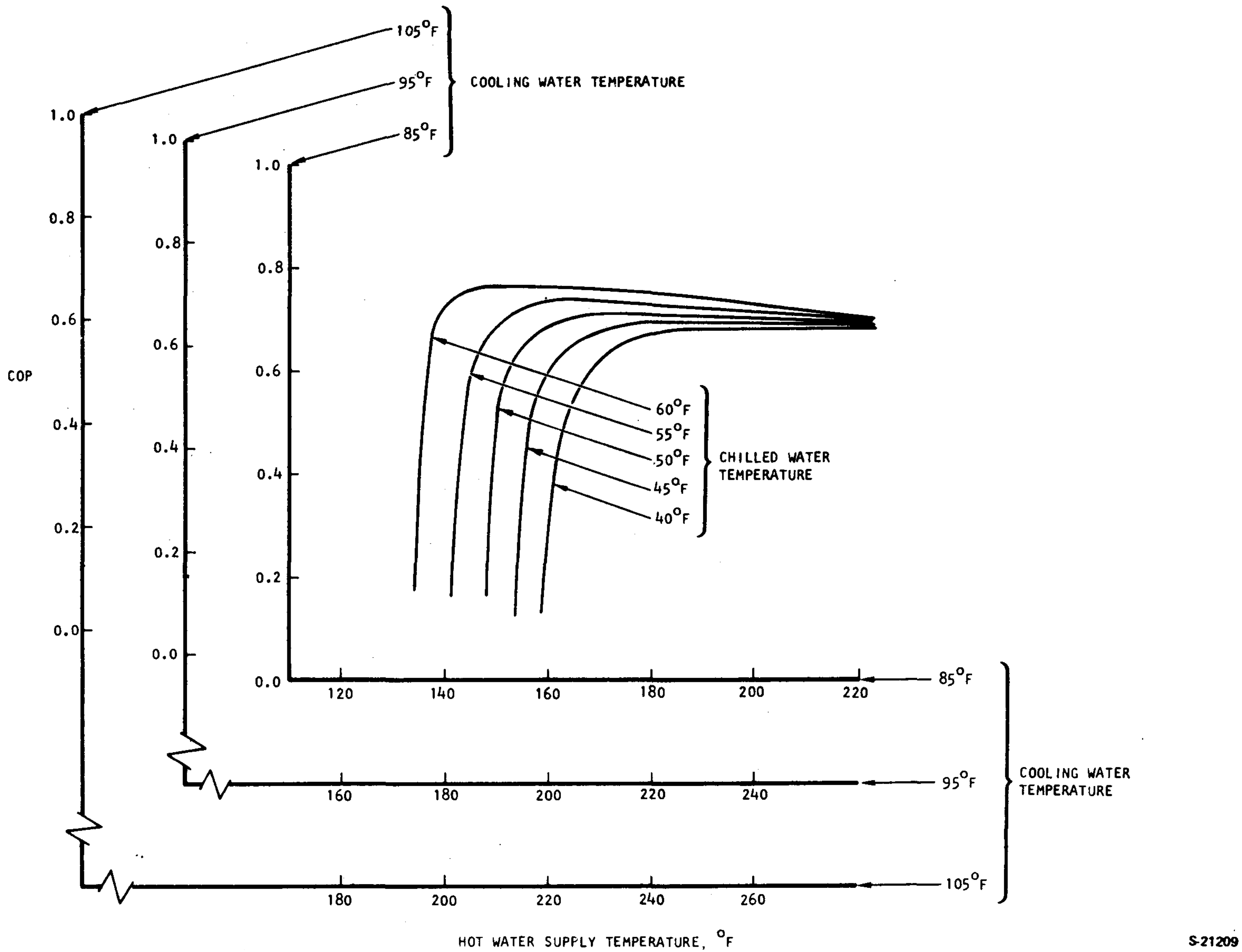

Figure H-3. Single Effect LiBr/H_2O Absorption Chiller Performance From Trane, Carrier, Arkla and AiResearch Performance Predictions

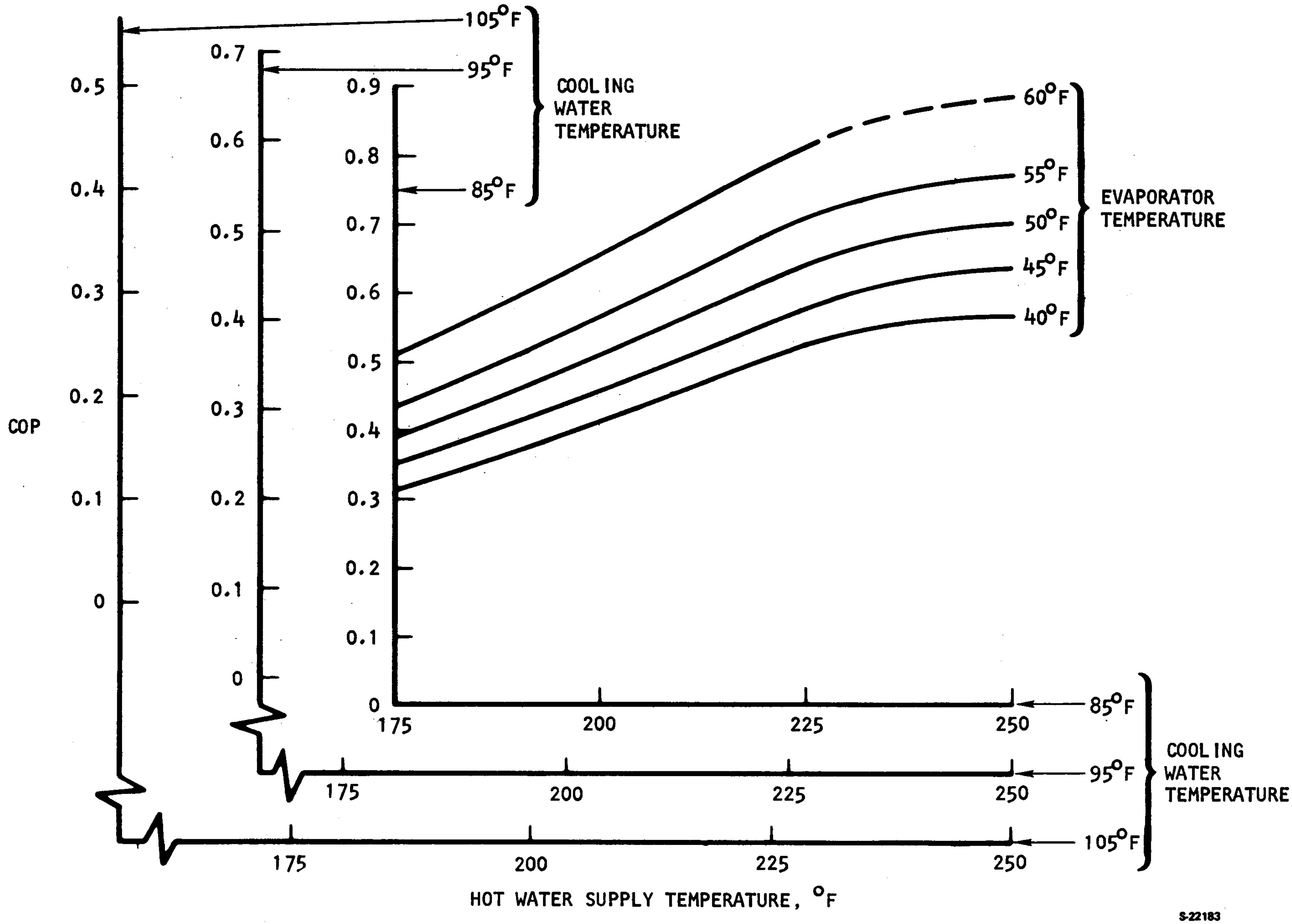

Figure H-4. AiResearch-NASA 3-Ton Rankine Cooling System Performance

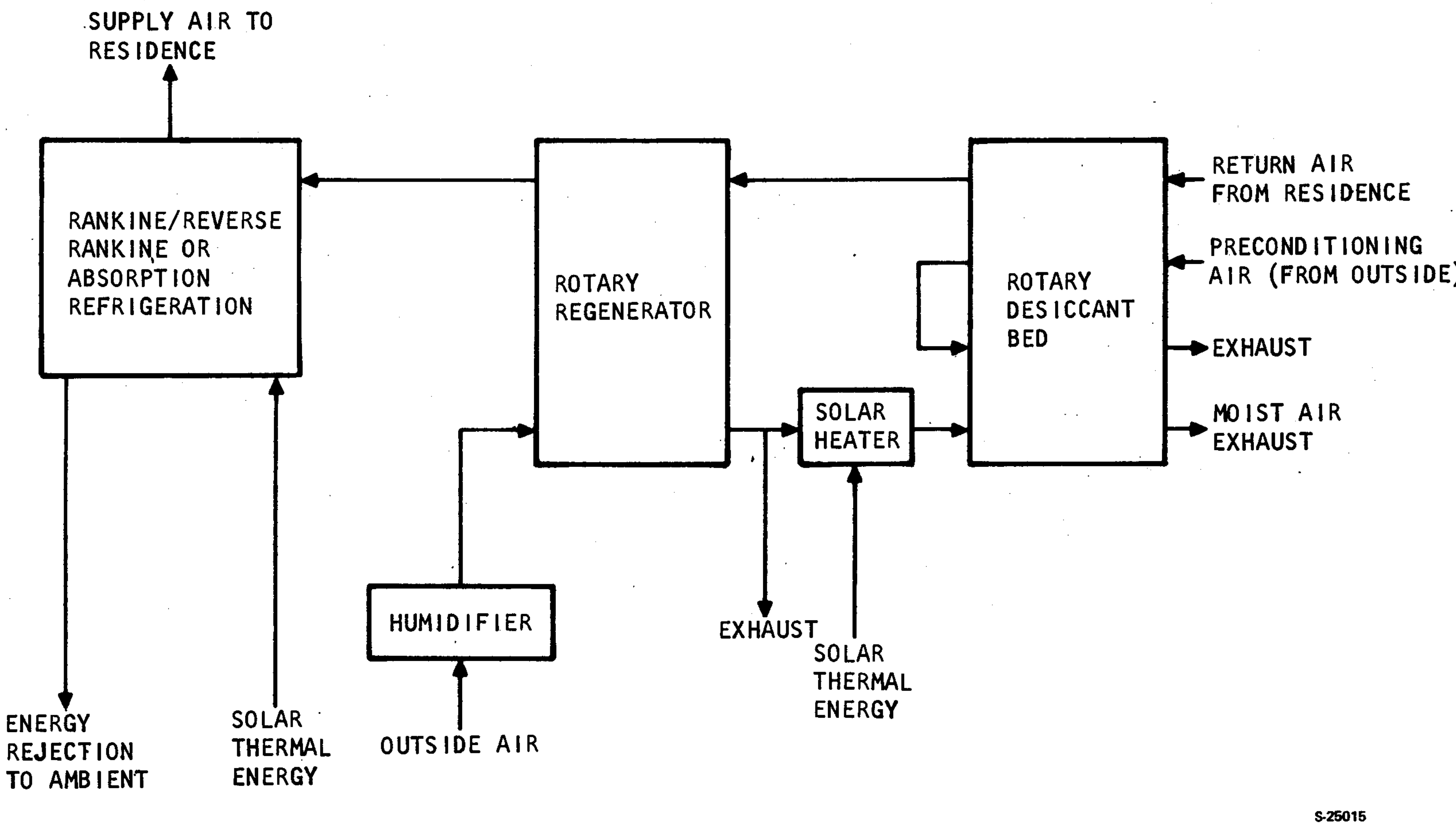

Figure H-5. Hybrid Solar Cooling System Block Diagram

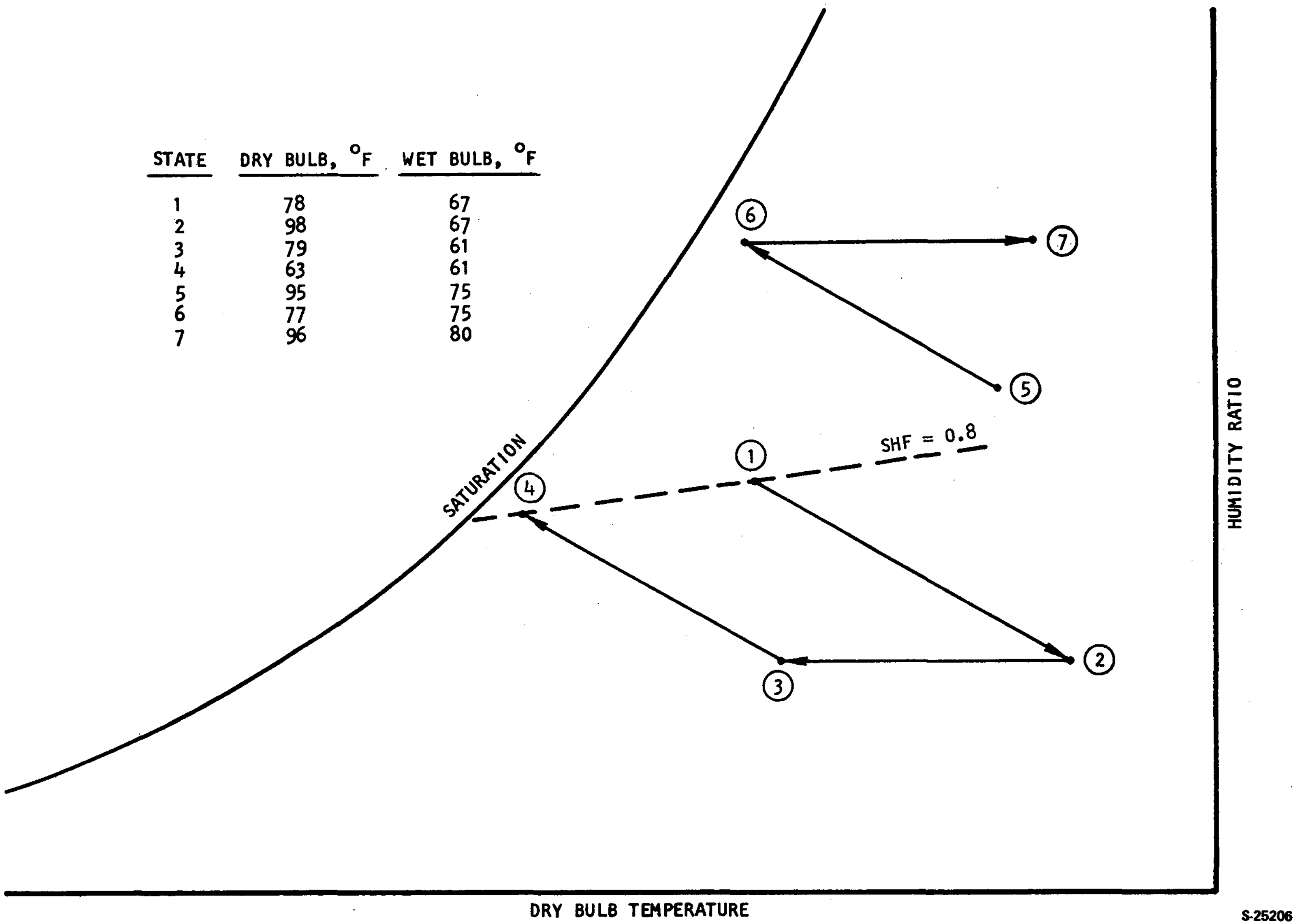

STATE	DRY BULB, °F	WET BULB, °F
1	78	67
2	98	67
3	79	61
4	63	61
5	95	75
6	77	75
7	96	80

Figure H-6. Case Al. Residence with Solar Desiccant-Evaporative Cooling System

Case AII. Residence with Solar Rankine or Absorption Refrigeration System

In this system the air is processed by direct cooling by coils. The coils could be either those of an absorption or Rankine system. Referring to Figure H-7, return air at state 1 is chilled by the coils to state 2, which is the point at which the SHF line intersects the saturation curve. This is about 58°F in this example. The saturated air at state 2 is mixed with some state 1 return air to form the supply air, state 3, at 63°F DB, 60.5°F WB.

All of the air cooling occurs by chilling state 1 air to state 2; therefore, the coil cold-side temperature must be about 53°F. From Figures H-3 and H-4, the COP will be 0.71 or 0.58 for absorption and Rankine chillers, respectively, assuming a hot water supply temperature of 200°F and a cooling water temperature of 85°F.

Case AIII. Residence with Solar Desiccant Dehumidifier-Solar Rankine or Absorption Refrigeration System

In this system, the residence air is first dehumidified by the solar desiccant system and then cooled by either an absorption or Rankine refrigerator. Referring to Figure H-8, return air at state 1 is dehumidified by contact with the desiccant bed to state 2. The air is then cooled by the regenerator to state 3 and by the refrigeration subsystem to state 4, the supply air state. Outside air at state 5 is humidified to state 6, used to cool the regenerator, and exhausted at state 7.

All of the cooling by the refrigeration system is done at a temperature slightly lower than state 4 temperature; i.e., about 58°F. From Figures H-3 and H-4, the absorption and Rankine COP's will be about 0.75 and 0.62. The cooling accomplished by the desiccant system will be done with a COP of about 0.52. The desiccant system provides about 17 percent of the total cooling (enthalpy change), so the overall COP will be 0.70 or 0.60 for absorption and Rankine hybrid systems, respectively.

Case BI. Kitchen with Solar Desiccant-Evaporative Cooling System

Case BI is the same as the baseline system of this project, but the change in return air conditions has caused a considerable improvement in performance. The COP of the desiccant system is predicted to be about 0.70. Referring to Figure H-9, return air at state 1 is dehumidified by the desiccant bed to state 2, cooled by the regenerator to state 3, and saturated to state 4. State 4 is the supply air state, falling on the SHF = 0.5 line drawn through state 1, the return air. Outside air, state 5, is humidified to state 6, and then used to cool the regenerator, exhausting at state 7.

Supply air, state 4, will be at about 66°F DB, 61°F WB. This system will operate with a COP of about 0.70 because all of the cooling is done by the desiccant system.

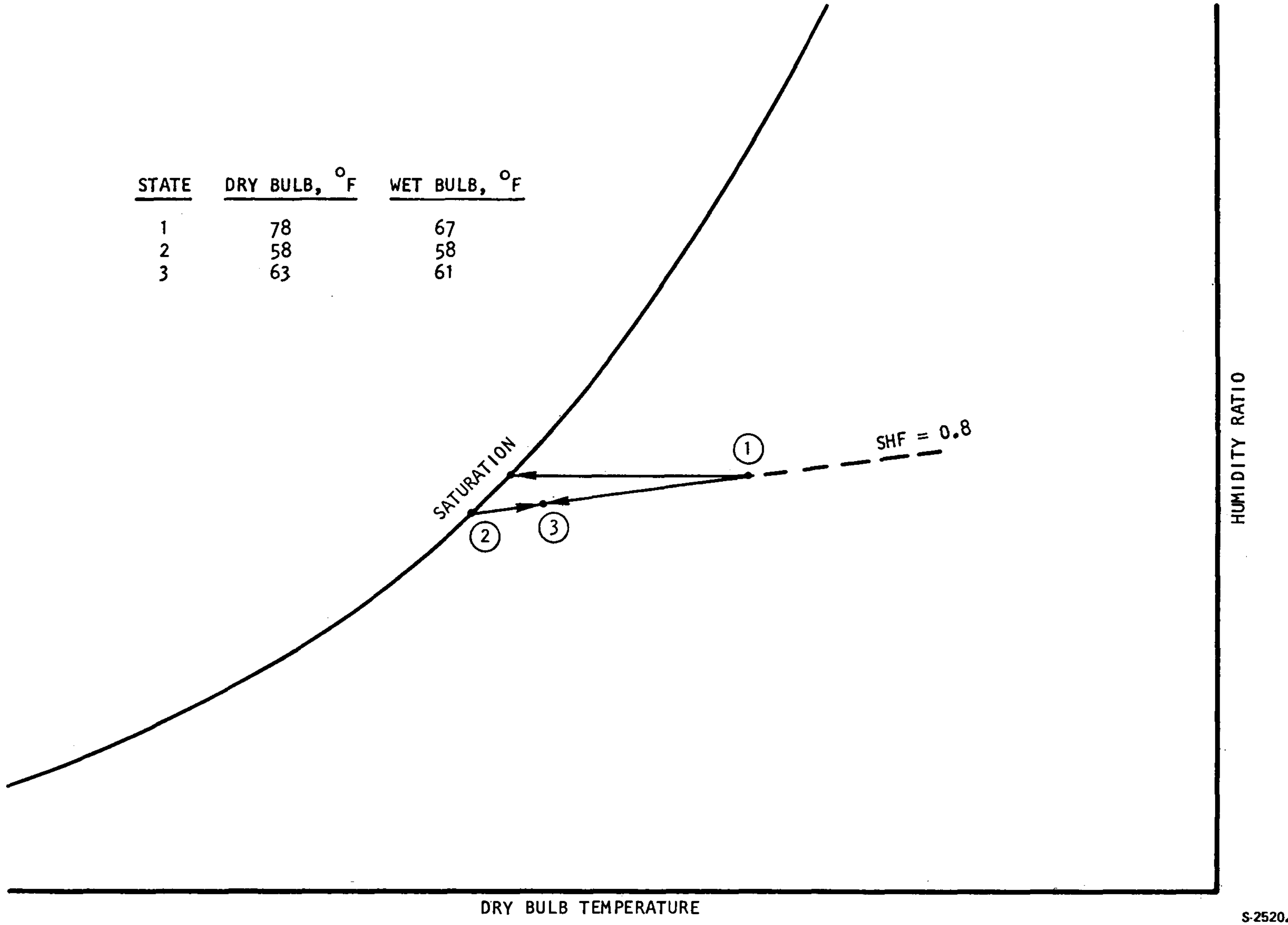

Figure H-7. Case All. Residence with Solar Refrigeration System

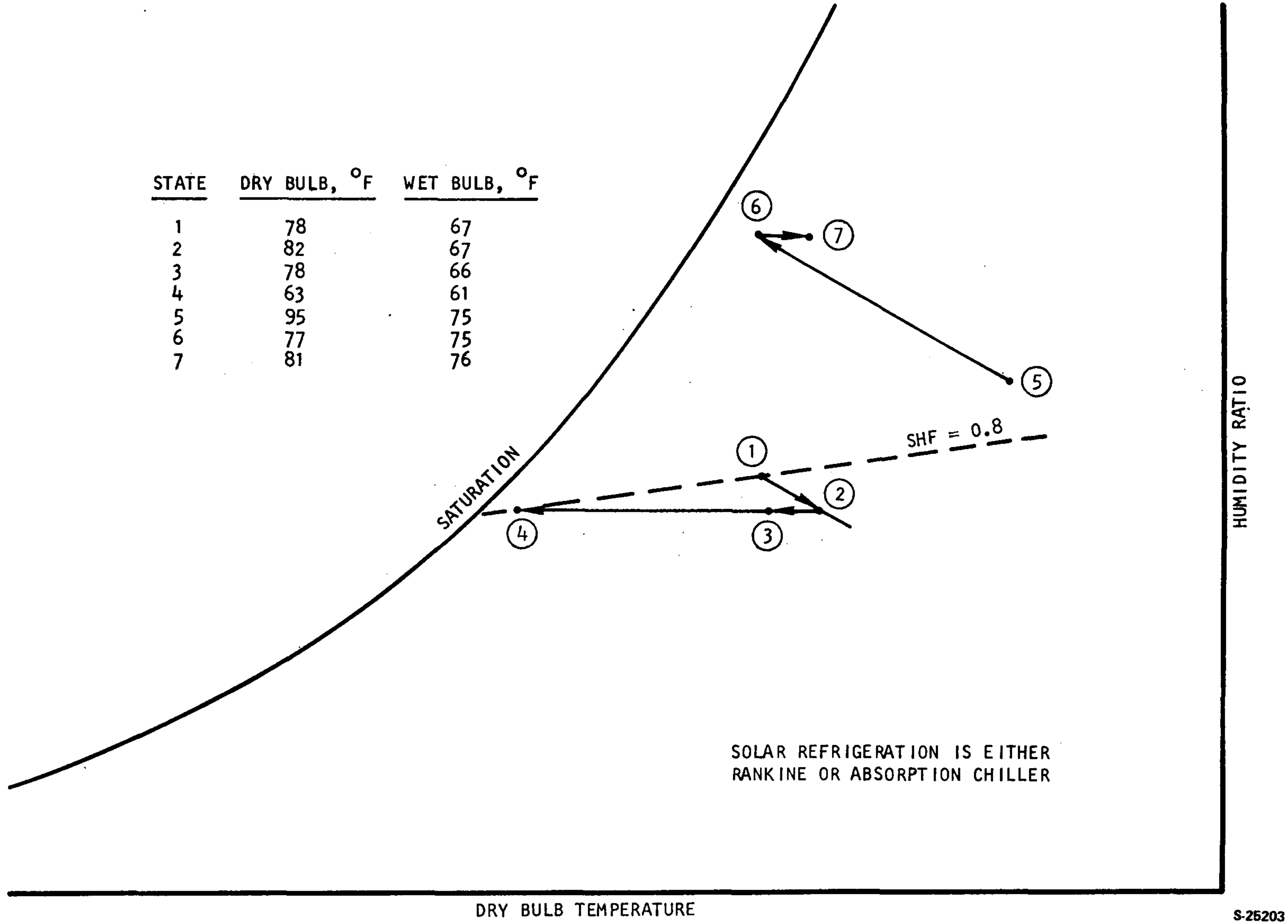

STATE	DRY BULB, °F	WET BULB, °F
1	78	67
2	82	67
3	78	66
4	63	61
5	95	75
6	77	75
7	81	76

Figure H-8. Case AIII. Residence with Solar Desiccant Dehumidifier-
Solar Refrigeration System

STATE	DRY BULB, °F	WET BULB, °F
1	80	70
2	108	70
3	80	61
4	66	61
5	95	75
6	77	75
7	105	82

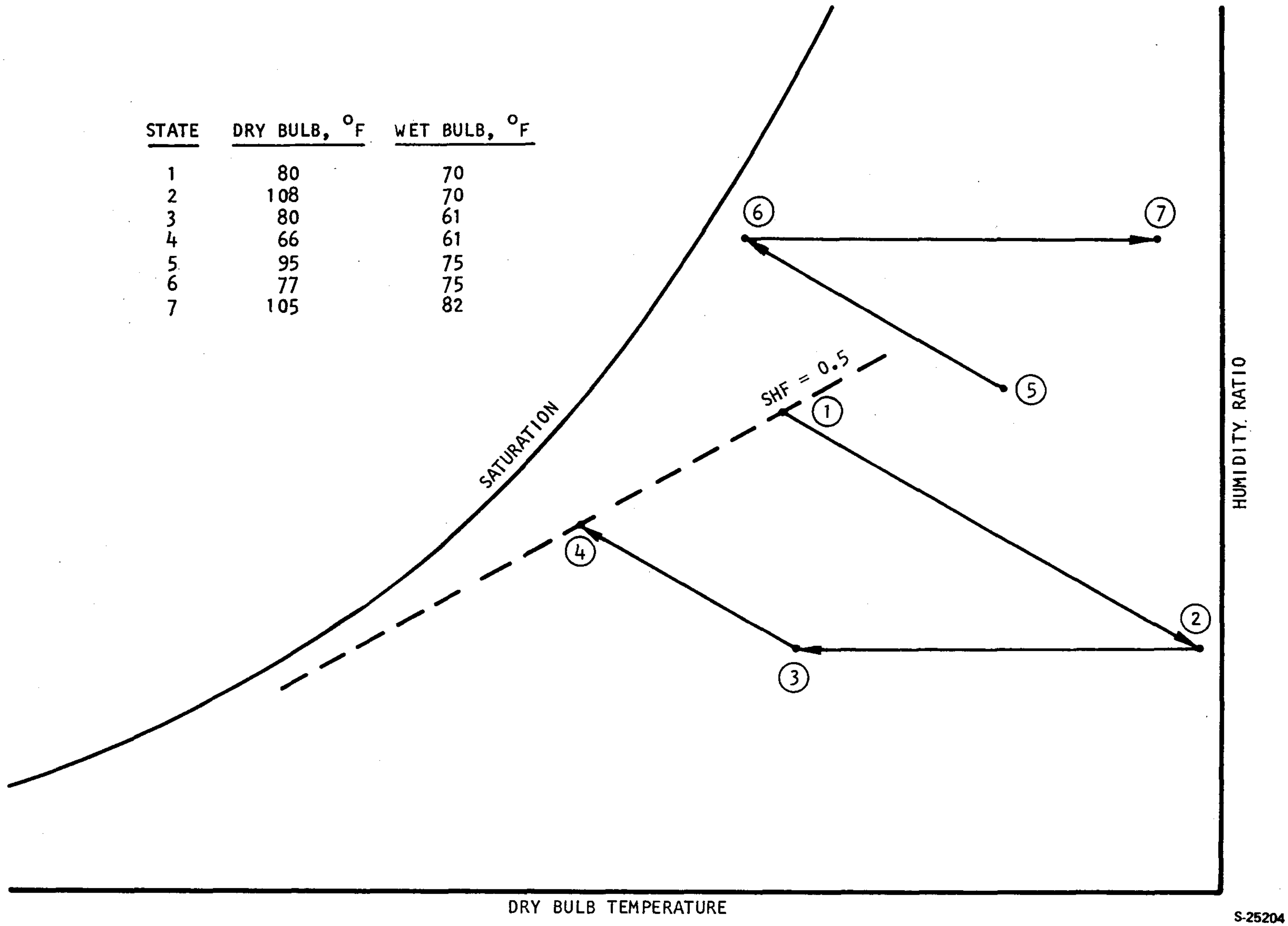

Figure H-9. Case BI. Kitchen with Solar Desiccant-Evaporative Cooling System

Case BII. Kitchen with Solar Rankine or Absorption Refrigeration System

In this system, the air is processed by direct cooling by coils. The coils could be either those of an absorption or Rankine system. Referring to Figure H-10, return air at state 1 is cooled by the coils to state 2, which has a humidity ratio corresponding to the desired supply air, state 3. The temperature at state 2 is 58°F, so the cold-side coil temperature must be about 53°F. The air is then reheated to 66°F, to be supplied to the kitchen at state 3.

An important problem with this type of system is that the air must be cooled substantially lower than the required supply temperature in order to obtain adequate humidity control. In this case, this amounts to 8°F sub-cooling. Most important, however, is the fact that the enthalpy change obtained in the refrigeration process is larger than the actually required change from the return air to the supply air. Therefore, to accomplish 1 ton of air conditioning, somewhat more than 1 ton of refrigeration must be performed.

Another disadvantage is that the reheating process, state 2 to state 3, may require an additional energy expenditure. However, in this example the supply temperature is low enough that the reheat can be done with waste energy. Therefore, no thermodynamic penalty will be assumed for this process.

From Figures H-3 and H-4, the COP's of absorption and Rankine chillers will be about 0.71 and 0.58, respectively. Because the cooling required is about 1.3 times the effective cooling, the COP's are effectively 0.54 and 0.44.

Case BIII. Kitchen with Solar Desiccant Dehumidifier-Solar Rankine or Absorption Refrigeration System

In this system, the return air is first dehumidified by the solar desiccant system and then cooled by either an absorption or Rankine refrigerator. Referring to Figure H-11, return air at state 1 is dehumidified by contact with the desiccant bed to state 2. The air is then cooled by the regenerator to state 3, and by the refrigeration subsystem to state 4, the supply air state. Outside air at state 5 is humidified to state 6, used to cool the regenerator, and exhausted at state 7.

With supply air, state 4, at 66°F DB, the cold-side coil temperature will be about 61°F. The COP's of the absorption and Rankine refrigerators will be about 0.73 and 0.67, respectively, from Figures H-3 and H-4. Cooling by the desiccant subsystem will be done with a COP of about 0.70. The desiccant system provides about 43 percent of the total cooling load (enthalpy change), so the overall COP will be 0.72 or 0.68 for absorption and Rankine hybrid systems, respectively.

STATE	DRY BULB, $^{\circ}F$	WET BULB, $^{\circ}F$
1	80	70
2	58	58
3	66	61

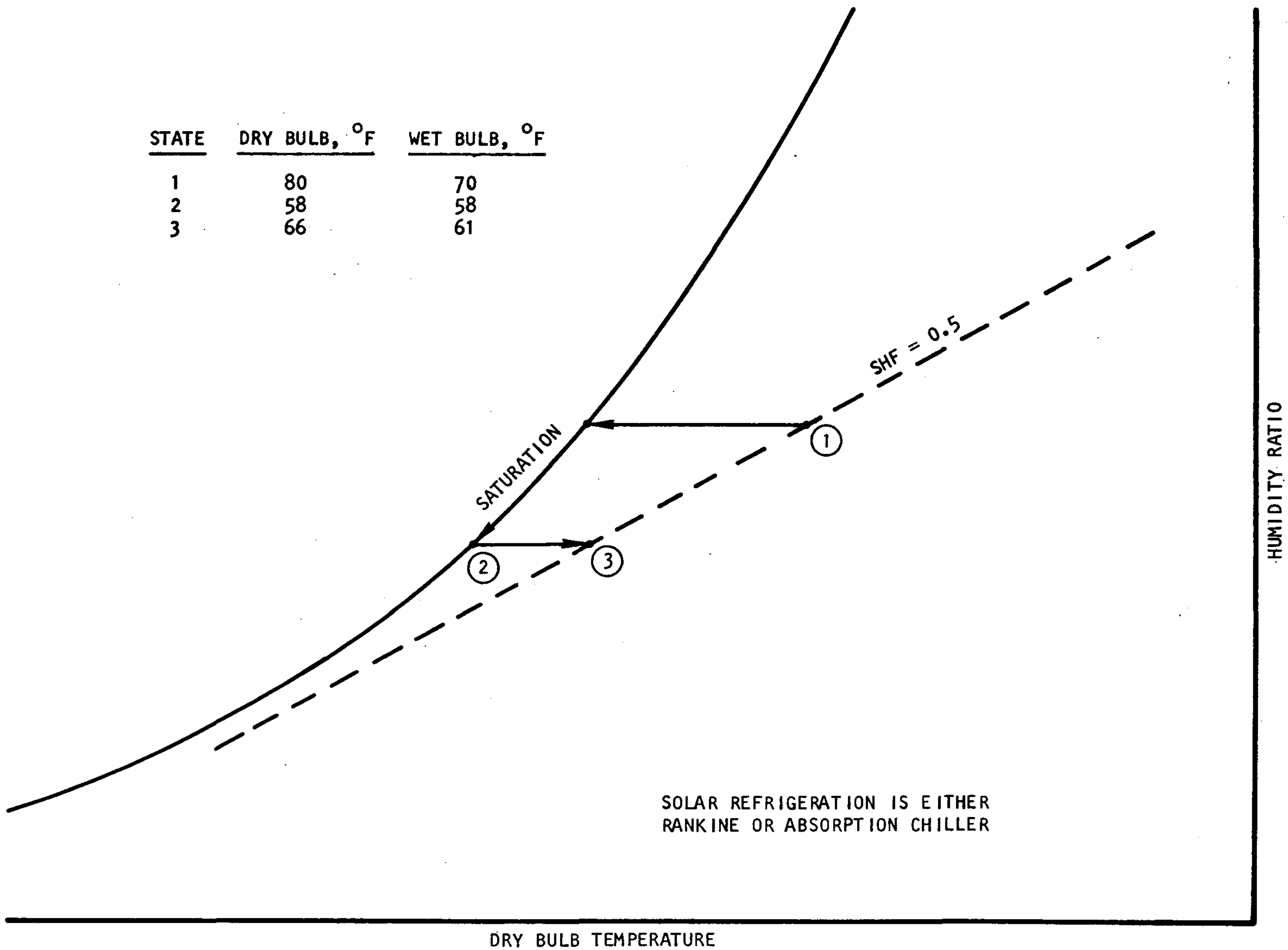

S-25205

Figure H-10. Case B11. Kitchen with Solar Refrigeration System

STATE	DRY BULB, °F	WET BULB, °F
1	80	70
2	94	70
3	79	66
4	66	61
5	95	75
6	77	75
7	92	79

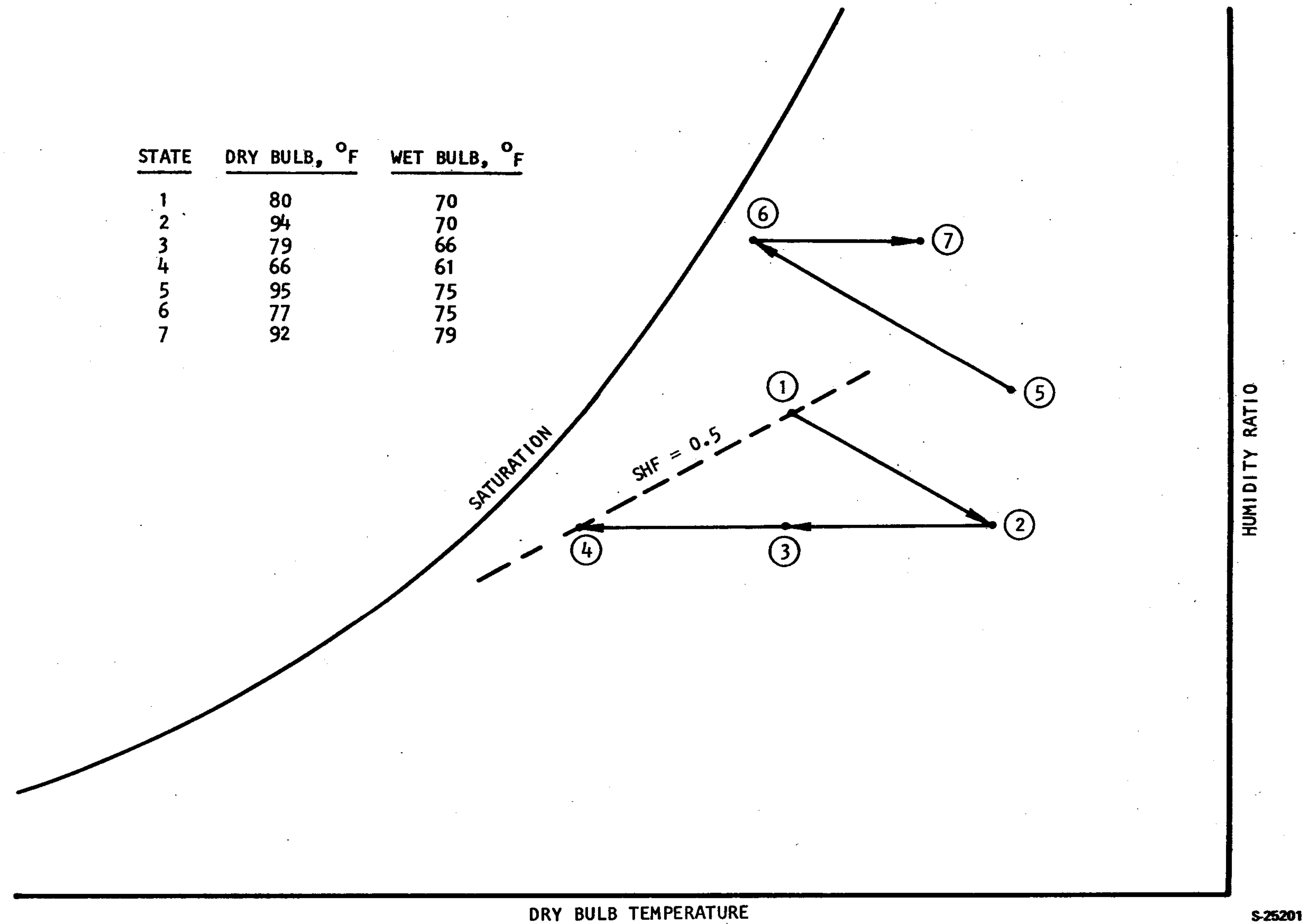

Figure H-11. Case BIII. Kitchen with Solar Desiccant Dehumidifier-Conventional-Refrigeration System

CONCLUSIONS

The preceeding examples have shown that, under certain conditions, considerable improvements in COP can be obtained over Rankine and absorption solar systems by hybrid desiccant-Rankine or desiccant-absorption systems. These results are summarized in Table H-1.

In the residence application, no advantage is gained over Rankine or absorption solar system performance. However, the commercial kitchen is quite different. The hybrid desiccant-absorption system (Case BIIIa) has a COP about 33 percent higher than the absorption system alone (Case BIIa). Similarly, the hybrid desiccant-Rankine system (Case BIIIb) shows about a 55 percent improvement over the Rankine system (Case BIIb). Neither BIIa nor BIIb include the required reheat energy input in the COP calculations. If this had to be supplied by additional primary energy input (solar or auxiliary), the differences would be much more significantly in favor of the hybrid systems.

The simple solar desiccant system (Case BI) has a COP about as good as either hybrid. However, substantial parasitic power savings would be realized with the hybrid systems, which does not show up in the solar thermal energy COP. The hybrid systems therefore represent a method to obtain good solar energy utilization with reasonable parasitic power consumption.

It is most important to make the final evaluation of any air conditioning system in terms of yearly solar and auxiliary energy consumption. Since design loads are commonly taken to be the most severe conditions normally encountered by an air conditioning system, the large majority of operation will be at loads that are significantly less than design point. This is particularly important with the standard and hybrid solar desiccant systems because capacity reduction is accomplished by airflow reduction. Considerable reductions in parasitic power will be the most significant improvement. COP will also improve somewhat.

TABLE H-1

COMPARISON OF COOLING SYSTEM PERFORMANCE

Case	System Configuration	Application	Sensible Heat Factor	Desiccant Subsystem COP	Cooling Subsystem COP	Overall COP
AI	Solar desiccant dehumidifier with evaporative cooling	Residence	0.8	0.52	--	0.52
AIIa	Solar absorption refrigeration system	Residence	0.8	--	0.71	0.71
AIIb	Solar Rankine refrigeration system	Residence	0.8	--	0.58	0.58
AIIIa	Solar desiccant dehumidifier with absorption refrigeration	Residence	0.8	0.52	0.74	0.70
AIIIb	Solar desiccant dehumidifier with Rankine refrigeration	Residence	0.8	0.52	0.62	0.60
BI	Solar desiccant dehumidifier with evaporative cooling	Commercial kitchen	0.5	0.70	--	0.70
BIIa	Solar absorption refrigeration system*	Commercial kitchen	0.5	--	0.54	0.54
BIIb	Solar Rankine refrigeration system*	Commercial kitchen	0.5	--	0.44	0.44
BIIIa	Solar desiccant dehumidifier with absorption refrigeration	Commercial kitchen	0.5	0.70	0.73	0.72
BIIIb	Solar desiccant dehumidifier with Rankine refrigeration	Commercial kitchen	0.5	0.70	0.67	0.68

*Requires reheat; not included in COP calculations. See text for discussion.

APPENDIX I

TASK I-4. SUBSYSTEM COMPUTER MODEL

INTRODUCTION

The design of a desiccant air conditioner involves the optimization of a number of parameters that define the sorbent bed and regenerator geometry and the conditions of system operation. The complex heat and mass transfer phenomena occurring in the desiccant bed and bed interaction with the process air stream require the use of sophisticated computer techniques to perform the numerous iterations necessary for the development of a design.

The approach taken in the evolution of the air conditioner described below was to design for a reasonable COP; also, system pressure drop as it relates to electrical energy consumption was a primary consideration.

The system designed on this basis is believed to be near optimum in terms of economic viability. Economic studies will be performed at a later date using baseline system data for evaluating year-round performance and energy requirements. Should these overall system investigations indicate the necessity for design changes, they will be incorporated after test evaluation of the prototype dehumidifier.

FUNCTIONAL DESCRIPTION

A schematic of the system is given in Figure I-1. The desiccant bed and the regenerator are two thin cylinders rotating around a common axis. The desiccant is granular silica gel and the regenerator matrix is a fine screen of galvanized steel. A top view of the package along the axis of rotation is shown in Figure I-2. The solar heater is located between the dryer and regenerator. Operation is as follows. Warm humid air from the residence is directed to the adsorbing side of the rotary dryer. Water is adsorbed from the air stream, which is heated in the process. The air is then cooled in the rotary regenerator. The specific humidity of this air stream is sufficiently low that its dry bulb temperature can be lowered by adiabatic humidification to levels adequate for sensible cooling while retaining reasonable latent cooling capacity. Ambient outside air is used to regenerate the sorbent bed and cool the rotary regenerator. This stream is humidified adiabatically and circulated through the rotary regenerator. About one-half of this air is then exhausted from the package without flowing through the dryer. The remainder is heated in a fixed-boundary heat exchanger by solar thermal energy and used to desorb the desiccant.

A minor amount of air directly from outside is circulated through the hot portion of the sorbent bed as it rotates from the desorbing zone to the adsorbing zone. In this manner the bed is cooled to a temperature level where it can adsorb moisture when exposed to the return air from the residence. This preconditioning air flow is then used to preheat the bed prior to desorption, thus reducing the solar thermal energy necessary for this process.

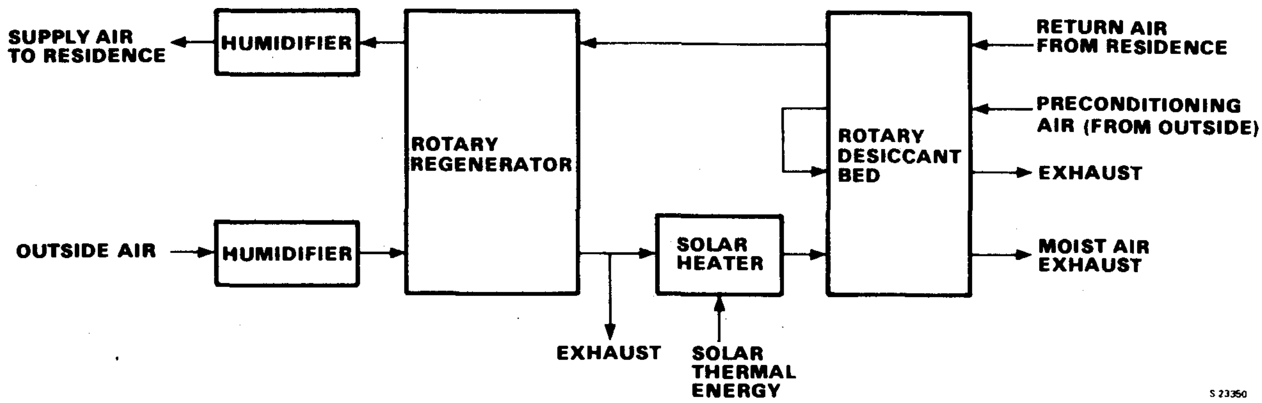

Figure I-1. Air Conditioner Schematic

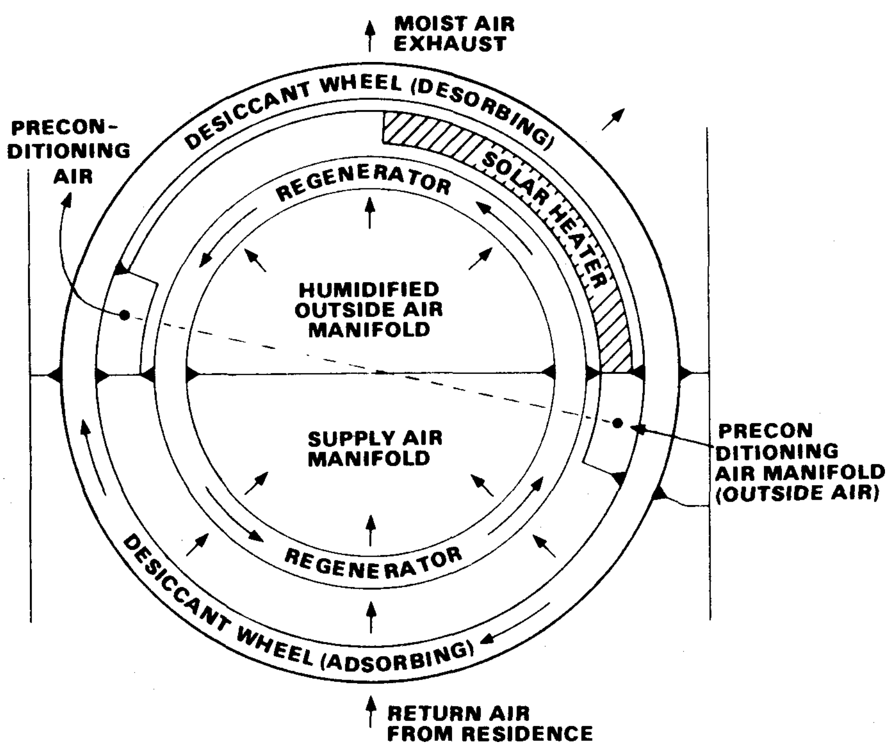

Figure I-2. Dehumidifier Arrangement

SYSTEM MODEL

System size and performance were estimated using a computer program developed to predict the transient performance of the dehumidifier assembly as the sorbent bed and regenerator rotate around their common axis.

Basic Sorbent Bed Model

A sorbent bed computer program developed under a NASA contract (Reference 1-1) was used to develop the sorbent bed model in this program. Existing equilibrium data and dynamic properties of the sorbent (Reference 1-2) also were used with the computer model. These data were supplemented by differential bed test data on granular silica gel.

The basic sorbent bed model accounts for the transient thermal and mass transfer phenomena occurring in the sorbent and the process gas as the gas proceeds through the bed. The mass transfer model includes gas phase diffusion and diffusivity within the sorbent particles. The heat transfer model is strictly between the gas and the particles; temperature gradients within the sorbent grains are ignored.

The rotating sorbent bed at any point around the periphery is essentially a small bed which has been exposed to the process air stream for a given time counted from the instant the bed enters the adsorbing (or desorbing) zone. The rotary regenerator model is the same as the sorbent bed model, where only heat is exchanged between the process air stream and the matrix; no mass transfer occurs in the regenerator.

In the use of the model, the calculation time interval is variable and determined by the behavior of the sorbent/regenerator at any point in the entire system. The time interval is set so that the sorbent loading rates (or temperature change) are maintained below 0.5 percent (or less than 1°F) for the selected time interval. The temperature criterion also is applicable to the regenerator model.

Dehumidifier Model

The dehumidifier computer program models the system depicted in Figure 1-2. Data inputs include the sorbent bed and regenerator matrix characteristics; geometry and rotating speed; and the process air flow rates, temperatures, and water content.

Initially, arbitrary bed loadings and bed and regenerator temperature profiles in the peripheral and radial directions are assumed. For the purpose of calculation, the sorbent bed is divided into ten discrete zones in the radial direction. In the peripheral direction, the width of the elemental beds is determined by the speed of rotation and the time interval criteria described above. The calculation procedure entails the sequence outlined in Table 1-1.

TABLE I-1

DEHUMIDIFIER MODELING CALCULATIONS

Step	Procedure
1	The thermal and mass transfer performance of the sorbent bed is calculated as the bed proceeds through the adsorbing zone. Bed loading and temperature in the peripheral and radial directions are calculated and stored. The temperature and specific humidity of the process air stream are calculated as it proceeds through the 10 radial zones of the elemental bed. The final values (as the air exits the bed) are stored for regenerator performance calculations.
2	The thermal performance of the regenerator is calculated in the same manner as that of the sorbent bed. Calculations start at the point where the regenerator enters the cooling zone, wherein the dehumidifier air is cooled. The air temperature profile from step 1 is used to determine the radial and peripheral temperature profiles within the regenerator, and the temperature profile of the air in this manifold and its water content are computed.
3	With the regenerator matrix temperature profile at the end of the cooling zone known from step 2, the regenerator performance when exposed to the humidified outside air stream is calculated. This sets the conditions for a repeat of the step 2 calculation procedures. Also, the air temperature distribution at solar heater inlet is calculated.
4	The temperature profile of the desorbing air stream at solar heater outlet is then calculated, accounting for the temperature drop of the water as it proceeds through the heat exchanger. Since the hot water and air flows through the heater are constant, the effectiveness of the heater at any point around its periphery will be constant.
5	The sorbent bed radial loading and temperature profile at the end of the adsorbing zone are used as the starting point for prediction of the bed conditions at the inlet of the desorption zone after exposure to the preconditioning air stream. The subroutine for the step 1 calculations is used for this calculation.
6	Bed conditions from step 5 and desorbing air temperature profiles and specific humidity from step 4 are used to calculate the peripheral and radial bed performance through the desorbing zone. In this manner, bed loading and temperature profile (when entering the precooling zone) are estimated.
7	The final step involves calculation of the sorbent bed performance in the preconditioning zone upstream of the adsorbing zone. The preconditioning air temperature and water content are calculated and used as input for step 5. Further, the bed moisture content and temperature profile as it enters the adsorbing zone are calculated.

The calculation procedure outlined in Table I-1 is repeated until stable conditions are achieved using constant process air flows, temperatures, and water content. Once stable conditions are achieved, the performance of the dehumidifier under transient process stream conditions can be estimated.

BASELINE SYSTEM CHARACTERISTICS

Physical Characteristics

The system was designed to provide 3 tons of air conditioning under the following conditions:

- Conditioned space temperatures: 78°F DB,
  67°F WB
- Outside air temperatures: 95°F DB,
  75°F WB
- Solar energy source temperature: 200°F

Pertinent characteristics of the major system components were determined from computer studies. These are listed in Table I-2.

TABLE I-2

COMPONENT CHARACTERISTICS

Desiccant Bed	Regenerator
Granular silica gel (8-10 mesh)	Diameter: 30 in.
Bed diameter: 45.8 in.	Height: 48 in.
Bed height: 48 in.	Thickness: 0.85 in.
Bed thickness: 1.15 in.	Matrix: Galvanized steel screen, 24 by 24 by 0.014 in.
Weight: 193 lb	Weight: 290 lb
Rotating speed: 5 rph	Rotating speed: 20 rpm
Working capacity: 3.7%	Effectiveness: 0.90

The effectiveness of the solar heater is 85 percent at any station along the periphery. It spans over an 86.6-deg arc in the space between the sorbent bed and the regenerator. The preconditioning (cooling and heating) sections of the sorbent bed between the adsorbing and desorbing zones extend over a 22.5-deg angle.

Design Point Performance

The performance of the system at the design conditions listed above is defined in Figure I-3. Pertinent data are listed below.

- The thermal COP of the system (cooling capacity/solar thermal energy input) is 0.52.
- The pressure drop through the system is 1.3 in. H_2O.
- The temperature gradient across the regenerator is about 27°F from the outer diameter to the inner diameter.
- The average temperature of the supply air at regenerator outlet is 81°F.
- The desorbing air temperature at solar heater outlet varies from 176°F to 186°F in the clockwise direction.

About 30 percent of the 3-ton capacity of the system at design point is for latent heat removal. The ratio of latent to sensible heat capacity increases rapidly as outside air wet bulb temperature drops. The latent capacity of the supply air stream could be increased by bypassing the humidifiers or using a less effective humidifier.

PARAMETRIC DESIGN DATA

The computer model was used to generate parametric performance data to permit final sizing of the bed, regenerator, and heater, and to define optimum operating conditions.

Regenerator Matrix

An essential part of the system is the rotary regenerator. As discussed subsequently, very high performance is necessary to achieve a high system COP. In the baseline design a regenerator effectiveness of 0.90 was assumed. A search for a regenerator matrix was initiated early in the program.

The requirements for a matrix involve considerations of thermal performance (specific surface area, density, specific heat, thermal conductivity, and surface heat transfer characteristics), pressure drop, and cost. A number of materials were investigated and characterized in terms of the parameters listed above (see Table I-3). Only materials that will not absorb moisture were considered as candidates.

To achieve 90 percent effectiveness, the conductance (hA) between the air stream and the matrix must be at least 35,000 Btu/hr-°F. This determines the minimum amount of material required. The smaller the characteristic diameter of a material, the greater the heat transfer coefficient and the surface area available per unit volume. In addition to the requirement for a high hA, the regenerator must be rotated at a speed that depends on the total heat capacity of the matrix so that the thermal loss caused by temperature swing is not excessive.

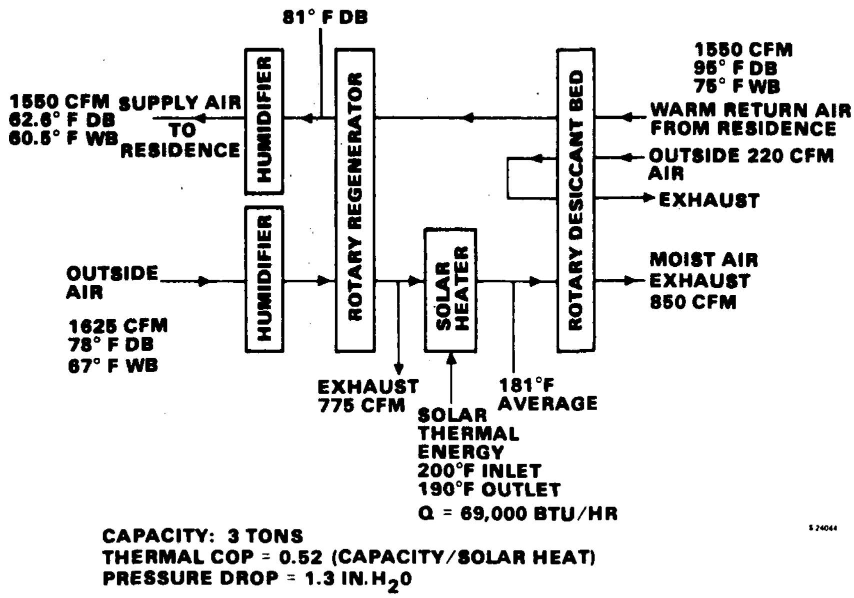

Figure 1-3. Air Conditioner Performance

TABLE 1-3

CHARACTERISTICS OF CANDIDATE REGENERATOR MATRICES

Material	Specific Heat (CP), Btu/ lbm-°F	Price (P), $/lbm	Bulk Density ρ_b, lb/ cu ft	Effective Bulk Thermal Conductivity k_b, Btu/hr-ft-°F	Specific Surface Area (S), sq ft/ cu ft	*Pressure Drop, (ΔP), in. H_2O	**Total Cost of Material, $
Soda lime glass beads (4-6 mesh)	0.20	2.00	99	0.068	280	0.7	1538
4-6 mesh crushed reclaimed glass	0.20	0.05	99	0.068	280	0.793	38
Aluminum turnings	0.22	0.90	85	0.12	500	0.5	333
Polyterephthalate (PTFE) pellets (4-6 mesh)	0.24	0.98	49	0.039	280	0.7	373
Polytetrafluroethylene (PTFE) pellets (4-6 mesh)	0.25	3.40	82	0.042	280	0.7	2166
Fluorinated ethylene propylene (FEP) pellets (4-6 mesh)	0.28	6.00	81	0.041	280	0.7	3776
Stainless steel turnings	0.12	1.10	240	0.044	500	0.5	1149
Polypropylene screen (24 by 24 by 0.014 in.)	0.48	37	16	0.34	980	0.193	1314
FEP screen (24 by 24 by 0.014 in.)	0.28	94	37	0.035	980	0.193	7721
Aluminum screen (24 by 24 by 0.014 in.)	0.22	2.60	47	0.053	980	0.193	271
Galvanized steel screen (24 by 24 by 0.014 in.)	0.11	1.00	132	0.049	980	0.193	293

*At average air velocity of 75 ft/min.
**For a 0.90 regenerator effectiveness.

Estimates of regenerator pressure drops were made for various types of matrices in the conditions corresponding to the operation of the dehumidifier. Pellet-type materials have pressure drops on the order of 0.7 in. H_2O, while screen-type materials have pressure drops of about 0.2 in. H_2O. This is significant since the dehumidifier is essentially a high-process air flow system. The pressure drops for the granular and screen types of matrices correspond to fan power levels of 0.61 and 0.17 kw, respectively. This difference is significant in a 3-ton system designed for energy savings. For this reason, all granular type regenerator matrices were eliminated. Steel and aluminum turnings were eliminated for the same reason. Of the screen-type materials, galvanized steel was selected as optimum based on its lower cost. Also, its bulk thermal conductivity is low and the corrosion resistance in wet air is high. Aluminum screens would require a special surface coating to prevent atmospheric corrosion. The cost of this material would increase well above that shown in Table I-3.

Rationale for Baseline System Definition

Preliminary sizing studies involving investigations of silica gel particle size, air flow rate, and air flow path were conducted to obtain a general definition of the system. Preliminary sizing of the system indicated that a 3-ton capacity could be achieved at reasonable performance with about a 4-ft-dia and 4-ft-high sorbent bed. These dimensions were considered as maximum for a 3-ton dehumidifier. Once the maximum size was determined, these investigations were refined and a systematic study of the various parameters affecting design was conducted. The results of these studies are discussed below. Data are presented for:

Granular silica gel, 8-10 mesh size
Galvanized steel screen regenerator matrix:
24 by 24 by 0.014 in. screen

Desiccant bed total face area of 48 sq ft,
corresponding to a bed diameter of 45.8 in.
and a bed height of 48 in.

1. Desiccant Bed Cycle Time (see Figure I-4)

A six-minute half-cycle time for the sorbent bed was selected because it is a good compromise between the parameters shown. Only slight COP improvement can be achieved with longer cycle time; however, the weight of the silica gel bed increases rapidly. Also, as the sorbent bed thickness increases the pressure drop through the system increases significantly. This cycle time yields the bed sizes and rotating speeds listed in Table I-2.

2. Regenerator Cooling Air Stream

Cooling of the regenerator prior to its entry into the dry residence process air stream is necessary to obtain low dry bulb temperature in the supply air manifold and high system capacity. However, the water content of this cooling air stream is high, and it must be exhausted from the package without flowing through the desiccant bed (see Figure I-2). The reduction in

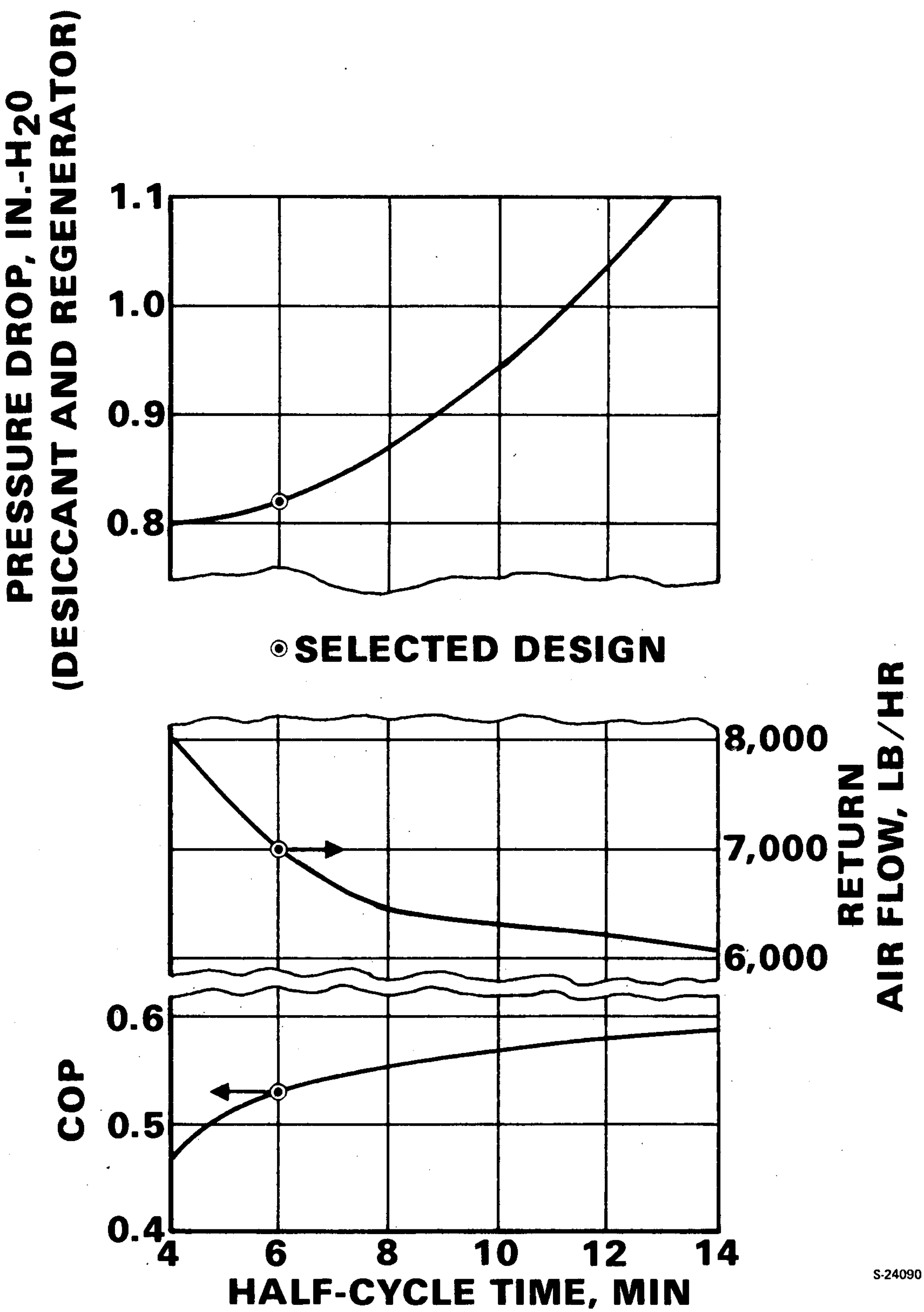

Figure 1-4. Parametric Design Data

system capacity and COP that would result if the regenerator cooling air flowed through the bed is shown in Table 1-4. To enhance baseline system performance, the regenerator cooling air stream is exhausted through the top of the package.

TABLE 1-4

EFFECT OF EXHAUSTING REGENERATOR
COOLING AIR THROUGH DESICCANT WHEEL

Configuration	Cooling Capacity, Btu/hr	COP
Design configuration	36,000	0.52
Regenerator cooling air through desiccant	30,400	0.42

3. Process Air Flow Rate

The sensitivity of the baseline system to air flow rate was investigated to determine its effect on capacity and COP (see Figure 1-5). The baseline system design assumes that the air velocity is the same in all air streams, with the exception of the regenerator cooling air flow, which is 10 percent higher.

As shown, the COP is relatively insensitive to process air flow rate. However, system capacity is nearly directly proportional to air flow. The baseline air flow through the adsorbing bed (21 sq ft face area) was taken as 7000 lb/hr. This yields a pressure drop through the desiccant bed and regenerator of 0.82 in. H_2O.

4. Preconditioning Air Stream

The bed temperature and water loading profiles at the end of adsorption and desorption are shown in Figure 1-6. As the sorbent bed exits the desorbing zone, its temperature is between 120° and 183°F; its moisture content is also relatively high. Should the bed be exposed to return air from the residence under these conditions, this air will be heated, and moisture will be released from the bed to the air. The resulting effect is a decrease in performance since heat and moisture are added to the supply air manifold.

In the baseline system, outside air (not humidified) is used to cool the bed prior to its entry into the adsorbing zone. This air is then collected and used on the opposite side of the bed to preheat the bed prior to desorption. A cross-over duct on top of the air conditioner package is used for this purpose.

The effect of the preconditioning air stream is shown in Figure 1-7; COP increases from 0.43 to 0.52; also, the capacity of the system increases by about 10 percent. At design point the preconditioning air stream transfers

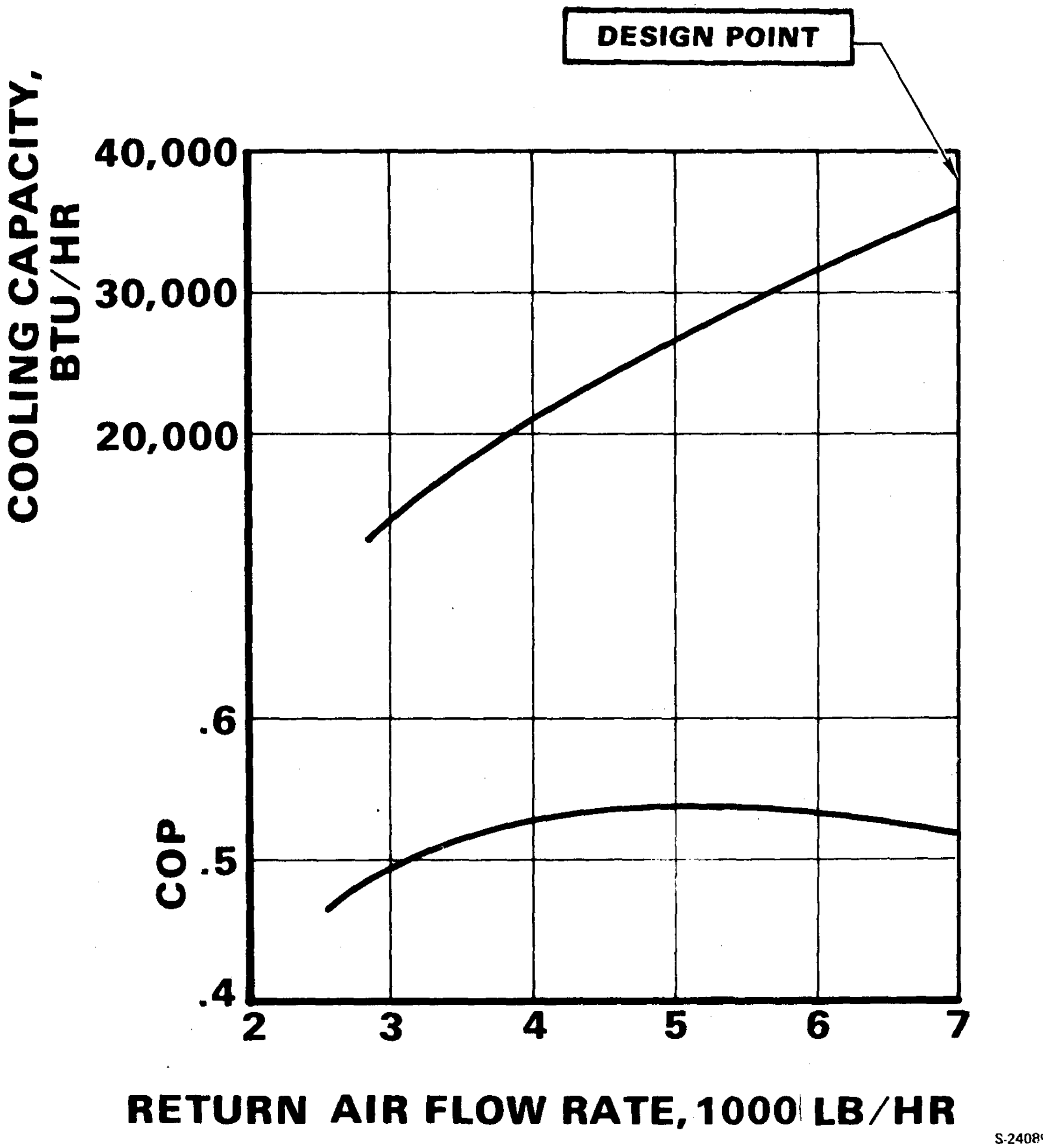

Figure 1-5. Effect of Process Air Flow Rate

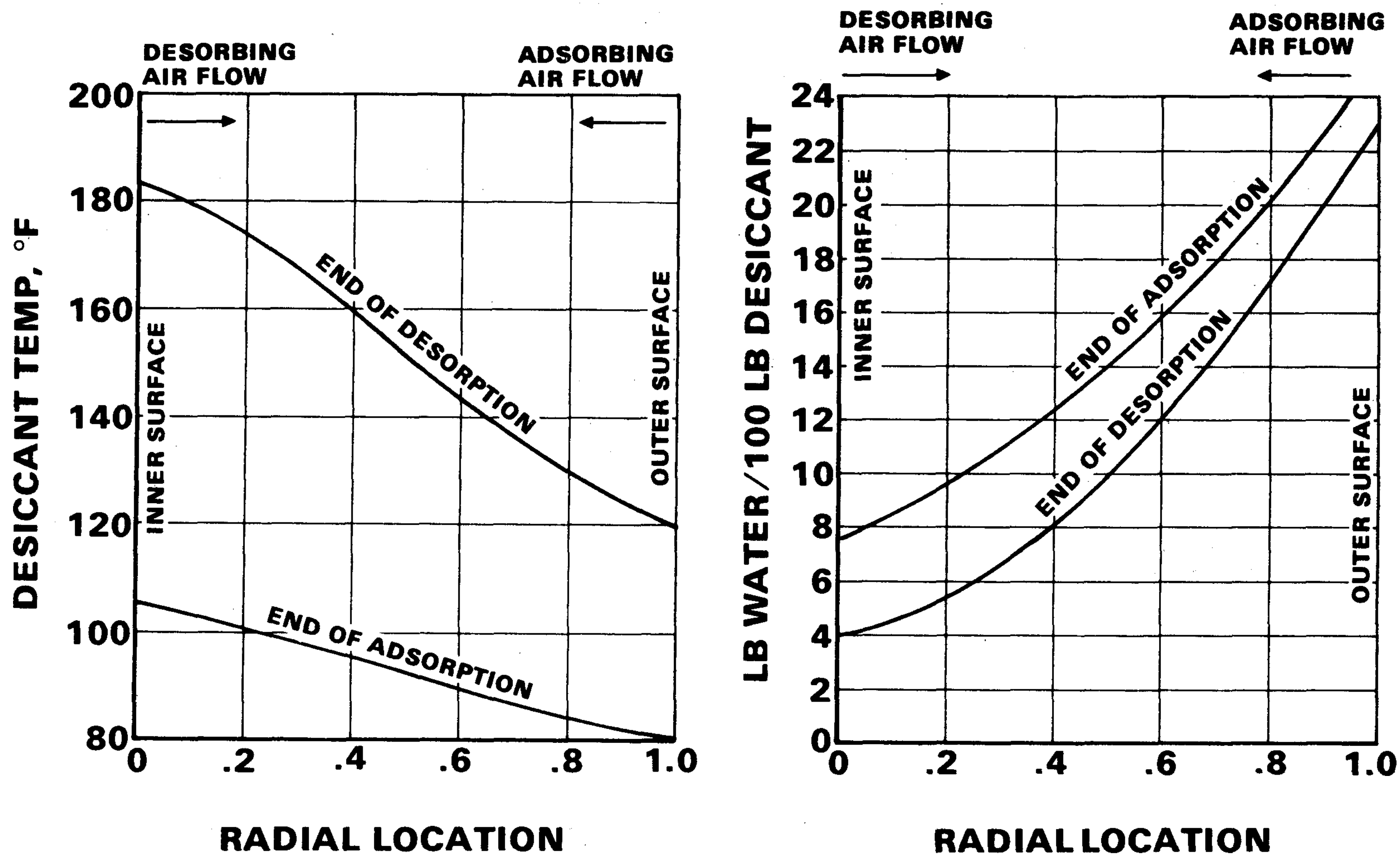

S-23308

Figure I-6. Sorbent Bed Loading and Temperature Profiles

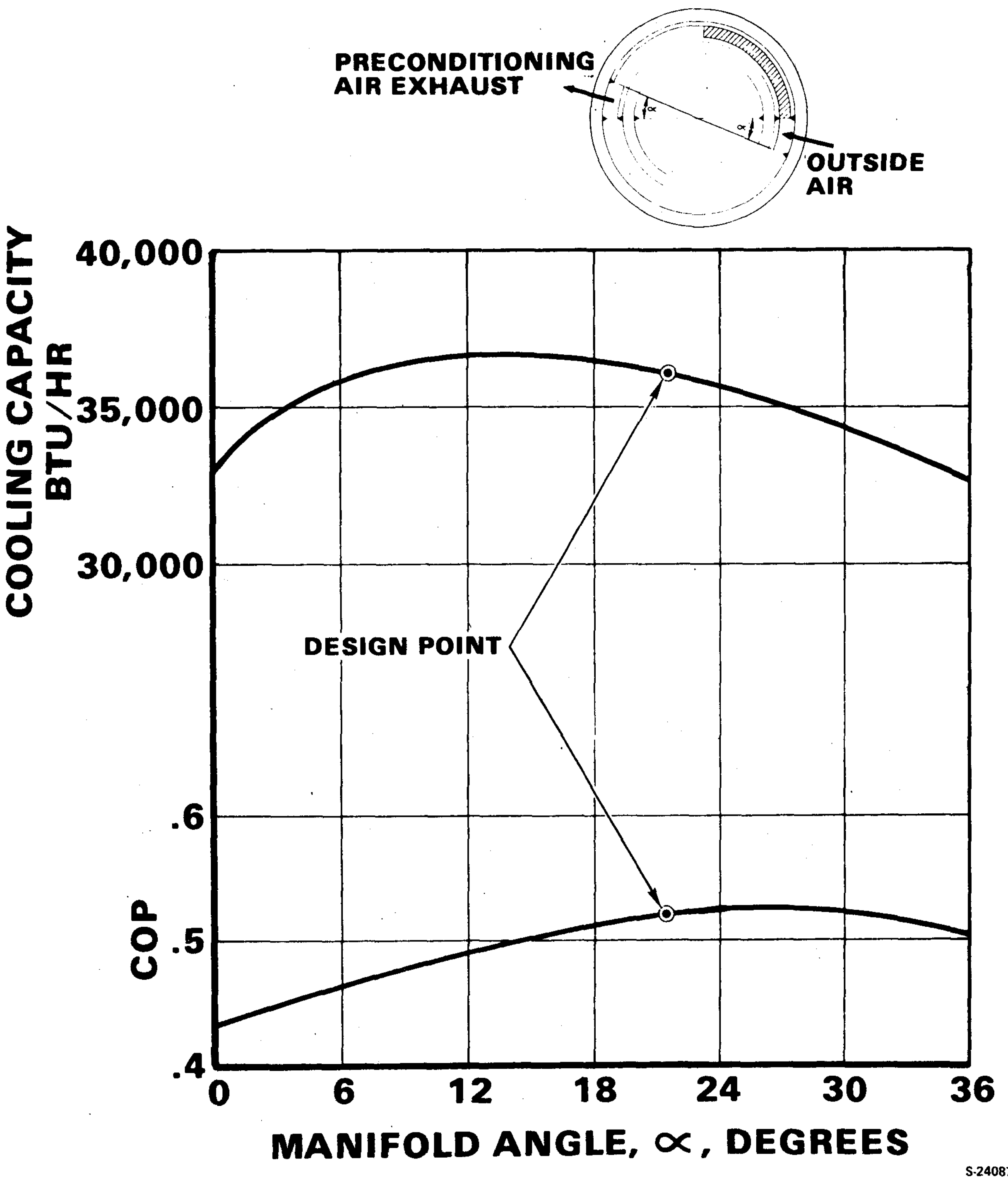

Figure I-7. Effect of Preconditioning Air Stream

15,000 Btu/hr from one portion of the bed to the other. This is very significant considering that the solar thermal energy input is 69,000 Btu/hr. Only very little desorption is affected by the preconditioning air. The major effect is sorbent bed heating.

5. Regenerator Effectiveness

The baseline system was designed with a rotary regenerator effectiveness of 0.90. Regenerator effectiveness is defined as:

$$\frac{Th\ in - Th\ out}{Th\ in - Tc\ in}$$

This component has a major effect on system capacity and COP, as illustrated in Figure I-8. The high effectiveness is achieved by increasing the relative air flow in the cooling segment of the regenerator. In this segment of the bed, the air flow is 10 percent higher than at other locations in the bed. In the design of the prototype, provisions are made for adjustment of this air flow rate if necessary.

6. Solar Heater Size

The depth of desorption of the silica gel bed is primarily a function of the temperature of the desiccant at the end of the desorption period. Prolonged exposure of any bed element at a given temperature results in inefficient energy use. Further, the bed loading at the inside surface actually determines the water content of the air in the supply manifold, so that deep drying the bed at the outside surface is neither necessary nor desirable. Bed temperature and loading profiles at the end of the adsorption and desorption zones are shown in Figure I-8.

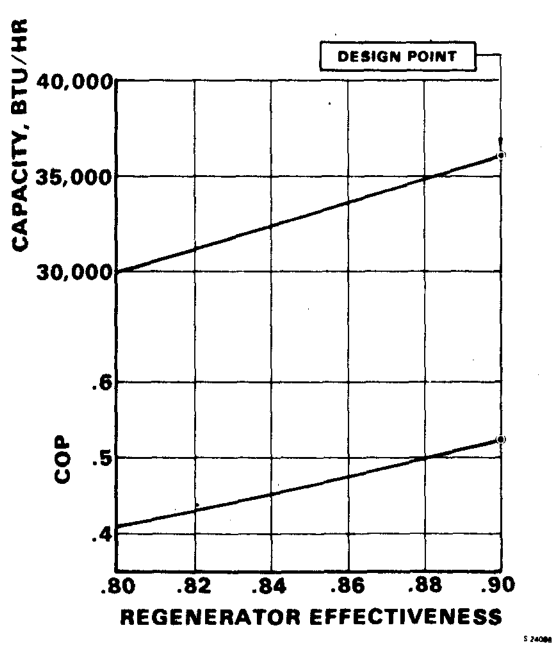

Figure I-8. Effect of Regenerator Effectiveness

The influence of the heater angle on system capacity and COP is shown in Figure I-9. As the angle increases, the bed capacity also increases because the bed is better desorbed in the radial direction so that its water loading capacity increases. However, the thermal energy used for this purpose is not used effectively in reducing the specific humidity of the process air. For this reason, the system COP drops as the heater angle increases.

The design configuration of the desiccant subsystem has been optimized using the subsystem computer model. The model has the capacity to generate off-design performance data as well. This work has been done in Task I-5, and is documented in Appendix J of this report.

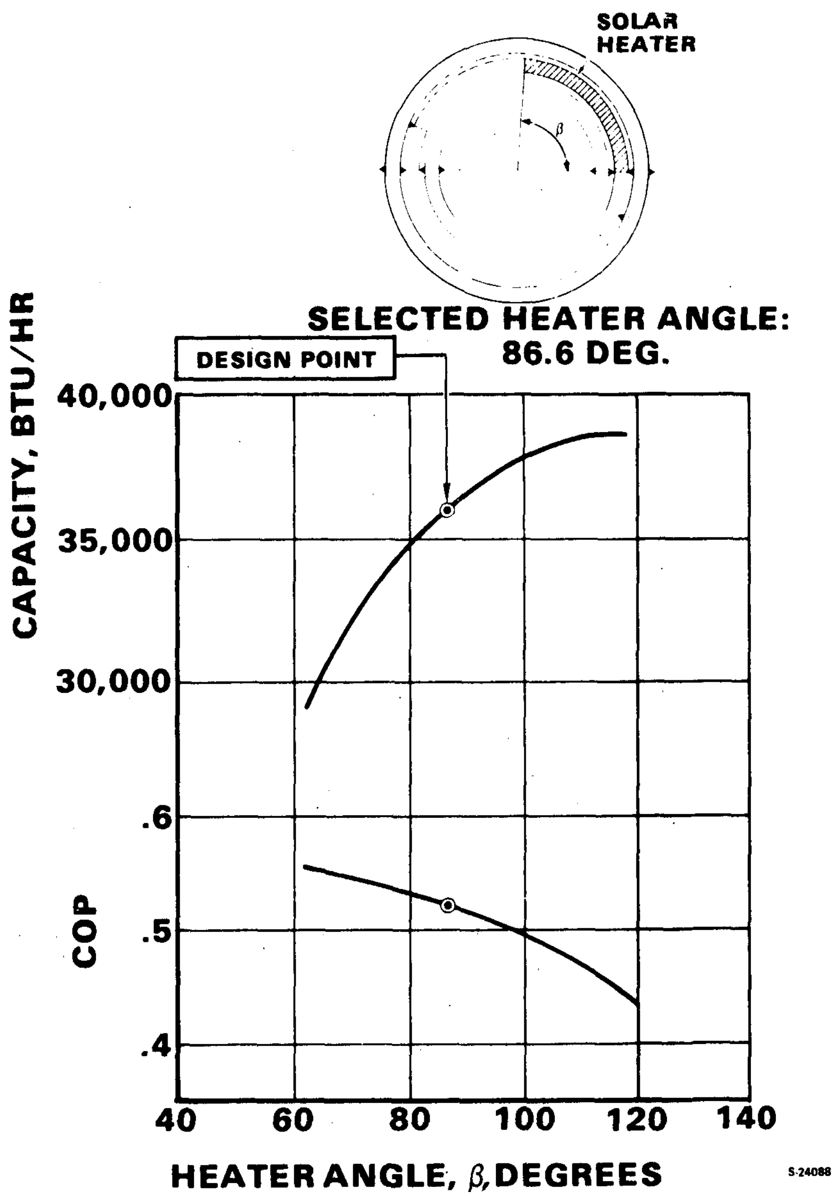

Figure I-9. Solar Heater Optimization

REFERENCES

I-1. Hwang, K. C., A Transient Performance Method for CO_2 Removal with Regenerable Adsorbents, NASA CR--112098, Oct. 1972.

I-2. Wright, R. M., et al., Development of Design Information for Molecular-sieve Type Regenerative CO_2-Removal Systems, NASA CR-2277, July 1973.

BIBLIOGRAPHY

Rousseau, J., and Hwang, K. C., Preliminary Design of a Solar Desiccant Air Conditioner, DOE Contract No. EG-77-C-03-1591, March 1978.

APPENDIX J

TASK I-5. SUBSYSTEM PERFORMANCE MAP

INTRODUCTION

The desiccant subsystem performance program developed in Task I-4 has been used to generate some subsystem performance predictions. In addition to the desiccant subsystem model, evaporative coolers with efficiencies of 90 percent were assumed in this work.

OFF-DESIGN PERFORMANCE

The baseline system was optimized for operating conditions that correspond to standard rating for air conditioning systems. Conditioned space and outside air temperatures were 78°F DB, 67°F WB inside and 95°F DB, 75°F WB outside. In addition, the solar energy temperature was taken at 200°F.

Effect of Hot Water Temperature

Baseline system capacity and COP were determined as a function of the hot water temperature for the solar source. These data are plotted in Figure J-1. As anticipated, the capacity of the baseline system is directly proportional to the hot water temperature, primarily because the equilibrium loading capacity of sorbent is nearly linear in the range of temperatures considered. The increase in cooling capacity of the system reflects the higher working capacity of the sorbent at higher desorption temperatures. However, system COP remains approximately constant because of the higher heating required to achieve the higher capacity at elevated temperature.

Effect of Operating Temperature Levels (DB and WB)

The performance of the system was determined for a range of inside and outside wet and dry bulb temperatures. Only one parameter was increased at the time; the others were kept constant. Two cases were considered: (1) the baseline configuration described in Appendix I, and (2) a modified configuration corresponding to a ventilated system rather than a recirculated system. In the ventilated system, outside air is processed through the dehumidifier to supply the conditioned space; return air from the residence is used to regenerate the bed and is then exhausted (the preconditioning air remains outside air).

The results of these studies are shown in Figures J-2 and J-3. The data illustrate the primary dependence of the system on the inside and outside wet bulb temperatures. Dry bulb temperatures have smaller effects on performance. These data may be misleading because only one parameter is varied while the other three are maintained the same. For example, in Figure J-2 it appears that significant gains will be achieved at the lower outside wet bulb. However, at lower ambient wet bulb the inside wet bulb will most probably also be lower, so that the net effect may not be as pronounced as shown in Figure J-3. These data show that off-design performance can only be determined accurately through the use of a complete system program incorporating a residence model. This work will be done as part of Task I-6, system performance model.

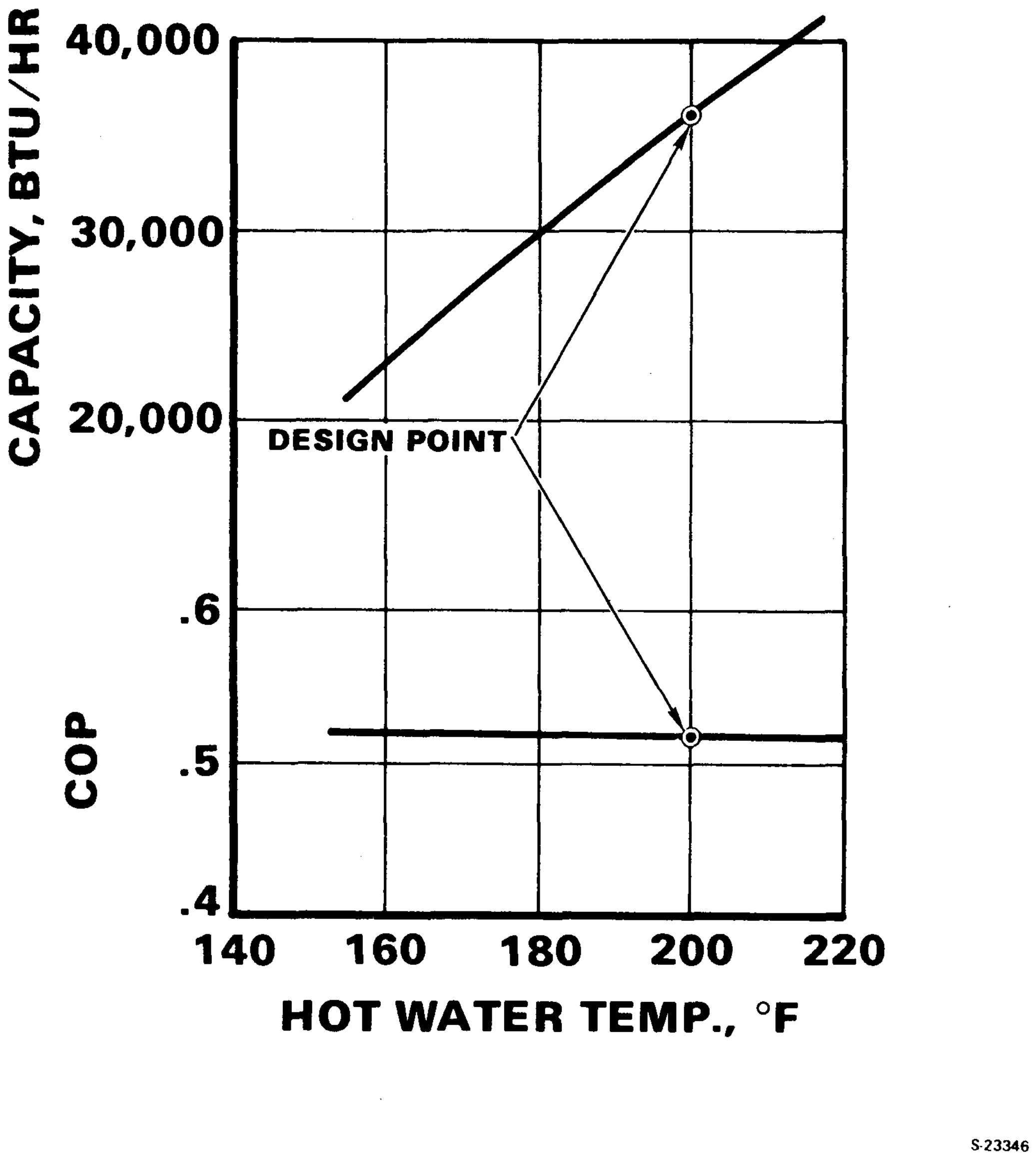

Figure J-1. Effect of Solar Source Temperature

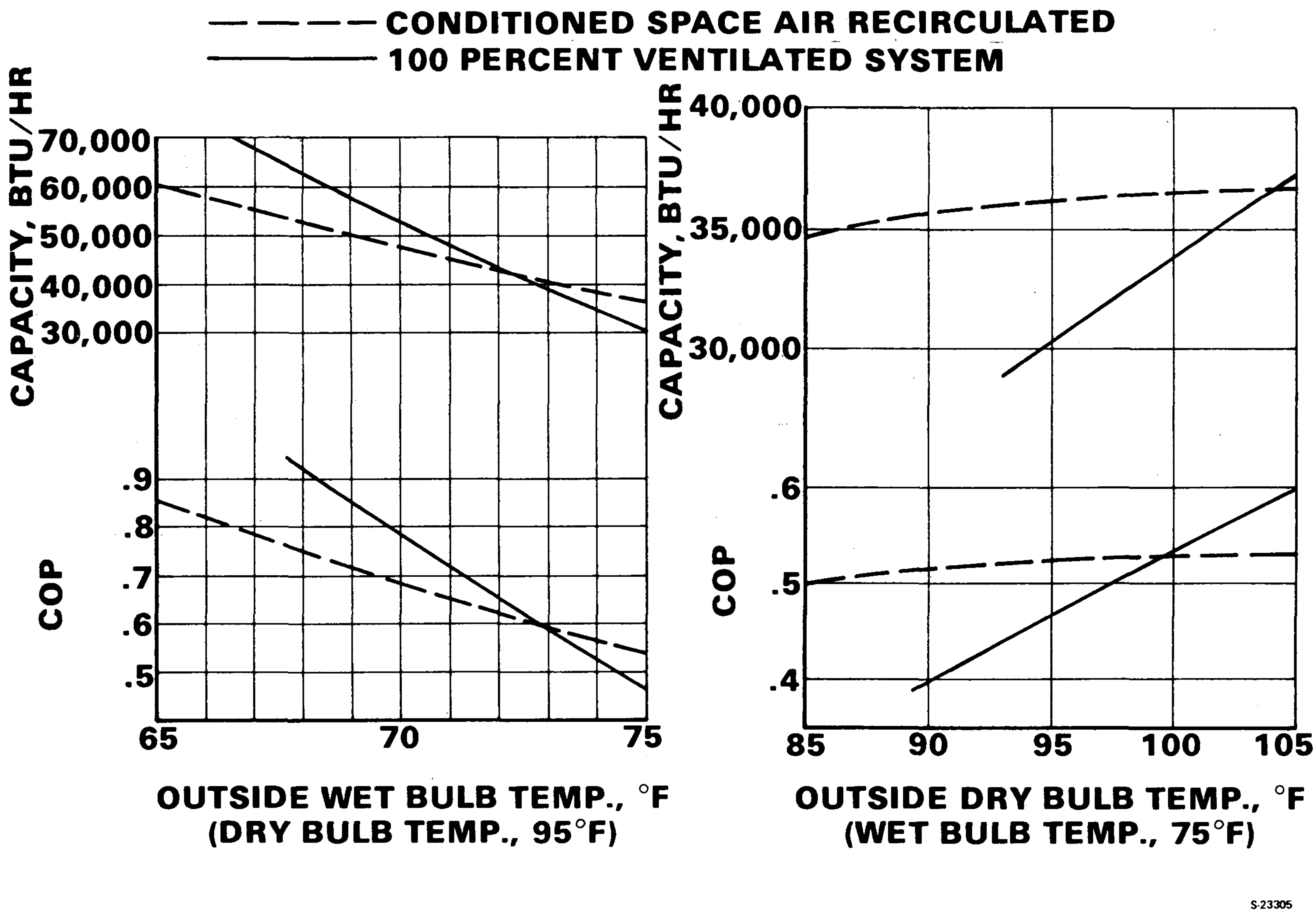

Figure J-2. Performance vs Outside Conditions

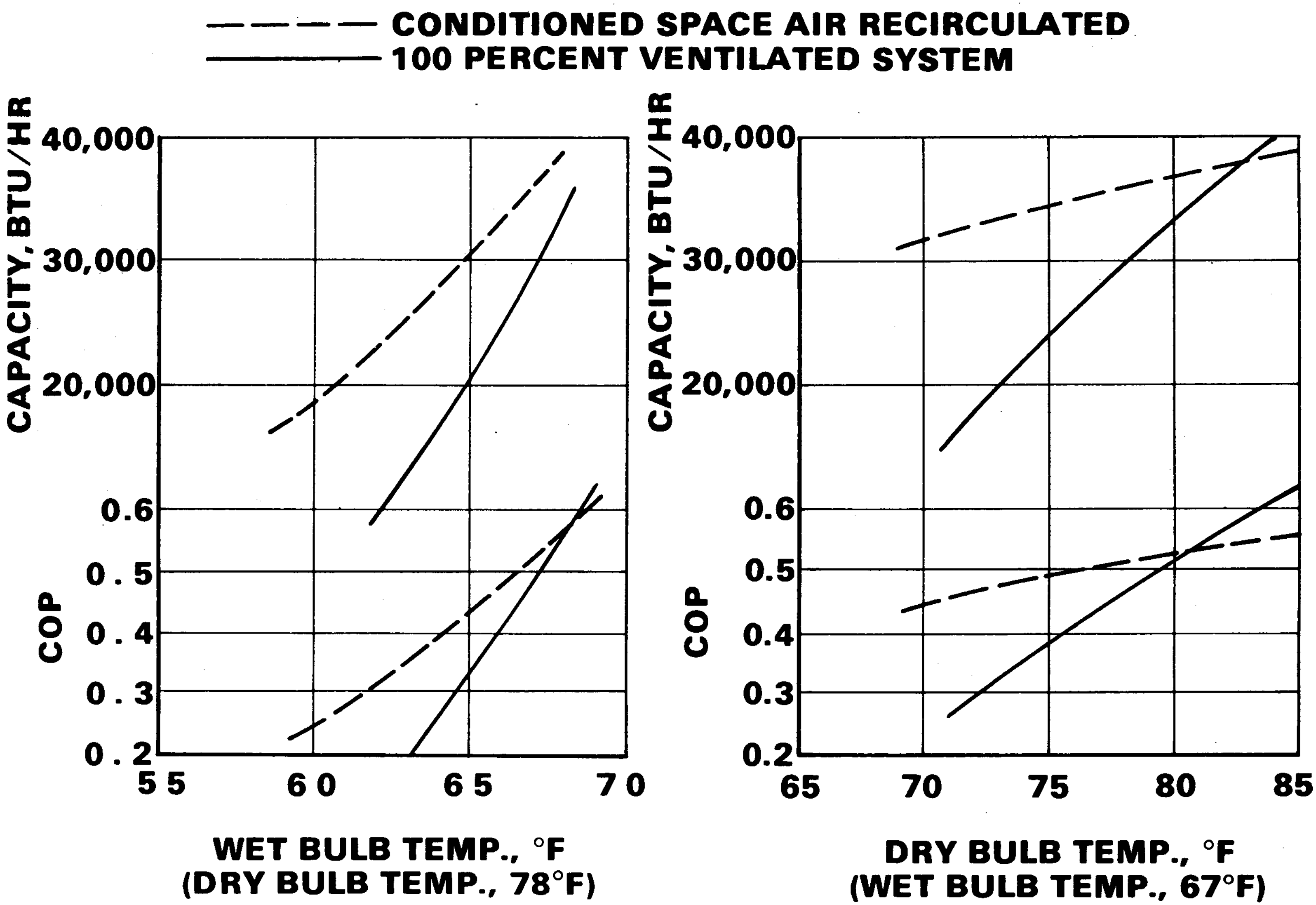

Figure J-3. Performance vs Conditioned Space Temperatures

APPENDIX K

TASK I-10. SUBSYSTEM PRELIMINARY DESIGN

INTRODUCTION

The present configuration of the solar desiccant subsystem matches the original configuration presented in the AiResearch technical proposal in most respects. However, at the beginning of this project, the approach taken was to examine all aspects of the subsystem in detail. The resulting preliminary design therefore represents an integrated subsystem, unrestricted by the concepts of the proposal wherever improvements could be made.

This appendix presents discussions of the facets of the preliminary design which have received the most attention to date. Drawings of the preliminary layout are presented at the end of this appendix. Although the layout is essentially completed, some details still remain to be worked out before a prototype can be constructed.

SUBSYSTEM CONFIGURATION

The primary function of the desiccant and regenerator transport mechanisms is to alternately expose the solid desiccant and regenerator matrix materials to the adsorbing air stream and the desorbing air stream. This can be accomplished in several ways. One of the possibilities is to use multiple stationary beds of materials, and to alternately direct the air streams through them. The other general method is to move the materials from one stationary air stream to the other.

There are two major drawbacks to the stationary multiple bed approach. The first is the nonuniform mass loading of the sorbent. As the adsorbing stream is first directed through a regenerated bed, the exiting air will be very dry. As the bed becomes loaded, the exit air conditions will change, resulting in nonuniform supply air to the conditioned space. A similar situation occurs with the desorbing air stream, resulting in poor utilization of the solar desorbing energy input. The second problem with stationary multiple beds is the large size of air manifolding and valves required to accomplish the switchover of the adsorbing and desorbing air streams. While this is not a fundamental problem, the added size and complexity would be undesirable, especially in small installations.

The simplest material transport mechanism is a porous disk. The desiccant or regenerator matrix would be enclosed by screens or other perforated material, and air would flow through the disk in an axial direction. Drive and support mechanisms for disks are quite simple compared to drum configurations. The main drawback to a disk is the large package size required to accommodate the diameter. For example, a disk of the same thickness and working capacity as the baseline desiccant drum selected in this preliminary design would be approximately 7.8 ft in diameter. This is too large to accommodate in a typical residence.

The size problem of a disk configuration is substantially improved by forming the desiccant and regenerator beds into concentric drums. Air flows in the radial direction, with manifolds in the center of the inner drum and outside of the outer drum. Largely because of the equipment that must be located between the drums, the drive system is somewhat complicated, but this does not seem to be a major problem.

With either a disk or drum configuration, it is important to minimize tumbling of the desiccant material. In some previous desiccant applications, it has been shown that agitation of the desiccant will cause fracturing and powdering, resulting in loss of desiccant and subsequent performance deterioration. This would most likely occur with either a disk or a drum rotating about a horizontal axis; rotation about a vertical axis eliminates this problem.

Based on these considerations, two concentric drums were chosen as the baseline configuration. The outer drum contains the desiccant material, and the inner drum holds the regenerator matrix. The two drums rotate in opposite directions. Desorbing airflow is from the central manifold, radially outward; absorbing airflow is from the outer manifold, radially inward. Desorption energy input is provided by the solar heat exchanger located in a sector of the annulus between the two drums, in the desorbing air stream.

Drum Construction

The selection of a material for the desiccant containment vessels depends on the nature of the materials to be contained. Appendix C contains a discussion of desiccants, leading to the selection of 8 to 10 mesh granular silica gel. Silica gel is normally chemically inert, fairly nonabrasive, and irregular enough in shape to eliminate the possibility of regular nesting with subsequent blockage of flow passages.

Several materials were considered for the desiccant drum. These include perforated metals, screens, plastics, and sintered glass. Sintered glass was examined as a possible method of making the desiccant itself into a structural drum, a concept found to be quite expensive. Plastics represent a variety of possibilities for large volume production units, but for prototype development, tooling costs would be prohibitive.

Screens and perforated metals are the most reasonable choices. Perforated metal can eliminate the need for a separate supporting frame or skeleton in order to maintain a rigid structure.

Perforated 20-gauge mild steel was chosen for both the desiccant and regenerator drums. A standard punch pattern of 0.050-in.-dia holes on 0.066-in. centers yields 225 holes per sq in., or 45 percent open area. This gauge and pattern combination is manufactured from a common stock material by most metal perforators. The steel is punched from flat stock, and then rolled into drums. Edges are joined by continuous butt welds.

Sheet steel stock with zinc cladding can be obtained from most of the major steel companies. Zinc cladding is produced by passing galvanized stock through a furnace at a temperature that allows an alloy to form between the zinc layer and the surface of the steel. The result is a surface that has the same anti-rust properties as galvanizing, but which is much less easily damaged by abrasion. The surface is also somewhat smoother than galvanizing, with the typical crystalline spangle eliminated. For these reasons, zinc-clad steel will be used for the drums.

Regenerator Matrix Materials

The selection of the regenerator matrix material is discussed in Appendix I, as part of Task I-4, subsystem computer model. Important characteristics of the materials are summarized in Table I-3.

Galvanized steel screen with 24 by 24 strands per inch and 0.014-in.-dia wire was selected. The regenerator will be assembled by winding the screen around the inner perforated drum in a continuous length. The outer drum will then be slipped over the outside of the screen bundle.

Seals

Inadequate sealing techniques and materials have been documented as major problems by most experimenters with desiccant systems. The large lengths and number of sealing surfaces lead to significant performance deterioration if even small leakages occur, and wear could lead to an expensive and complicated overhaul.

An ideal solution to both the wear and leakage problems would be a molded seal strip made of Teflon, or other high lubricity material, with the desiccant and regenerator drums coated with a low friction coating, also perhaps Teflon. This would be prohibitively expensive, however, and a nearly equal solution using less exotic materials has been found. Zinc-clad steel will provide a smooth and fairly slippery surface for the drums. Flat silicone rubber strips, 2-in. wide and 0.1-in.-thick, will be used for the seals. This material is extruded instead of molded, which is much less expensive. The rubber selected meets Federal Specification ZZR-765, Grade 2B, 70 durometer.

Seals of this basic design have been used for years by Bry-Air, Inc. in their industrial dehumidifiers, an application similar to this project. No exact life expectancy figures are available based on this experience, but Mr. Stephen Fitch of Bry-Air has given his opinion that wear should not be significant as long as the surface finish of the drum is reasonably good.

Drum Drive Mechanisms

The concentric, counterrotating drum configuration makes the drive design somewhat complicated. In general, the drums can be driven either from the rim by belts, chains, peripheral gears, or friction wheels, or from central concentric shafts. All of these possibilities were considered for this project. Peripheral drives require that the drums be supported at the edge. This can be done by ball bearing rollers. The main drawback to this type of support is the noise that would be caused by the regenerator, which rotates at about 20 rpm. Both timing and V belts are inexpensive and easy to use for this application, but because of the stationary roller supports and nonrotating partitions between the drums, it would not be possible to change a belt without removing one or both of the drums.

Peripheral gears and chain drives were not seriously considered because of the cost of manufacturing large diameter gears and sprockets. Also, assembly tolerances for gears would have to be held closely. This would be too expensive especially considering the out-of-round limits that would have to be specified for the drums.

Friction wheel drives are a potentially inexpensive way to manufacture a production unit. Successful design of a friction drive requires a close estimate of total frictional loading to be expected in operation. Seal friction is somewhat difficult to predict within about 50 percent, so the prototype unit will not use a friction drive. Subsequent units will probably be redesigned based on measurements of the prototype friction.

A central shaft drive was chosen for the preliminary design. The two drums are supported by concentric shafts mounted in ball bearings. The shafts connect to gearmotors by roller chains.

In the preliminary design, separate adjustable-speed gearmotors are used to drive the two drums. This is done to provide flexibility in testing because it will be desirable to vary the drum speeds. In production units, a single constant-speed motor will be used.

Solar Heat Exchanger

The desorption air heater will be a multiple-pass crossflow unit of finned tube construction. The heat exchanger must fit into an annular sector between the regenerator and desiccant drums, a location which suggests a curved core. However, the unit will be constructed as two small rectangular cores to minimize manufacturing costs. Each core will have five rows of tubes, each making four vertical passes. Hot water enters at the top of the first pass, flows down, returns up the second pass, and so on. Each pass is approximately 44-in. high. The tubes will be Dunham-Bush 3/8-in. "Wolverine" aluminum tubes, with 14 fins per inch.

The pressure drop across the air side is predicted to be 0.1-in. H_2O at design. The water-side pressure drop will be about 4 psi. The general configuration of the solar heat exchanger is shown in Figure K-1.

Controls

The design point performance of the baseline design represents a series of compromises intended to provide good performance in a reasonable package. Significant improvements in design point performance can only be achieved by substantial increases in desiccant drum size. However, off-design operation can benefit from improved thermal performance and parasitic power reduction as long as the proper control techniques are employed. This is an important consideration since system operation is almost always at the off-design point; substantial solar thermal energy and parasitic power savings can thereby be reduced.

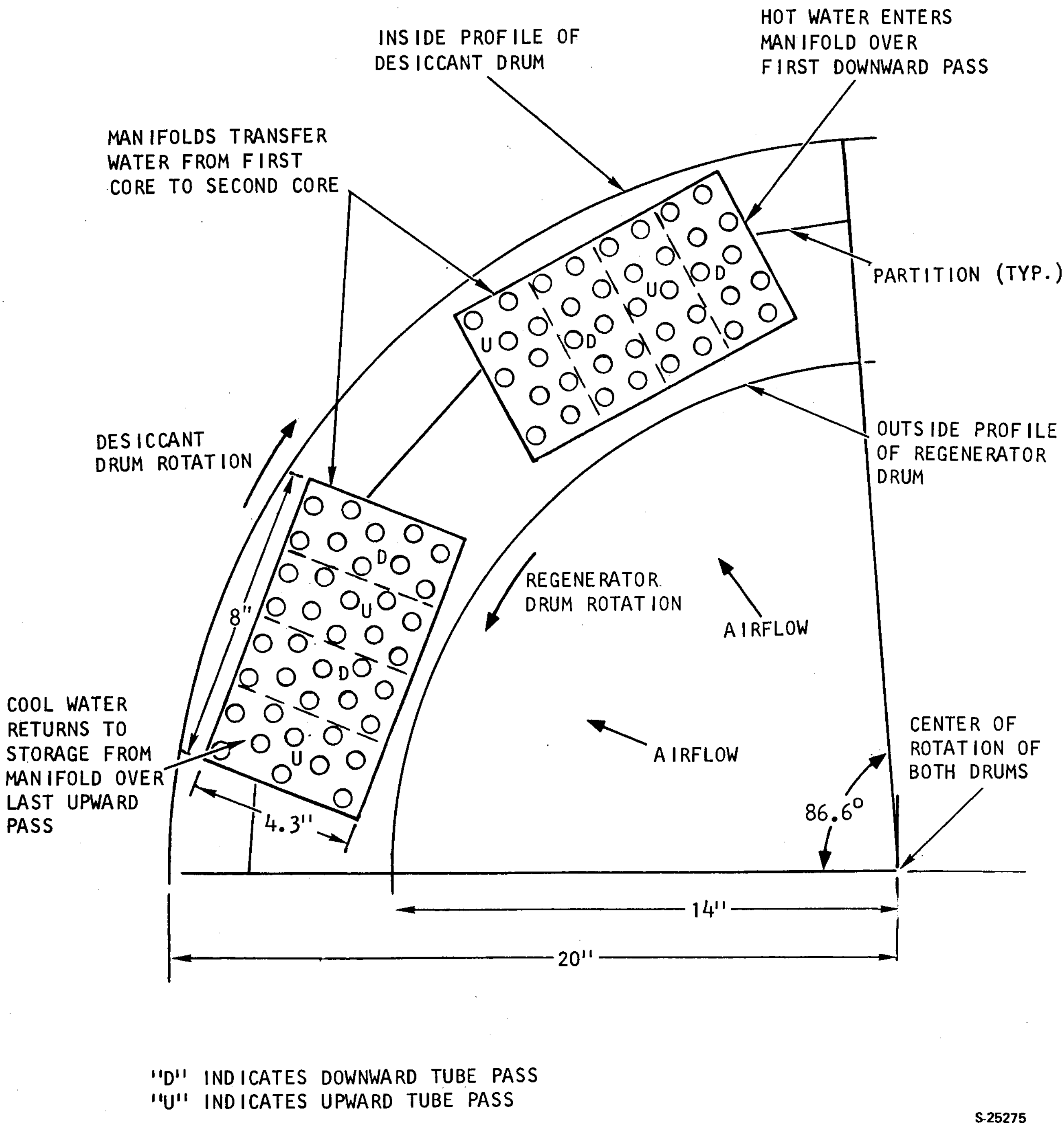

Figure K-1. Top View Illustration of Solar Heat Exchanger

Another problem inherent in the desiccant system also can be solved by proper control techniques. The problem is the time lag encountered when the system is first started. Depending on the various air conditions involved, approximately two complete revolutions of the desiccant drum are required before steady-state operation is reached. This precludes the ability to switch the system on and off, as is commonly done with a conventional air conditioner, to control the temperature in the conditioned space.

The primary control technique will be the use of multiple speed fans. When the system is first switched on, say in the morning, the fans will run at top speed until the system stabilizes and the cooling requirements are met. Then, assuming that the load is less than the design point load, the airflow will be lowered by reducing the fan speed. The thermal COP will stay about the same, but the cooling capacity will be reduced, so the solar energy consumption rate will also drop. Most important will be the drop in fan power. If the airflow rate is dropped by 50 percent, the capacity will also drop by 50 percent, approximately. However, the pressure drop of the air streams will drop by about 75 percent, resulting in a 50 percent reduction in parasitic power consumption per ton of cooling. Two- or three-speed fans appear to be the most practical, but continuously variable speed motors are being investigated.

An improvement in COP also can be made by slowing the desiccant bed rotation at part-load conditions. This may not be practical for a production unit, however, because it would require separate motors for the desiccant and regenerator drums.

Cabinet, Structure, and Ductwork

The enclosure and ductwork have been designed according to conventional air conditioning practice so that the desiccant subsystem can be easily manufactured by Dunham-Bush and no special skills or techniques will be required by installers. AiResearch designs have been reviewed by Dunham-Bush designers, and their comments have been incorporated wherever possible. In general, the structural members of the enclosure are made of "hat" section beams. These will be made from sheet metal stock in the lengths and cross-sections required. Structural fastening will mainly be done with spot welds. Nonstructural cabinet sections and parts that must be removable will be fastened with sheet metal screws.

SUBSYSTEM LAYOUT

The preliminary layout of the subsystem is shown on the following pages.

☆U.S. GOVERNMENT PRINTING OFFICE: 1979- 640- 092 1180

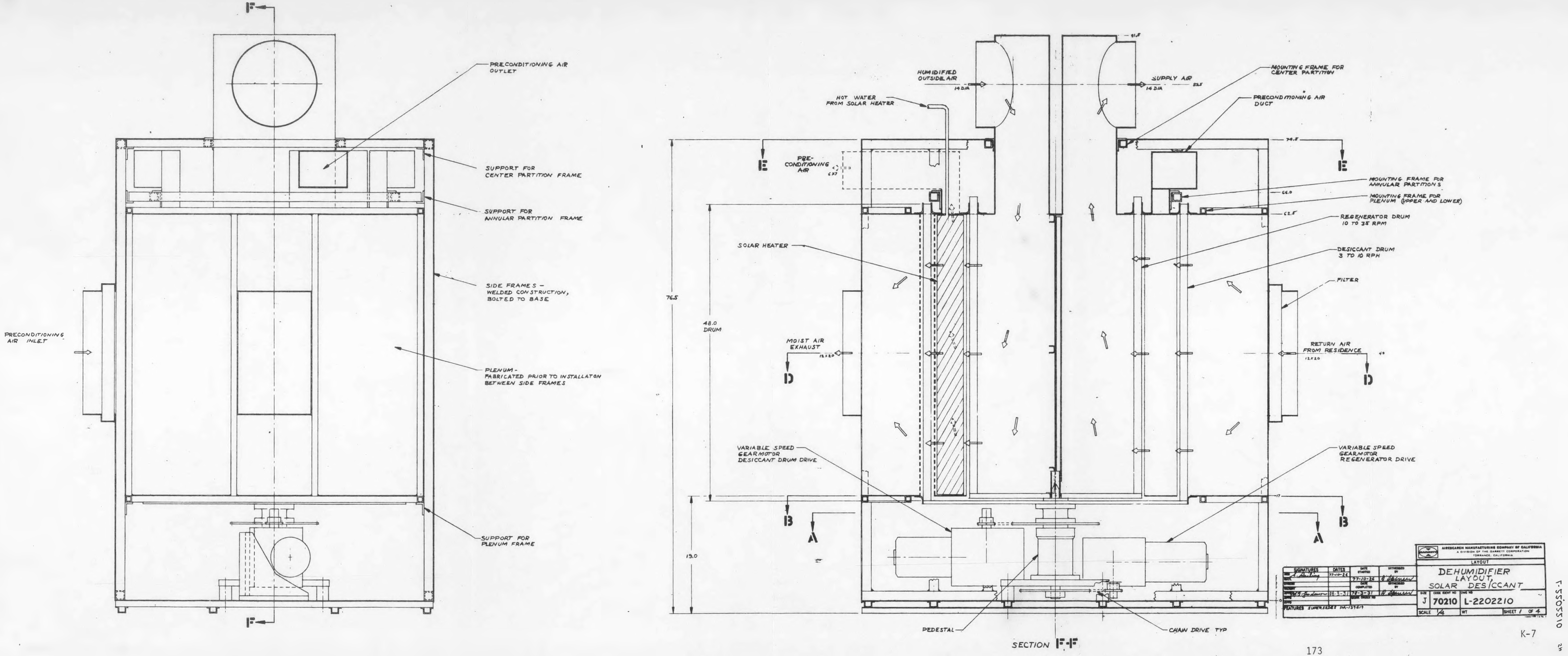
PRECONDITIONING AIR OUTLET
SUPPORT FOR CENTER PARTITION FRAME
SUPPORT FOR ANNULAR PARTITION FRAME
SIDE FRAMES — WELDED CONSTRUCTION, BOLTED TO BASE
PRECONDITIONING AIR INLET
PLENUM - FABRICATED PRIOR TO INSTALLATON BETWEEN SIDE FRAMES
SUPPORT FOR PLENUM FRAME
F
HUMIDIFIED OUTSIDE AIR
14 DIA
SUPPLY AIR
HOT WATER FROM SOLAR HEATER
MOUNTING FRAME FOR CENTER PARTITION
PRECONDITIONING AIR DUCT
PRE-CONDITIONING AIR
E
MOUNTING FRAME FOR ANNULAR PARTITIONS
MOUNTING FRAME FOR PLENUM (UPPER AND LOWER)
REGENERATOR DRUM 10 TO 35 RPM
DESICCANT DRUM 3 TO 10 RPH
SOLAR HEATER
FILTER
76.5
48.0 DRUM
MOIST AIR EXHAUST
12 x 20
RETURN AIR FROM RESIDENCE
D
VARIABLE SPEED GEARMOTOR DESICCANT DRUM DRIVE
VARIABLE SPEED GEARMOTOR REGENERATOR DRIVE
B
A
13.0
PEDESTAL
CHAIN DRIVE TYP
SECTION F-F
AIRESEARCH MANUFACTURING COMPANY OF CALIFORNIA
A DIVISION OF THE GARRETT CORPORATION
TORRANCE, CALIFORNIA
LAYOUT
DEHUMIDIFIER LAYOUT, SOLAR DESICCANT
SIGNATURES
DATES
77-10-26
DATE STARTED
77-10-26
WITNESSED BY
DATE COMPLETED
78-3-31
78-3-31
FEATURES SUPERSEDES PA-139619
SIZE J
CODE IDENT NO 70210
DWG NO L-2202210
SCALE 1/4
WT
SHEET 1 OF 4
T-550510

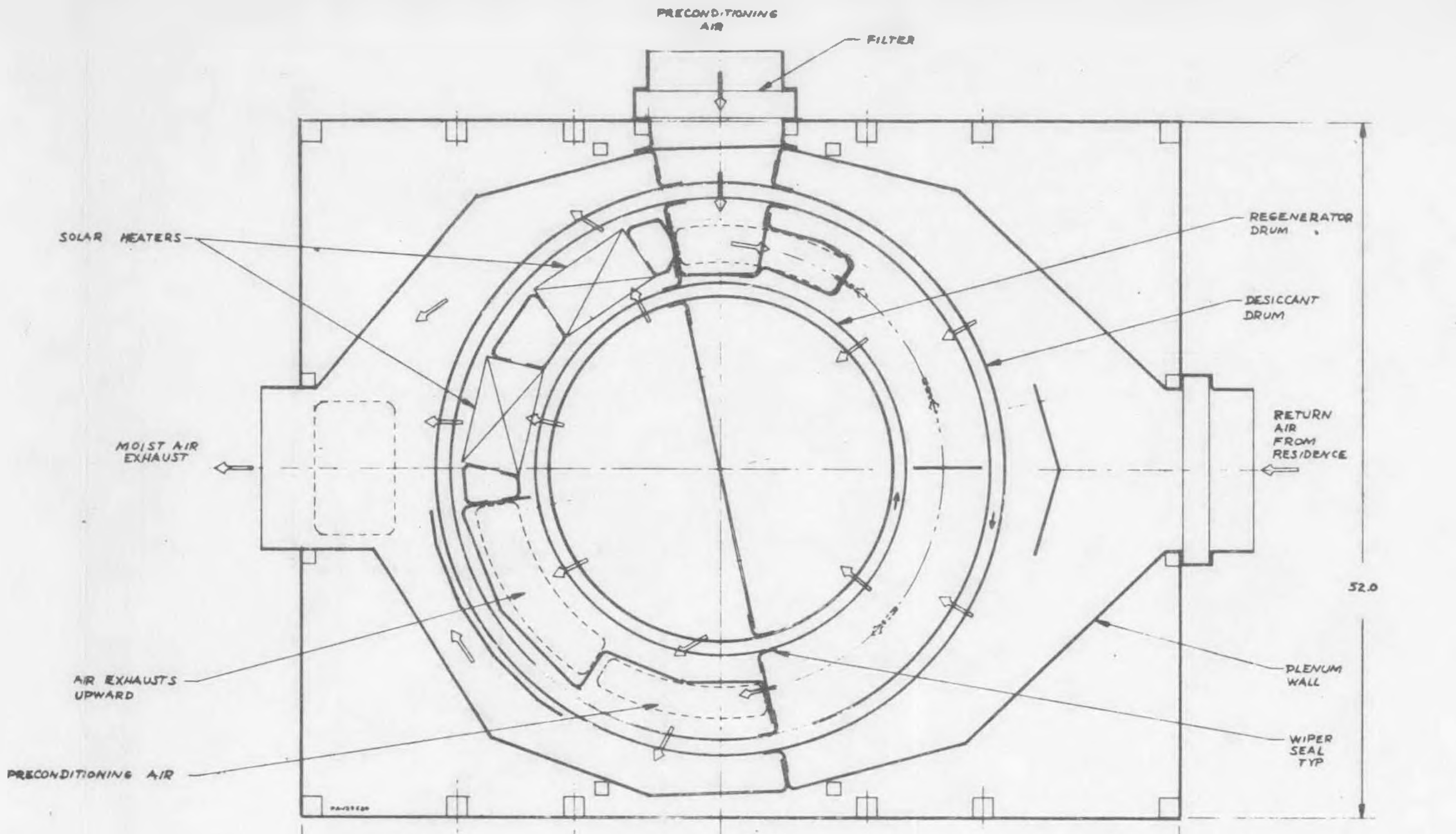

SECTION D-D

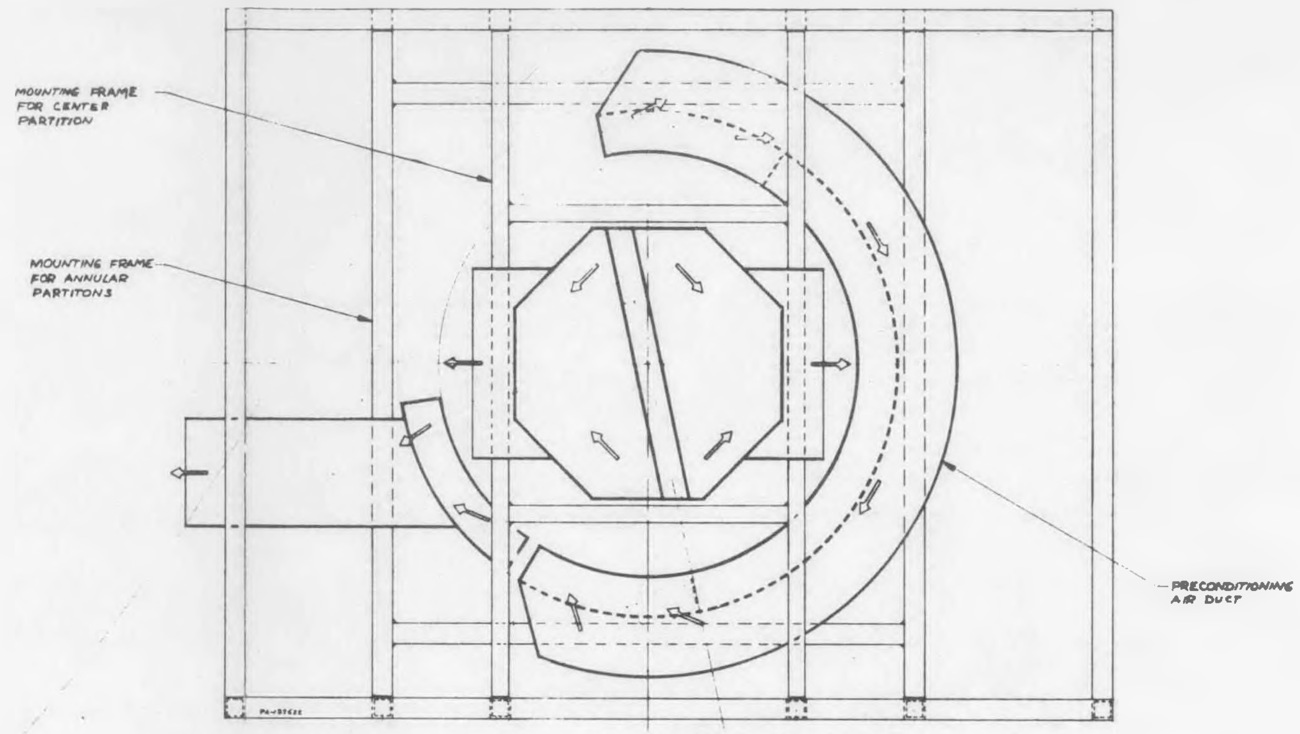

VIEW E-E
WITH ROOF PLATES REMOVED

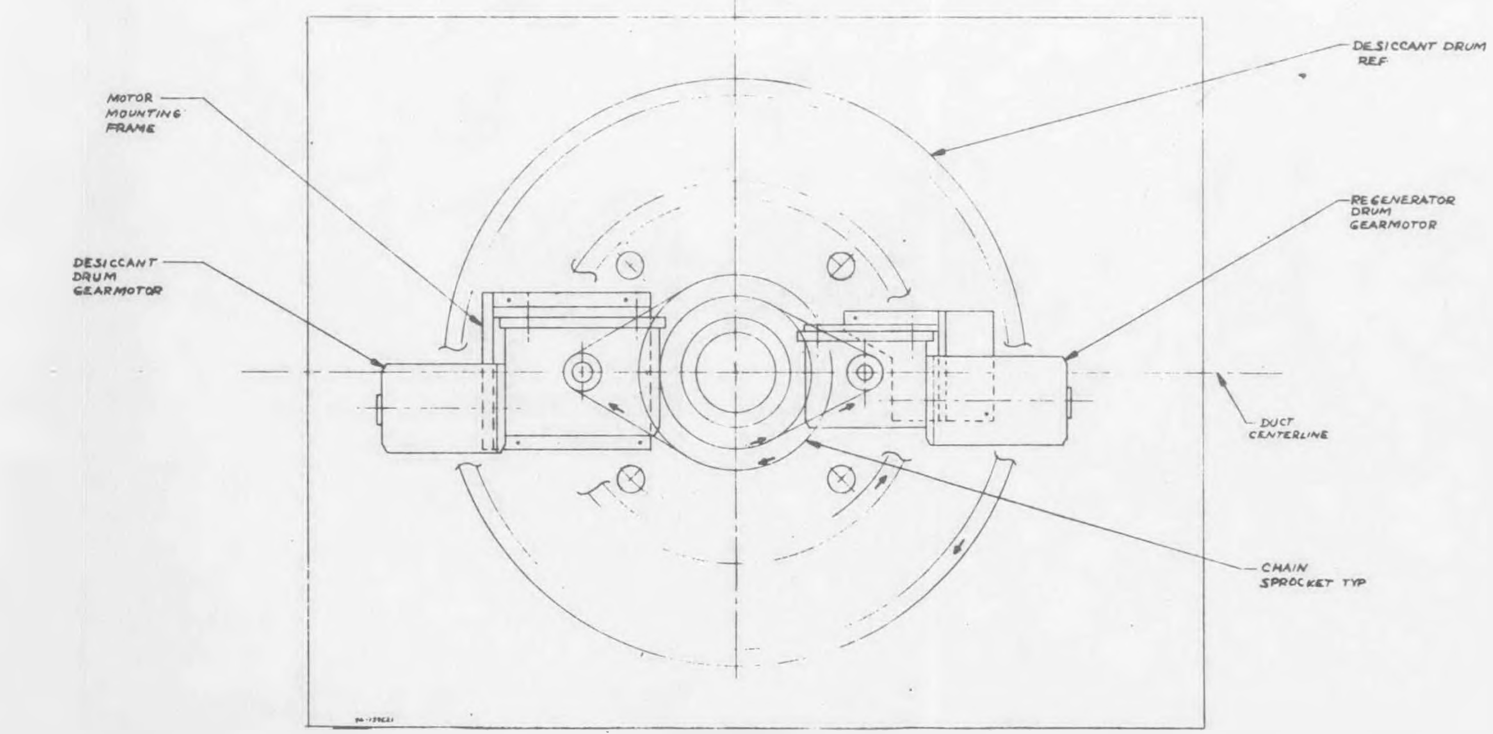

SECTION A-A
DRIVE MECHANISM

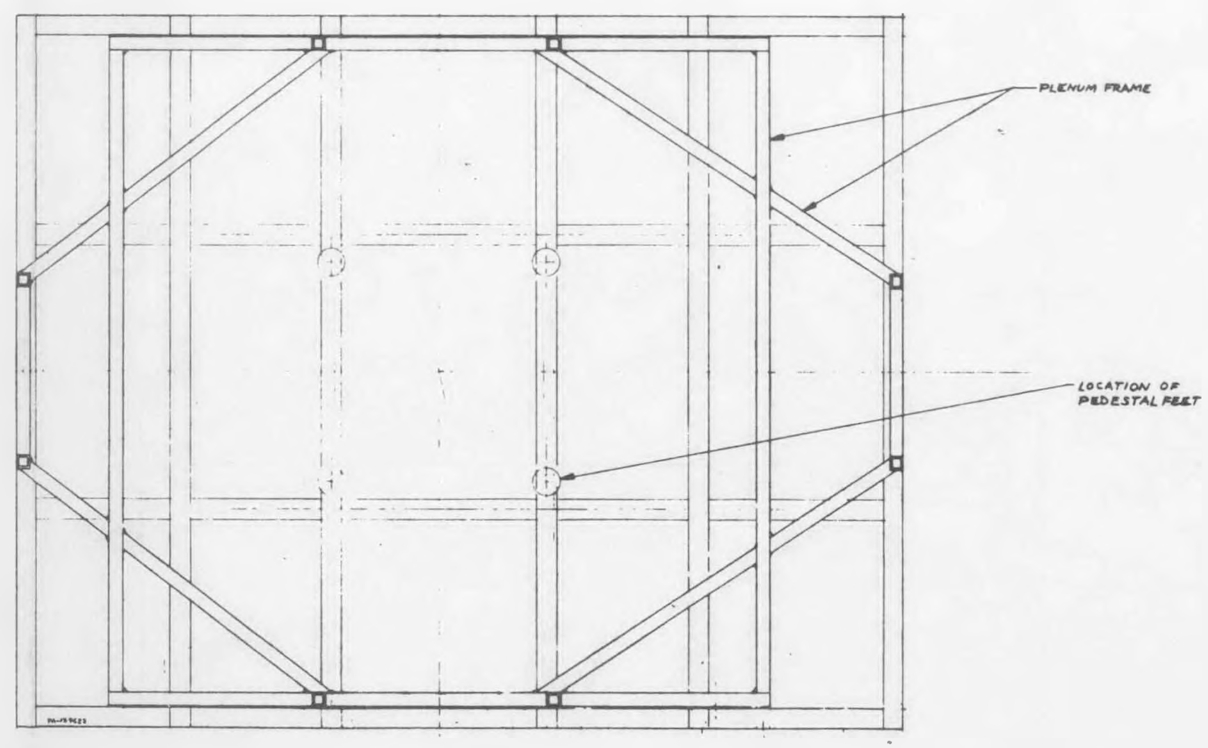

SECTION B-B
PLENUM FLOOR FRAME AND UNDER FLOOR STRUCTURE

0 2 4 6 8 10 INCHES 40

J	70210	L-2202210

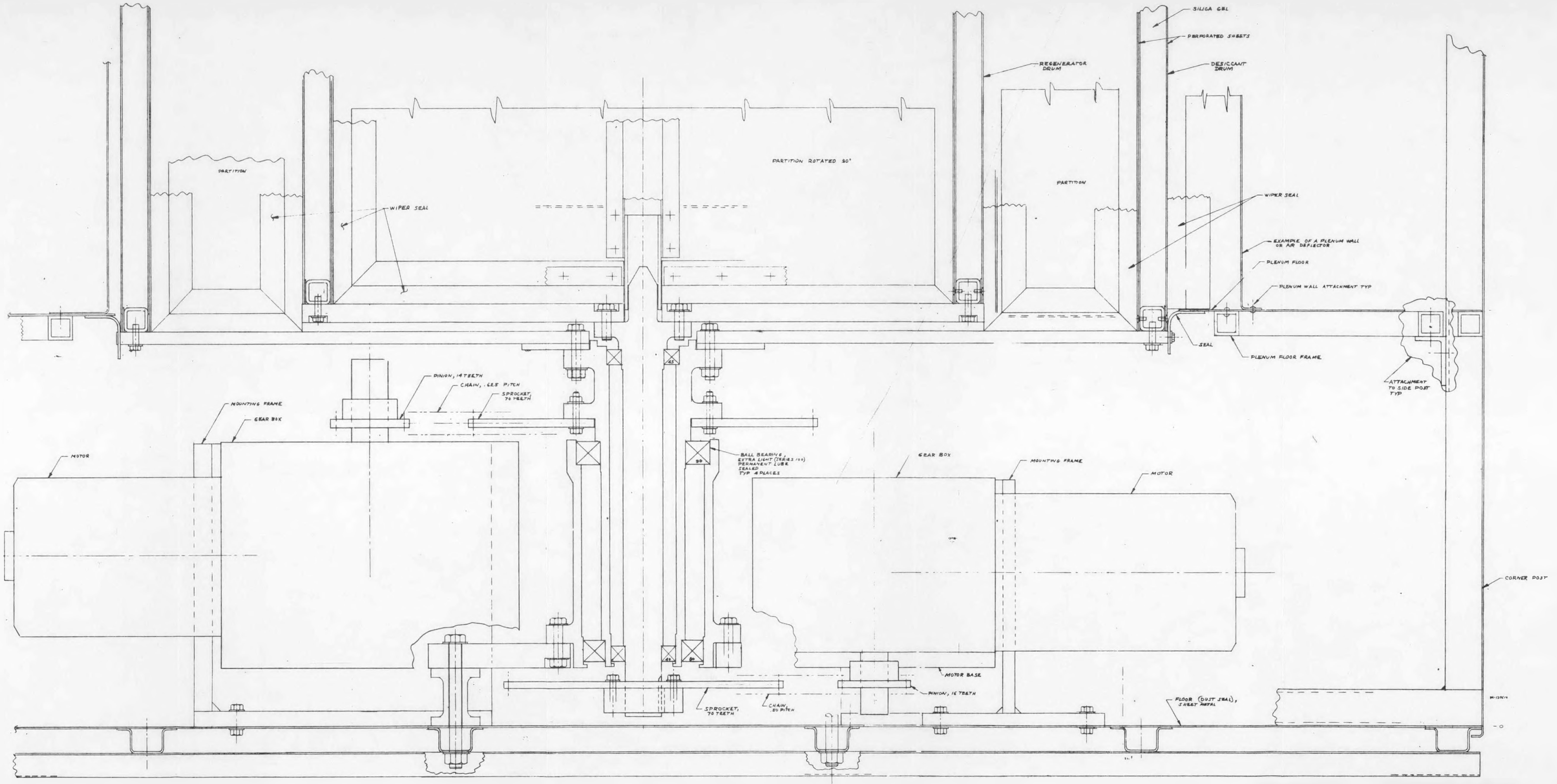

DETAILS, LOWER HALF

J	70210	L-2202210
SCALE 1/1		SHEET 3 OF 4

K-9

0155051

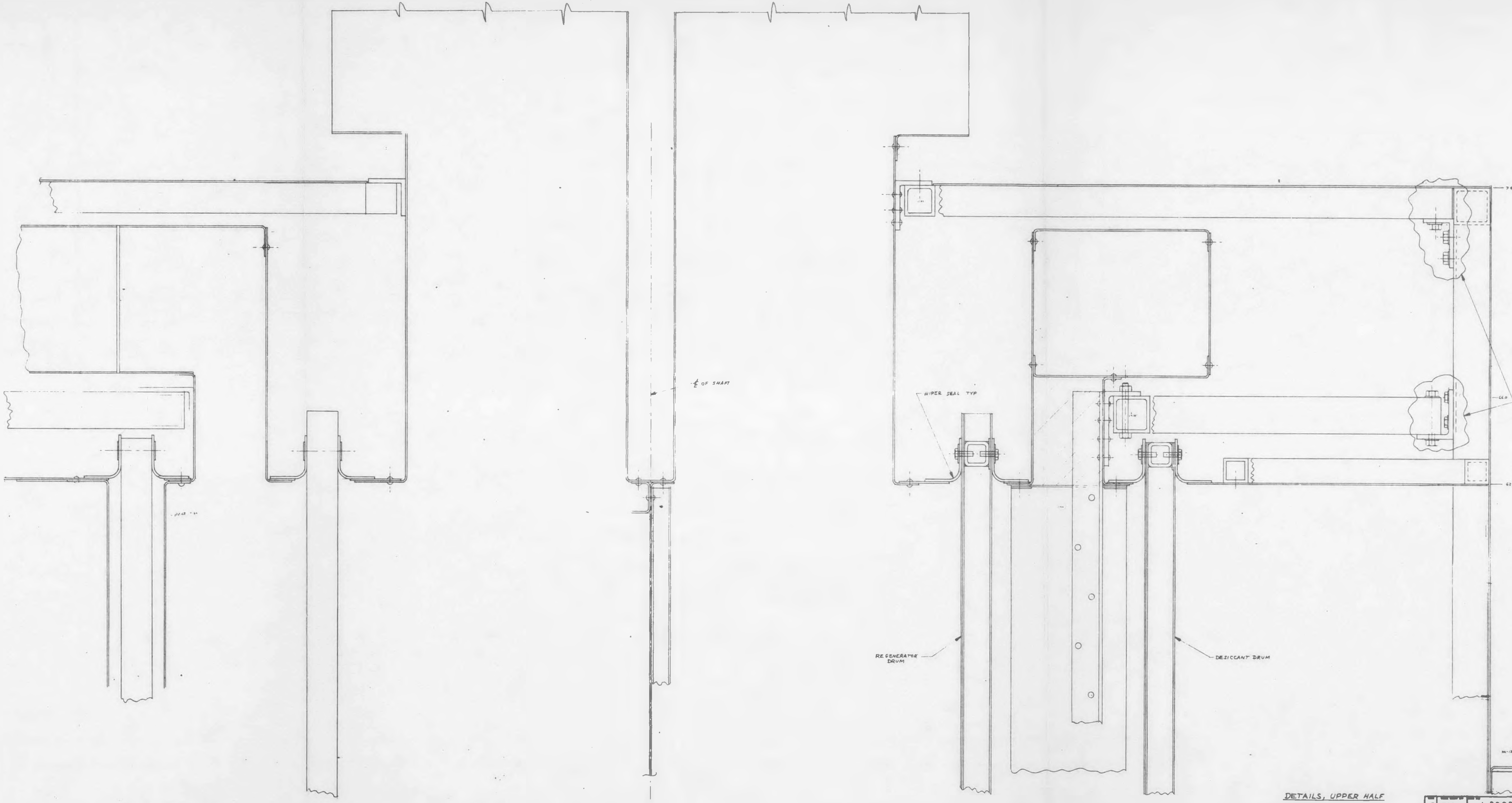

DETAILS, UPPER HALF

J	70210	L-2202210
SCALE 1/1		SHEET 4 OF 4

K-10

T-550551D